

National Chiao-Tung University PhD Thesis

國立交通大學博士學位論文

Functional study of the phosphodiesterase YjcC and the second messenger cyclic di-GMP in the stress response regulation in *Klebsiella pneumoniae* CG43

克雷白氏肺炎桿菌 CG43 磷酸二酯酶 YjcC 與二級訊息分子 c-di-GMP
在壓力反應調控之功能性研究

分子醫學及生物工程所

學生:黃靜柔

Student: Ching-Jou Huang

指導教授:彭慧玲 博士

Advisor: Hwei-Ling Peng, Ph.D.

中華民國一〇二年七月

July, 2013

克雷白氏肺炎桿菌 CG43 磷酸二酯酶 YjcC 與二級訊息分子 c-di-GMP
在壓力反應調控之功能性研究

**Functional study of the phosphodiesterase YjcC and the second
messenger cyclic di-GMP in the stress response regulation in
Klebsiella pneumoniae CG43**

研究生：黃靜柔

Student: Ching-Jou Huang

指導教授：彭慧玲

Advisor: Hwei-Ling Peng



國立交通大學
分子醫學及生物工程所
博士論文

National Chiao Tung University
Institute of Molecular medicine and Bioengineering
PHD Thesis

July 2013

中華民國 102 年七月

謝誌 (Acknowledgement)

時間總是過得很快，轉眼來到交大已經七年了，博士班期間最感謝的就是我的指導教授彭慧玲老師，很感謝老師不嫌棄我學術背景的薄弱，總是很有耐心的訓練我獨立思考的能力，也常常在我學習過程中訓練並導正我的邏輯。雖然我自己覺得走的很慢但還好老師願意陪我慢慢走，這是我始終非常感謝的。除了給予我們的專業知識的訓練，老師也很關心我們的生活，這是一般教授不會做的事，所以我真的由衷感謝我的彭老師，再多的感謝我也無法用言語或文字表達。

謝謝清華大學張晃猷老師，對於我的研究上，提醒我除了實驗結果的探討，必需對自己所研究的相關新領域，都要有追根究底的態度，而不是只是走馬看花的帶過去。很謝謝老師在我最後口試的時候給的一些建議，提醒自己，整理實驗結果時除了主觀的相信自己所做的之外，還是要謹慎探討可能會出錯的部分。

感謝中興大學鄧文玲老師，在專業領域上給予我一些建議及幫助，也感謝老師抽空參與了我在學期間重要的兩次口試，鄧老師熱心與直爽的個性，是我應該學習的榜樣。雖然最後一次的論文口試，鄧老師沒有機會參與，但我還是很謝謝老師寫信給我的鼓勵。

感謝林志生老師撥冗參與我在學期間的三次重要口試，雖然都是藉著口試的機會接觸林老師，但可以很確定老師真的很關心我們將來出社會後，面對事情時，應持有的正確態度。也很謝謝老師提醒我，外面的世界不像學校那麼單純，勉勵我要繼續努力，努力不懈後才能嚐到甜的果實。

謝謝楊昀良老師總是很親切的給予我指導與建議，老師和善的態度也讓非常容易緊張且自認有上台恐慌症的我，口試時的壓力減輕不少，雖然我的畢業口試沒能邀請到楊老師，但是也是很謝謝老師參與我的資格考以及非論文口試。

謝謝中國醫藥大學林靖婷老師，林老師正好參與我的非論文及畢業口試論文，雖然曾是實驗室的學姐，但隨著時間的累積，也讓我見識到靖婷學姐努力耕耘後的成績。這是我們做為學弟妹所該學習的榜樣。也謝謝梁美智老師參與我最後畢業論文的口試，梁老師提醒了我在表現口試的答問上，須考慮如何才能以條理分明的方式，把自己的研究充分的表現出來。感謝過去彭老師實驗室眾多的學長姐

及學弟妹。首先是九子，盈蓉學姐，當我實驗遇到瓶頸或生活上有煩惱時，總是帶著我一起去跳街舞，排解當時的煩惱與壓力，是我的精神支柱之一。謝謝健誠與小新，在我博士班修讀期間，兩位彭家大學長總是能一針見血且精闢的指正我們的實驗設計可能會遇到的缺失，也給予我很多的建議。除此之外，也很感謝健誠在離開交大後，當我遇到問題，想尋求同儕意見時，樂意提供了一些建議或幫忙，也常給我精神打氣。謝謝哲充學弟，在我博班後期，我們還一起合作把文章搞定。

感謝在我博士班前幾年一起打拼的學弟妹，特別是雅雯、家華、秉熹、顛峰、佩君、蕙如，謝謝你們總是很關心我的健康，也常拿好吃的零食、補品還有出國買回來送給我的禮物，都是支持我一步一步往前走的動力，真的很謝謝你們。還要感謝可愛學弟妹，品瑄、歲云、小波、力成、郁勝，總是默默的鼓勵我繼續往前。最後要感謝陪伴我在博班後期時的學弟妹與生力軍：補教界未來名師：冠男、多才多藝的正妹燕曦、講義氣的子祥、細心個性好的偉豐、可愛且聲音爽朗的珍儀、溫柔體貼的俐君、閩南語天后兼彭家主計處處長蕙瑜、思慮清楚的專題生豐碩，非常感謝你們在我最後要畢業時，所帶給我的歡笑以及鼓勵。新彭家生力軍碩班學弟妹瑋芝、家睿、專題生煥義，期待大家能在彭家一起茁壯。

最後我要感謝我的爸媽，一直給我很大的鼓勵及讓我無後顧之憂，父母對我的愛是無人能及的。也很感謝我的大姐、大姐夫、二姐、二姐夫以及小妹，一直以來都代替我陪伴媽媽與爸爸，家人給予我的支持才讓我勇敢的走下去。還要感謝台北三重的家人，包括大阿姨、小阿姨、小姨丈、兩個表妹依倫與李盈，更要感謝從小就把我跟二姐帶大，已經在天上的三重阿嬤，很遺憾，在你生前沒來的及把喜悅帶給你，我想阿嬤現在一定知道，也很開心我畢業了。謝謝北投三姨、三姨丈給我的鼓勵及關心。感謝所有參與我生命過程的你(你)們，才成就了現在的我。

論文摘要

克雷白氏肺炎桿菌是一株伺機性的革蘭氏陰性病原菌，可造成肺炎、原發性肝膿瘍、尿道和化膿性感染、及敗血症等廣泛疾病。我們實驗室先前利用小鼠活體表現技術（in vivo expression technology），由克雷白氏肺炎桿菌 CG43 基因庫中分離出只在小鼠體內表現、影響其毒性且會受巴拉刮（1,1'-二甲基-4,4'-聯吡啶氯化物）誘導表現的 *yjcC* 基因，分析此基因序列顯示此具 534 個殘基的蛋白質 N 端具有 2 個穿膜的二級結構和可能接收訊息的 CSS 功能區，其 C 端具有磷酸二酯酶（phosphodiesterase; PDE）活性的功能區。本論文的第一部份，我們證實 YjcC 可受巴拉刮和過氧化氫誘導表現；剔除 *yjcC* 基因除了使 CG43 抗氧化壓力的能力減低外，也降低其莢膜多醣的合成及對小鼠的毒性；而 *yjcC* 基因缺損株中的活性氧自由基、氧化傷害化、第三型線毛單位蛋白 MrkA 表現及生物膜活性相對增加；同時，經純化的 YjcC 磷酸二酯酶功能區重組蛋白被證實具有 PDE 活性；進一步，在 CG43 增加 YjcC 表現使 c-di-GMP 濃度降低後的 mRNA 定序結果顯示有 34 與 29 個基因分別因而提高和降低其表現量，而其中包括與氧化壓力相關的基因。這些結果顯示 YjcC 在氧化壓力反應中扮演正向調控的角色（詳述於第二章）。

細菌的二級訊息分子 cyclic di-GMP（c-di-GMP）由雙鳥苷酸環化酶（diguanylate cyclase; DGC）環化合成，被磷酸二酯酶所分解，因此，c-di-GMP 於細胞內的濃度由此兩群酵素活性來調控。最近許多的報導顯示 c-di-GMP 訊號

傳遞系統主導許多基因的表現與生理功能的調控。為了進一步探討克雷白氏肺炎桿菌中 c-di-GMP 濃度是否參與調控細菌對抗各種壓力的反應，我們將具有 DGC 活性的質體 pRK415-*ydeH* 轉殖至 *K. pneumoniae* CG43S3 提高 c-di-GMP 的濃度後，再以轉錄體 RNA 定序與定量分析受影響的基因，結果顯示除了已被證實受 c-di-GMP 濃度正向調控的基因 *mrkABCDF* 和 *mrkHI* 表現量明顯升高外，熱休克反應及其它壓力反應相關的基因 *ibpA*、*clpB*、*dnaK*、*grxA* 和 *dinI* 也大量表現；而比較 *K. pneumoniae* CG43S3[pRK415]和 CG43S3[pRK415-*ydeH*]發現細胞內的 c-di-GMP 濃度上升使細菌抵抗 50°C 的熱休克反應的能力增加，相對的卻降低細菌對抗氧化及酸壓力，此結果暗示細菌可藉改變 c-di-GMP 濃度來調控抵抗惡劣環境的反應（詳述於第三章）。

K. pneumoniae CG43 基因體已於今年初定序完成，序列分析結果顯示至少有 25 個與 c-di-GMP 濃度調節相關的基因，釐清這些基因的表現調控和功能性，將有助於建立 c-di-GMP 主導調控的基因網路，也將有利於了解 c-di-GMP 在細菌對抗壓力反應的調控機制。另外，最近研究證實 c-di-GMP 可與 STING 蛋白結合而增強人類干擾素的表現，又因其增強免疫反應的特性，可提供作為疫苗佐劑；未來，如何應用 c-di-GMP 配合抗生素的使用來降低細菌的感染將是一個值得深入探討的課題。

Thesis abstract

Klebsiella pneumoniae is an opportunistic Gram-negative pathogen that causes a wide range of infections, including pneumonia, urinary tract, purulent infections, primary liver abscess and septicemia. We have previously identified from *K. pneumoniae* CG43, using *in vivo* expression technology (IVET), *yjcC* gene which was shown to be inducible by paraquat and affect its virulence to mouse. Sequence analysis of YjcC shows a signal peptide followed by 2 transmembrane domains and a CSS motif at the N-terminal region, whereas the C-terminal contains a conserved EAL domain of the PDE enzyme. For the first part of the thesis, we have demonstrated that *yjcC* is induced expression by paraquat and H₂O₂. The *yjcC* deletion reduced the bacterial oxidative stress resistant activity, capsular polysaccharide production, and virulence to mouse. In addition, the *yjcC* deletion mutant exhibited increased production of reactive oxygen species, oxidative damage, type 3 fimbriae MrkA pilin, and biofilm. The recombinant protein containing the YjcC-EAL domain was demonstrated to exhibit phosphodiesterase (PDE) activity. Moreover, transcriptome analysis via RNAseq of CG43S3[pRK415-*yjcC*] compared to the CG43[pRK415] gene expression revealed 34 upregulated and 29 downregulated genes, which include stress related genes. The results suggest that *yjcC* plays a positive role in the anti-oxidative stress regulation in *K. pneumoniae* CG43S3

(Detailed description in Chapter 2).

In bacteria, the second messenger c-di-GMP is regulated by diguanylate cyclase (DGC) enzymes and phosphodiesterases (PDEs) that catalyze synthesis and hydrolysis of this molecule, respectively. Many recent reports show that the c-di-GMP-mediated signal transduction system is a major regulator for many gene expression and physiological response. In order to investigate if c-di-GMP level is involved in the stress response regulation in *K. pneumoniae*, the DGC expression plasmid pRK415-*ydeH* was used to transform *K. pneumoniae* CG43S3 to elevate the intracellular c-di-GMP level. Subsequently, transcriptome analysis via RNAseq was employed and then qRT-PCR analysis used to confirm the affected genes. The results showed that, in addition to the reported c-di-GMP upregulated genes *mrkABCDF* and *mrkHI*, the heat shock response and other stress response genes including *ibpA*, *clpB*, *dnaK*, *grxA*, and *dinI* are also increasingly expressed. Compared to CG43S3[pRK415], CG43S3[pRK415-*ydeH*] had increased the heat shock (50°C) resistant activity, but had reduced the bacterial resistance to oxidative and acid stress by the increase of the c-di-GMP levels. The results imply that bacteria could resist to the harsh environment by modulating the intracellular c-di-GMP levels.

Analysis of the recently resolved genome sequence of *K. pneumoniae* CG43 revealed 25 genes coding for GGDEF- or EAL-domain proteins that are responsible

for the intracellular c-di-GMP level modulation. To clarify how these gene expression are regulated and what are their functional roles in the bacteria should help to establish a c-di-GMP-dependent gene network. These data should also provide much more insights of the c-di-GMP role in the stress response regulation. Besides, several recent reports have demonstrated that c-di-GMP is able to bind STING protein, the stimulator of interferon gene, thereby enhances the immune response. It is proposed to be used as vaccine adjuvant because of the potent immune modulator property. In the future, the issue of how to apply c-di-GMP together with antibiotic treatment to decrease bacterial infections deserves an in depth investigation.

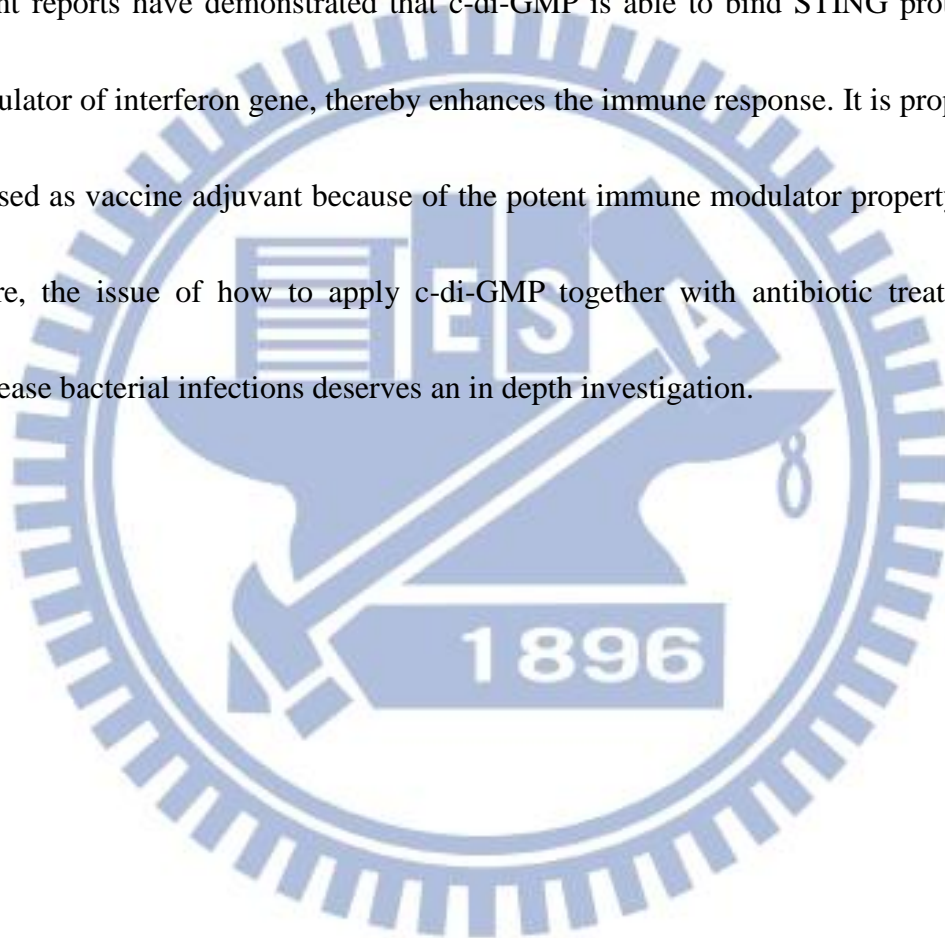


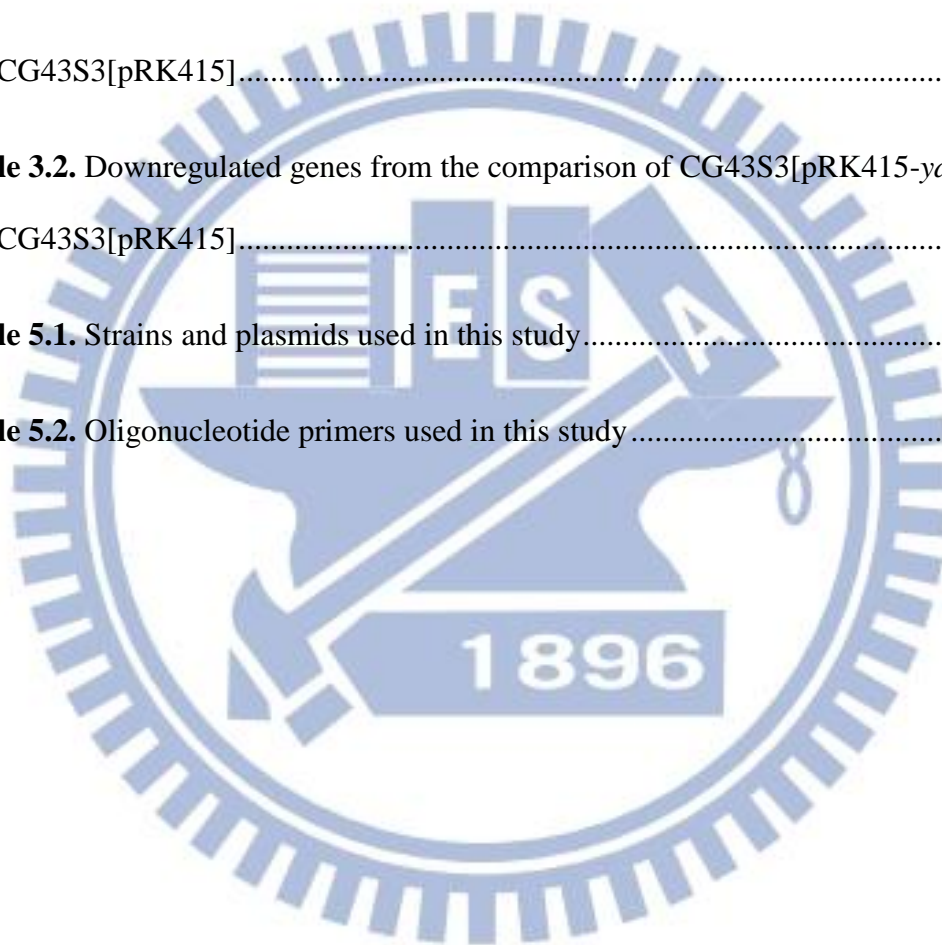
Table of Contents

謝誌.....	III
論文摘要(Thesis Abstract in Chinese).....	V
Thesis Abstract.....	VII
Table of Contents.....	X
List of Tables.....	X II
List of Figures.....	X III
Abbreviations.....	X IV
Chapter 1	
General Introduction.....	1
1.1 <i>Klebsiella pneumoniae</i>	2
1.1.1 <i>K. pneumoniae</i> infections.....	2
1.2 <i>K. pneumoniae</i> virulence factors.....	4
1.2.1 <i>K. pneumoniae</i> type 1 fimbriae.....	6
1.2.2 <i>K. pneumoniae</i> type 3 fimbriae.....	6
1.3 Cyclic-di-GMP signaling system.....	7
1.3.1 The GGDEF- and EAL domain proteins.....	8
1.3.2 Regulatory mechanism of c-di-GMP.....	9
1.3.3 Role of c-di-GMP in virulence.....	10
1.3.4 Domain structure of GGDEF- and EAL- domains in <i>K. pneumoniae</i> CG43S3.....	11
1.4 Oxidative stress.....	13
1.4.1 Oxidative stress response in bacteria.....	14
1.5 Transcriptome analysis.....	16

1.5.1 RPKM measure	18
Chapter 2	
YjcC, a c-di-GMP phosphodiesterase protein, regulates the oxidative stress response and virulence of <i>Klebsiella pneumoniae</i> CG43	
2.1. Abstract	20
2.2. Introduction.....	21
2.3. Results.....	23
2.4. Discussion.....	29
Chapter 3	
Transcriptome analyses of the c-di-GMP effect on the stress response in <i>Klebsiella pneumoniae</i> CG43S3	
3.1 Abstract.....	49
3.2 Introduction.....	49
3.3 Results.....	50
3.4 Discussion.....	52
Chapter 4	
Conclusion and Perspectives.....	60
Chapter 5	
Experimental Section.....	65
References.....	82
Publication	102
vita.....	103

List of Tables

Table 2.1. YjcC effect on the mouse virulence	34
Table 2.2. Significantly upregulated genes by <i>yjcC</i> overexpression.....	35
Table 2.3. Significantly downregulated genes by <i>yjcC</i> overexpression.....	36
Table 3.1. Upregulated genes from the comparison of CG43S3[pRK415- <i>ydeH</i>] and CG43S3[pRK415].....	53
Table 3.2. Downregulated genes from the comparison of CG43S3[pRK415- <i>ydeH</i>] and CG43S3[pRK415].....	54
Table 5.1. Strains and plasmids used in this study.....	80
Table 5.2. Oligonucleotide primers used in this study.....	81

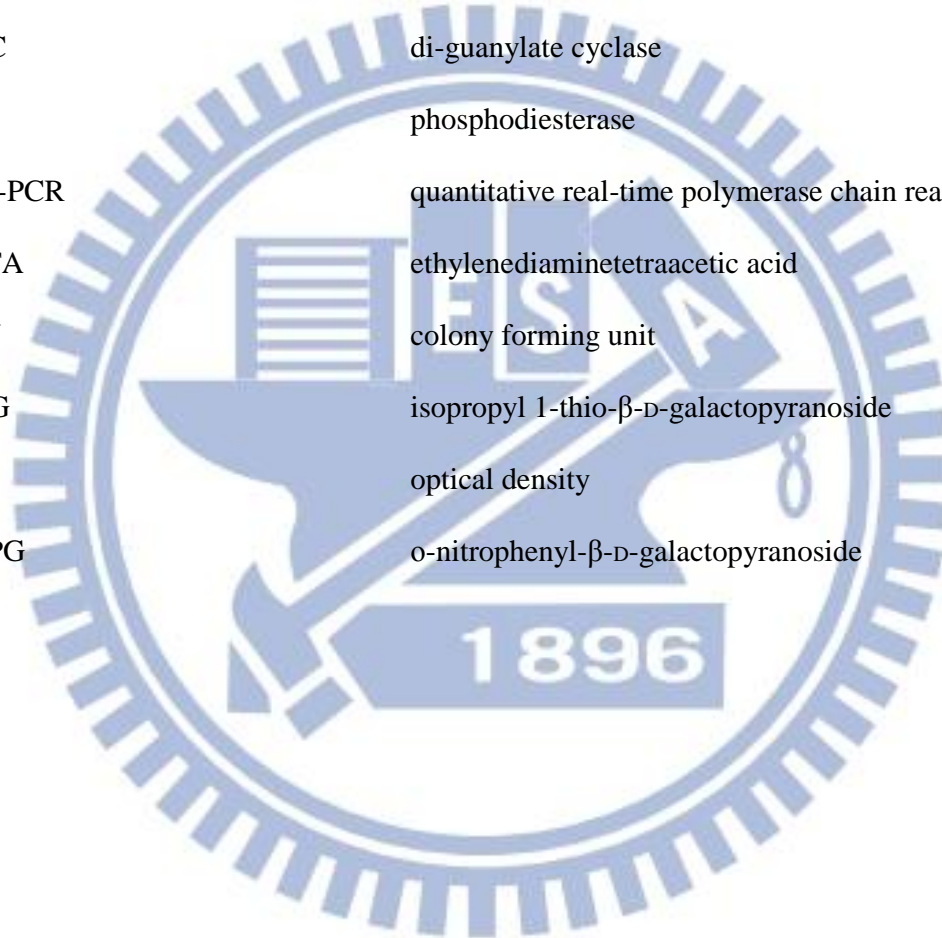


List of Figures

Fig. 1.1 Domain architecture of putative c-di-GMP signaling proteins encoded of <i>K. pneumoniae</i> CG43	12
Fig. 2.1 <i>yjcC</i> gene is paraquat inducible, and <i>SoxRS</i> and <i>RpoS</i> dependent	38
Fig. 2.2 Analysis of the deletion effects of <i>yjcC</i> upon exposure to oxidative stress ...	40
Fig. 2.3 Deletion of <i>yjcC</i> places bacteria in an oxidative stress state	42
Fig. 2.4 YjcC affects the CPS biosynthesis, biofilm formation and MrkA production	45
Fig. 2.5 The qRT-PCR analysis of the expression of <i>mrkA</i> , <i>mrkH</i> , and <i>mrkI</i> of <i>K. pneumoniae</i> CG43S3	47
Fig. 3.1 The cyclic di-GMP content.....	56
Fig. 3.2 qRT-PCR analysis of the selected up-regulated genes.....	57
Fig. 3.3 Heat shock stress survival analysis	58
Fig. 3.4 Responses to acid stress and oxidative stress treatment.....	59

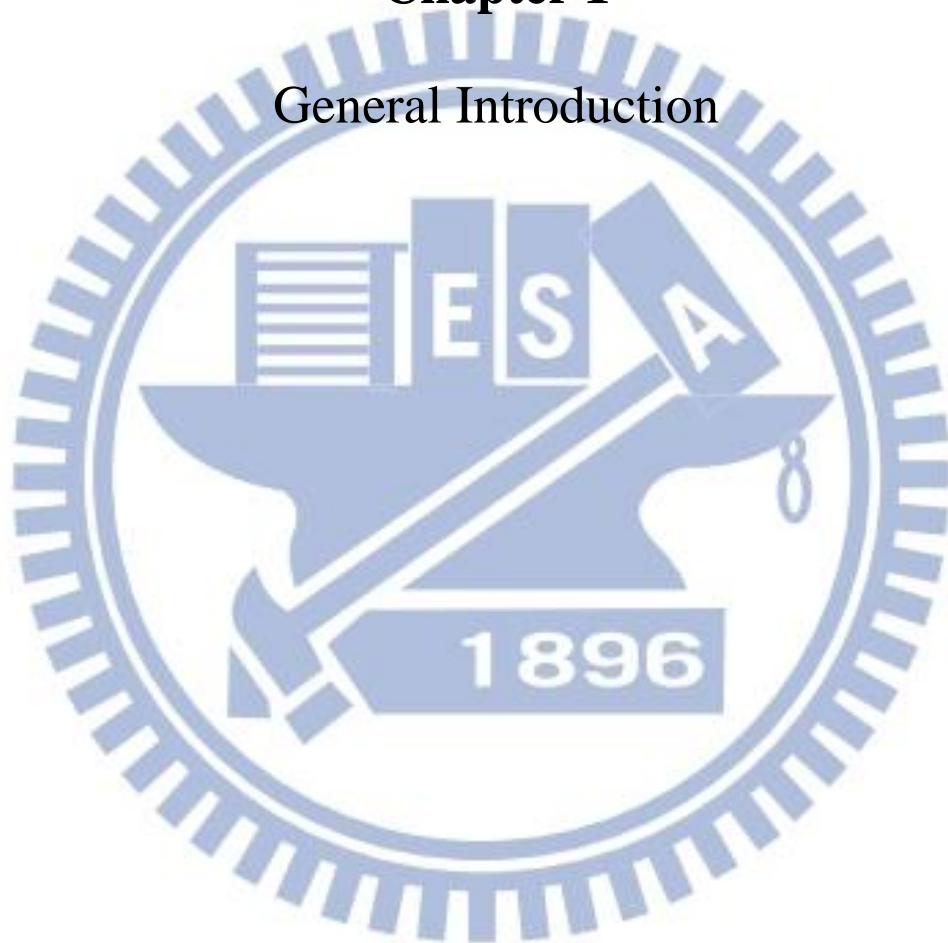
Abbreviations

PLA	pyogenic liver abscess
ESBL	extended-spectrum β -lactamase
CPS	capsular polysaccharide
LPS	lipopolysaccharide
C-di-GMP	Bis-(3'-5')-cyclic dimeric guanosine monophosphate
DGC	di-guanylate cyclase
PDE	phosphodiesterase
qRT-PCR	quantitative real-time polymerase chain reaction
EDTA	ethylenediaminetetraacetic acid
CFU	colony forming unit
IPTG	isopropyl 1-thio- β -D-galactopyranoside
OD	optical density
ONPG	o-nitrophenyl- β -D-galactopyranoside



Chapter 1

General Introduction



1.1 *Klebsiella pneumoniae*

Klebsiella pneumoniae is a rod-shaped, non-motile, heavily-encapsulated gram-negative bacterium belonging to the *Enterobacteriaceae*. As an opportunistic human nosocomial pathogen, it primarily attacks immunocompromised individuals. Mostly community-acquired *K pneumoniae* infections cause pneumonia or urinary tract infections [1]. Since 1980s, liver abscesses patients infected with *K. pneumoniae* were start to be described in reports and case series in Taiwan [2,3].

1.1.1 *K. pneumoniae* infections

K. pneumoniae has emerged as the leading cause of pyogenic liver abscess in Asia, with over 900 cases reported in Taiwan by 2004 [4]. Smaller series have been reported from other countries in Asia, including the Peoples Republic of China, Korea, Japan, Singapore, Hong Kong, Thailand and India [5]. Diabetes mellitus or impaired glucose tolerance is significant comorbidity, present in 40–75 % of these cases. A significant minority of patients (8–15%) had infection at other anatomical sites, including brain abscess, endophthalmitis, pyogenic meningitis, empyema, septic pulmonary emboli, osteomyelitis, septic arthritis, prostatic and psoas abscesses. Mortality ranged from 4 to 11 %, which is notably lower than historical mortality rates reported for pyogenic liver abscesses [6,7]. In 1999, *K. pneumoniae* was first reported as a cause of community- acquired, mono-microbial pyogenic liver abscess

in North America [6,8]. In Europe, single cases have been reported from Spain, Belgium, the Netherlands, Sweden, Italy and France [9-13]. One larger case series from France published in 2011 detailed seven cases of invasive liver abscess from hospital [14]. In addition, it was identified as the commonest cause (23/79 cases) of pyogenic liver abscess at two New York City hospitals, between 1993 and 2003 [15].

Invasive isolates typically belong to capsular serotypes K1 and K2, both of which express a distinct hypermucoviscous phenotype [16]. Heavy encapsulation confers the bacteria resistance to phagocytosis and prevent from intracellular killing. Two plasmid-encoded virulence factors have been well characterized, *rmpA*, a regulator of mucoid phenotype that upregulates the capsule synthesis, and the iron siderophore aerobactin, which enables the bacterium to obtain iron. Other virulence factors include the genes *kfu*, which codes for an iron uptake system, and *allS*, which is associated with allantoin metabolism. All have been associated with severe pyogenic infections [17,18].

In the hospital environment with the extensive use of antibiotics, multiple drug resistance has been increasingly observed in *K. pneumoniae*, especially the extended-spectrum β -lactamase (ESBL)-producing strains [19-21]. Carbapenems are considered to be the preferred agents for the treatment of serious infections caused by ESBL-producing *K. pneumoniae* because of their high stability against β -lactamase

hydrolysis and observed retained susceptibility of ESBL producers [22-24]. Nevertheless, it is rare occurrence for liver abscesses caused by ESBL- *K pneumoniae* have been reported in Taiwan. Carbapenem-resistant *K pneumoniae*, such as strains producing NDM-1, has been increasingly reported [25,26]. Antibiotics such as ampicillin–sulbactam, a third-generation cephalosporin, aztreonam, and a quinolone can be used to treat these hyper-resistance strains [27].

1.2 *Klebsiella pneumoniae* virulence factors

The virulence factors that allow *K. pneumoniae* to overcome innate host immunity and to maintain infection in a mammalian host factors include capsule, lipopolysaccharides, adhesins, iron acquisition systems, serum resistance factor, and biofilm formation regulators [28,29]. CPS acts to protect the bacteria from phagocytosis, from killing by polymorphonuclear granulocytes and from killing by bactericidal serum factors [30-32]. Besides the physical hindrance to fimbrial binding, the role of *Klebsiella* CPS in mediating the bacterial resistance to antimicrobial peptides has also been reported [33,34]. *K. pneumoniae* strains expressing K1 and K2 CPS are the most virulent to mice [35]. In addition to the 77 serotypes distinguished, a new K serotype has been identified in 2008 [36]. Serotypes K1, K2, K4 and K5 are highly virulent in experimental infection in mice and are often associated with severe infections in humans and animals [37]. The K1 and K2 serotypes were also found to

be the most prevalent capsular serotypes in liver abscess-causing *K. pneumoniae*. The *rmpA* (regulator of the mucoid phenotype A) gene correlated with abscess formation in patients with community-acquired *K. pneumoniae* bacteremia has been attributed to be a risk factor for metastatic infection in patients with *K. pneumoniae* liver abscess [38]. The *rmpA* together with *rmpA2* gene both located on the large virulence plasmid pLVPK are able to enhance the CPS biosynthesis thereby confer *K. pneumoniae* a hypermucoviscosity phenotype [39].

Animal experiments have been performed to assess the role of iron-acquisition systems in *K. pneumoniae* pathogenicity [40,41]. Analysis of the genomic sequence of *K. pneumoniae* NTUH-K2044 revealed 10 putative iron-acquisition systems, whereas *K. pneumoniae* strain MGH78578 and CG43 possess only 6 and 8 of these systems, respectively [42].

The LPS O-antigen and the lipid A are responsible for the resistance to serum factors and the establishment of septic shock [43]. Antimicrobial peptides, such as polymyxin B, are bactericidal agents that exert their effects by interacting with the LPS of Gram-negative bacteria. Our previous studies have shown that regulation of the gene expression for LPS modification determine the polymyxin B resistance [44,45]. The adhesion factors, including the type 1 [46,47] and 3 fimbriae [48] play crucial roles in adhesion to host cells, persistence in infection site, and biofilm

formation.

1.2.1 *K. pneumoniae* type 1 fimbriae

Type 1 fimbriae are approximately 7 nm wide and 1-2 μm long surface organelles are found in many bacteria in the family *Enterobacteriaceae* [49,50]. Type 1 fimbriae are encoded by *fimAICDEFGH* gene cluster coding for the fimbrial structure and assembly. The fimbrial rod consists of the major subunits FimA and the minor subunits FimI, FimF, and FimG. The adhesive properties of type 1 fimbriae are exerted by the FimH adhesin which locates at the tips of the fimbriae. FimC and FimD are respectively chaperone and usher that are required for the fimbrial assembly. [51,52]. Type 1 fimbriae, which are able to cause mannose-sensitive agglutination of yeast cells or erythrocytes (mannose-sensitive haemagglutination, MSHA) from guinea pig are regulated via phase- variation [47,51,53-57].

The *fimK* gene, locating downstream to the *fimH* gene and unique to the *K. pneumoniae* *fim* gene cluster, encodes an EAL domain protein [56]. We have recently demonstrated that FimK may influence type 1 fimbriation by binding to *fimS* via the N-terminal domain, and thereafter, the altered protein structure activates C-terminal PDE activity to reduce the intracellular c-di-GMP level[58].

1.2.2 *K. pneumoniae* type 3 fimbriae

Type 3 fimbriae that are originally characterized in *Klebsiella* strains are 2-4 nm

wide and 0.5-2 μm long surface organelles. The fimbriae are able to agglutinate the tannic acid-treated human erythrocytes which could not be competitively inhibited by mannose and hence designated MR/K haemagglutination [59]. Besides playing an important role in biofilm formation on biotic and abiotic surfaces, type 3 fimbriae are able to attach the endothelial and bladder epithelial cell lines [60-65]. The fimbriae are encoded by chromosomally- or plasmid-borne *mrkABCDF* [61,65,66]. MrkD is the adhesin that mediates binding specificity and biofilm formation on extracellular matrix-coated surfaces, which can bind to type IV and/or type V collagen [63].

1.3 Cyclic-di-GMP signaling system

In bacteria, there are having various ways to sense environmental signals and to adapt their behavior and physiology through different signaling transduction systems. In bacteria, there are various ways to sense environmental signals and to adapt their behavior and physiology through different signaling transduction systems. Cyclic AMP (cAMP) is a global second messenger involved in bacterial transcription regulation, while the signaling role of cyclic di-GMP (c-di-GMP) which was first discovered in *G. xylinus* [67] as an allosteric activator of the cellulose synthesis has not been recognized until recently. The second messenger c-di-GMP exclusively found in bacteria is involved in many fundamental behaviors such as motility, sessility and virulence. It also plays key roles in adhesion to surfaces, aggregation and

biofilm formation, and developmental transitions [68,69] [70].

1.3.1 The GGDEF- and EAL-domain proteins

In general, GGDEF domains are approximately 170 amino acids long and GG(D/E)EF motif is an integral part of the active site [71]. Stand-alone GGDEF domains are usually not enzymatically active, but require activation through an N-terminal signaling domain for activation. Besides the EAL motif, there are several other highly conserved motifs involved in catalysis, substrate binding and divalent ion coordination. Usually, EAL domains show significant enzymatic activity without N-terminal allosteric activation. Both GGDEF and EAL domain containing proteins can be enzymatically active [72-74]. Alternatively, only one domain possesses enzymatic activity, while the enzymatically inactive domain serves a regulatory function [75].

GGDEF or EAL domain proteins often contain additional sensory and signal transduction domains such as PAS, GAF, HAMP REC, and HTH domains [69,76,77]. It has been shown that oxygen, amino acids, electrons, and photons can modify the activity of DGC or PDE proteins. For example, PAS is a conserved protein domain involved in sensing oxygen, redox or light [78]; PleD is a GGDEF domain protein that carries the REC domain that gets phosphorylated to activate the DGC activity for c-di-GMP synthesis [79].

Many GGDEF domain proteins possess c-di-GMP diguanyl cyclase (DGC) activity, while EAL or HD-GYP domain proteins exert c-di-GMP phosphodiesterase (PDE) activity [72,80,81]. The concentration of c-di-GMP is modulated through the action of DGC and PDE respectively to synthesize and hydrolysis of c-di-GMP [82,83].

1.3.2 Regulatory mechanism of c-di-GMP

Through binding to diverse receptors or effectors, the c-di-GMP exerts a regulatory activity. The small 'effector' called PilZ domain, transcription factor or riboswitch [84-86]. The c-di-GMP-mediated regulation can occur at the level of transcription, post-transcription or post-translation, such as in the allosteric effect on cellulose synthesis or regulation of protein turnover [70]. In general, c-di-GMP is involved in positive regulation of exopolysaccharide production, biosynthesis of adhesive fimbriae and biofilm formation [58,82,87-93]. By contrast, motility is commonly negatively regulated by c-di-GMP. Various types of motility, including flagella-mediated swimming and swarming, type IV pili-mediated twitching motility are all affected by c-di-GMP [87,94]. In *S. typhimurium*, high levels of c-di-GMP generated by overexpression of the DGC AdrA inhibited swarming and swimming motility while reduction of c-di-GMP levels by overexpression of the PDE YhjH stimulated motility [95-97]. The binding of c-di-GMP to the PilZ domain protein

YcgR leads to a conformational change in the protein and consequently the c-di-GMP loaded YcgR form a complex with FliG and FliM to impair the flagella activity [85,98,99].

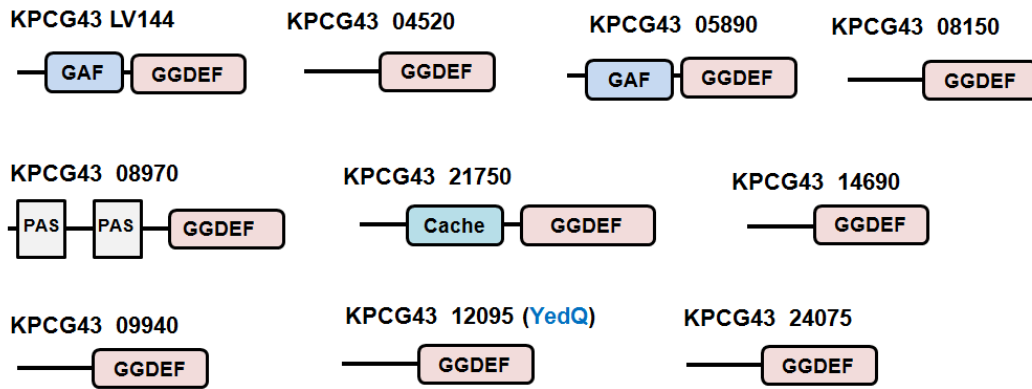
1.3.3 Role of c-di-GMP in virulence

C-di-GMP signaling is involved in regulating virulence of many bacteria which include *E. coli*, *S. Typhimurium*, *Vibrio cholerae*, *Pseudomonas aeruginosa*, *Bordetella pertussis*, *Xanthomonas campestris*, *Legionella pneumophila*, *Brucella melitensis* and *Anaplasma phagocytophilum* [75,93,98,100-105]. In *V. cholera*, downregulation of c-di-GMP levels by the PDE VieA leads to activation of cholera toxin [106]. *P. aeruginosa* c-di-GMP signaling is required for biofilm formation in chronic infection and also the acute infection phenotype [90,107,108]. The plant pathogen *X. campestris* pathovar *campestris* (Xcc) causes disease through a HD-GYP domain protein expression to regulate the production of extracellular enzymes and extracellular polysaccharide[109], and motility. In *S. typhimurium*, the EAL-domain like protein STM1344 causes resistance to oxidative stress, inhibits rapid macrophage killing and is required for virulence in the typhoid fever mouse model. Intriguingly, STM1344 has no PDE activity nor has bind activity to c-di-GMP, and hence the involvement of c-di-GMP signalling in these phenotypes remains to be investigated [110].

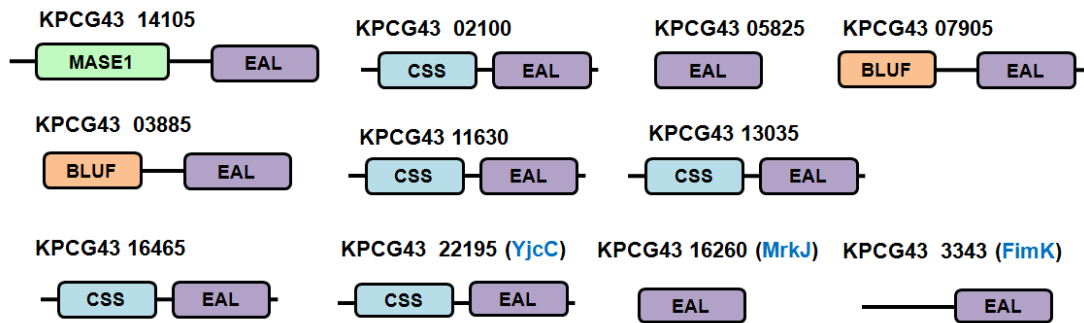
1.3.4 Domain structure of GGDEF- and EAL-protein encoding genes in *K. pneumoniae* CG43S3

GGDEF and EAL domain proteins are widespread in bacterial genomes. Very often one bacterial genome contains more than one GGDEF and EAL domain protein. The sequenced genome of *S. typhimurium* codes for 20 GGDEF/EAL domain proteins; 5 contain a GGDEF, 8 an EAL domain and 7 contain both. On the other hand, *E. coli* K-12 has 12 GGDEF, 12 EAL and 7 GGDEF-EAL domain proteins [111]. A recent study search for conserved GGDEF and EAL domains in three sequenced *K. pneumoniae* genomes revealed multiple copies of GGDEF and EAL containing proteins: 21 for *K. pneumoniae* Kp342, 18 for *K. pneumoniae* MGH 78578 and 17 for *K. pneumoniae* NTUH-K2044 [112]. The *K. pneumoniae* CG43 genome sequence has recently been resolved and the annotation results show 24 GGDEF- and EAL-domain protein encoding genes. As shown in Fig. 1.1, 10 GGDEF-, 11 EAL- and 4 GGDEF-EAL-domain protein encoding genes are identified. The sensor domains identified include MASE, CHASE, CACHE and CSS motif [113]. Genome-wide approach to study these proteins might shed light on their functional roles in different environmental settings.

(A) GGDEF domain



(B) EAL domain



(C) GGDEF-EAL domain

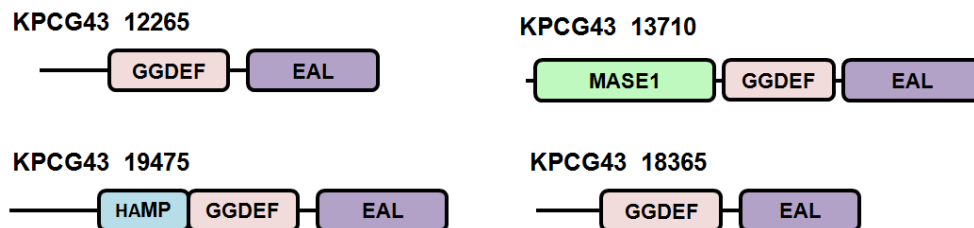


Fig. 1.1. Domain architecture of putative c-di-GMP signaling proteins encoded by the *K. pneumoniae* CG43. The genome of *K. pneumoniae* CG43 encoding (A) GGDEF, (B) EAL, and (C) GGDEF/EAL, the analysis of protein functional domain,

as indicated, was performed using the Pfam database provided online ([http://www.sanger.ac.uk /Software/Pfam/](http://www.sanger.ac.uk/Software/Pfam/)). The identities of the proteins are also shown in blue: four EAL domain proteins (YjcC, FimK and MrkJ) that have been described in *K. pneumoniae* [58,91,114,115] and (chapter 2).

1.4 Oxidative stress

The most commonly discussed oxidants that cause damage to DNA, proteins, and cell membranes and often results in cell death are the reactive oxygen species (ROS) including superoxide anion (O_2^-), hydrogen peroxide (H_2O_2), and the hydroxyl radical (HO^\cdot), and the reactive nitrogen species (RNS), which include nitric oxide (NO^\cdot) and peroxynitrite ($ONOO^\cdot$). During infection, pathogens have equipped to protect themselves from the oxidative burst of phagocytic cells and the challenging oxidative environments within cellular and extracellular compartments.

The oxygen species can be excluded from active sites by electron transfer to the redox cofactors. Reactions of this type occur by the formation of reactive oxygen species (ROS) and their subsequent inactivation of enzymes. Intracellular molecular oxygen can adventitiously abstract electrons from the exposed redox moieties of electron-transfer enzymes, thereby generating partially reduced oxygen species. A mixture of O_2^- and H_2O_2 is formed, reflecting the fact that either one or two electrons can be transferred in an oxidation event. Flavoenzymes, which is ubiquitous and

abundant, in particular are responsible for all aerobic organisms to experience a steady flux of endogenously generated oxidants [116]. The overall reaction rate is proportional to collision frequency; thus, O_2^- and H_2O_2 fluxes depend directly upon the ambient concentration of oxygen [117,118]. Several source of oxidative stress have been identified that include (a) intracellular enzyme autooxidation. In exponentially growing *E.coli*, both O_2^- and H_2O_2 are generated by the auto-oxidation of components of the respiratory chain [119]. (b) environmental redox reactions, (c) H_2O_2 released by competing microbes, (d) phagosomal NADPH oxidase and (e) redox cycling antibiotics, plants or microorganisms secrete redox-cycling antibiotics that diffuse into the competing bacteria, chemically oxidize redox enzymes and transfer the electrons to molecular oxygen [118].

1.4.1 Oxidative stress response in bacteria

The defense mechanisms, which play an important role in determining the bacterial virulence, include sensing, avoiding, and removing the oxidants. In *Escherichia coli*, superoxide is removed by SODs (SodA, SodB, SodC) [120], generating hydrogen peroxide which is then removed by catalases (KatE, KatG) and peroxidases (AhpC). The transcriptome analysis of *Pseudomonas aeruginosa* or *Staphylococcus aureus* response to H_2O_2 revealed many more genes including the

virulence genes, the genes encoding products involved in DNA repair and anaerobic metabolism were induced. Nevertheless, many of the genome-wide analysis revealed the expression of more than 100 genes were induced in responding to either H₂O₂ or paraquat indicating the complexity of the antioxidant strategies [121-123].

Many of the defenses are controlled by regulators that respond to iron (e.g., Fur), oxygen tension (e.g., FNR and ArcAB), superoxide (e.g., SoxRS), and hydrogen peroxide (e.g., OxyR). In *E. coli*, OxyR is known to regulate more than nine genes including *katG* (hydroperoxidase I), *ahpC* (alkylhydroperoxide reductase), *gorA* (glutathione reductase), *oxyS* (regulatory RNA), and *fur* that are involved directly or indirectly in the oxidative stress response. The antioxidant genes *katE*, *katG*, and *sodC* have been reported to be components of RpoS regulon. While the expression of superoxide dismutase SodA and SodB are respectively controlled by at least 3 global regulators including SoxRS, ArcAB, and Fur [124].

RpoS is a sigma factor which regulates expression of a variety of genes in both *E. coli* and *Salmonella* spp. that allows the bacteria to adapt, resist, and survive under stress condition. The deletion of *rpoS* in *V. vulnificus* was found to down-regulate the expression of *fur*, indicating a cascade regulation between the two global regulators. Fur, which is complexed with iron as an iron responsive regulator, binds to multiple sites (a 19-bp Fur box) with differential affinities to repress the transcription of genes

required for iron acquisition, acid and oxidative stress responses. However, Fur has also been demonstrated to function as a transcriptional activator for several genes including *fur* itself (*Hp* and *Vv*), and virulence associated genes [125-127].

In *K. pneumoniae* CG43, the 2CS response regulator encoding gene *kvgA* deletion was found to reduce the expression of *katG* and *sodC*. KvgAS has also been shown to be induced expression in upon treatment with 0.2 mM paraquat, which suggesting an involvement of the 2CS in oxidative stress defense in the bacteria. Moreover, we have reported in *K. pneumoniae* CG43 that *rpoS* deletion reduced the *kvgAS* expression which also showing a cascade regulation on the expression of 2CS. This suggests complex signaling networks with inter-connection regulatory circuits are required for multiple stress signal integration [128].

1.5 Transcriptome analysis

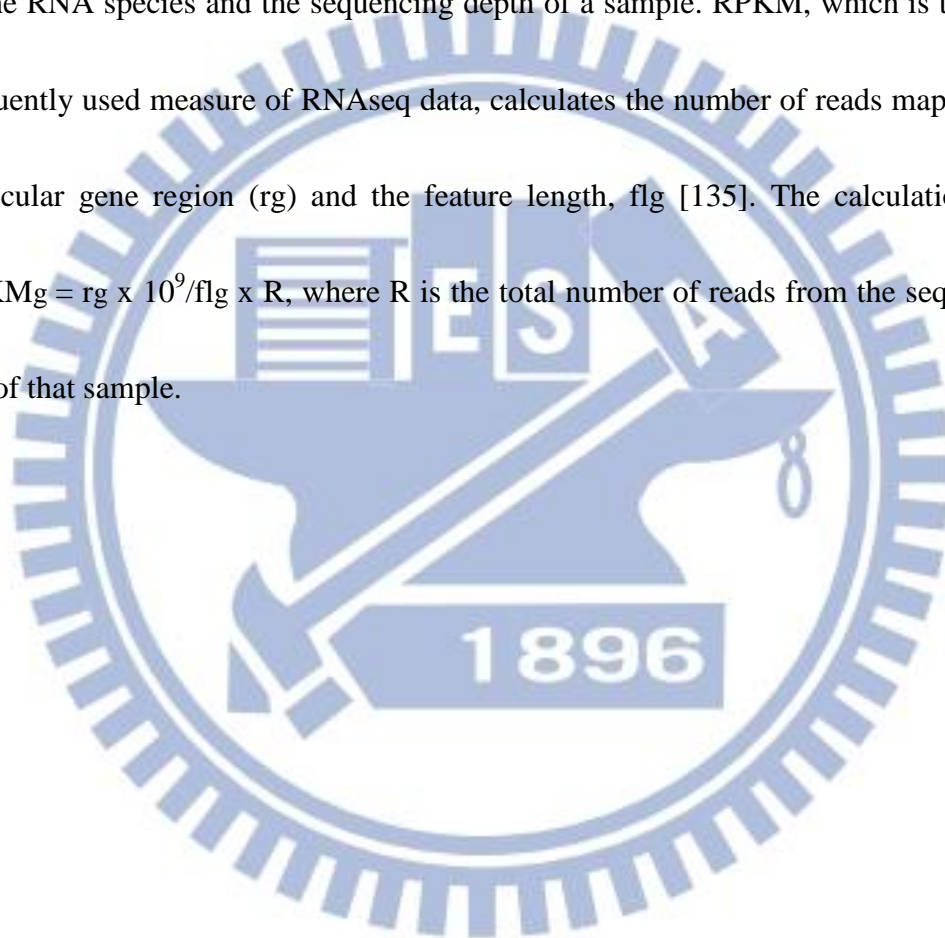
Transcriptome analysis of gene expression can be profiled by high throughput techniques including SAGE, serial analysis of gene expression [129], microarray [130], and sequencing of clones from cDNA libraries [131]. Microarrays have been the method of choice providing high throughput and affordable costs. However, the microarray technology has limitations including insufficient sensitivity for quantifying lower abundant transcripts, narrow dynamic range and non-specific hybridizations.

Sequencing-based methods such as SAGE rely upon cloning and sequencing cDNA fragments. This approach allows quantification of mRNA abundance by counting the number of times cDNA fragments from a corresponding transcript are represented in a given sample, assuming that cDNA fragments sequenced contain sufficient information to identify a transcript. The currently used RNAseq is a SAGE-based technology that allows for high-throughput analysis of transcriptomes. Its decrease in the cost allows routinely used in research, increasing application and fast development. In RNAseq method, complementary DNAs (cDNAs) generated from the mRNA of interest are directly sequenced using next-generation sequencing (NGS) technologies. The obtained reads can then be aligned to a reference genome for a whole-genome transcriptome map.

The NGS technology enables massive parallel sequencing at a reasonable cost [132,133]. Current NGS platforms include the Roche 454 Genome Sequencer, Illumina's Genome Analyzer, and Applied Biosystems' SOLiD. These platforms can analyze tens to hundreds of millions of DNA fragments simultaneously, generate giga-bases of sequence information from a single run, and have revolutionized SAGE and cDNA sequencing technology [134].

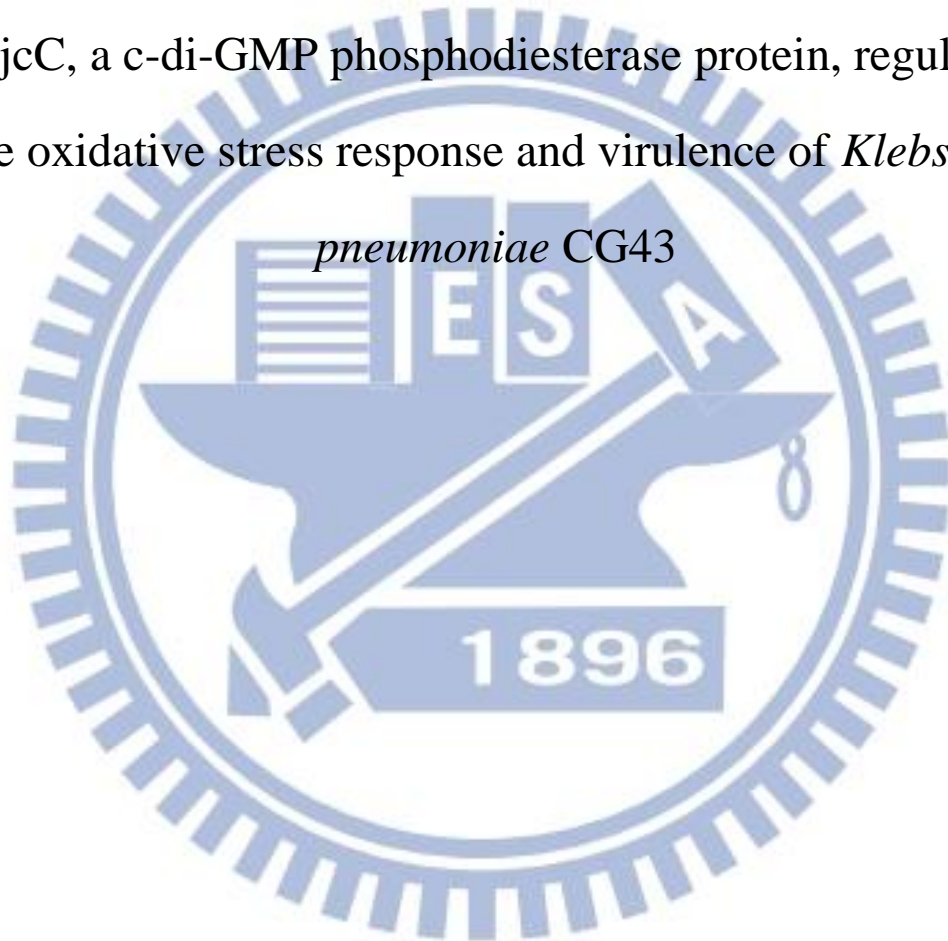
1.5.1 RPKM measure

Measures of RNA abundance are important for many areas of biology and often obtained from RNAseq using Illumina sequence data. These measures need to be normalized to remove technical biases in the sequencing approach, such as the length of the RNA species and the sequencing depth of a sample. RPKM, which is the most frequently used measure of RNAseq data, calculates the number of reads mapped to a particular gene region (rg) and the feature length, flg [135]. The calculation is as $RPKM_g = rg \times 10^9 / flg \times R$, where R is the total number of reads from the sequencing run of that sample.



Chapter 2

YjcC, a c-di-GMP phosphodiesterase protein, regulates the oxidative stress response and virulence of *Klebsiella pneumoniae* CG43



2.1. Abstract

This study shows that the expression of *yjcC*, an in vivo expression (IVE) gene, and the stress response regulatory genes *soxR*, *soxS*, and *rpoS* are paraquat inducible in *Klebsiella pneumoniae* CG43. The deletion of *rpoS* or *soxRS* decreased *yjcC* expression, implying an RpoS- or SoxRS-dependent control. After paraquat or H₂O₂ treatment, the deletion of *yjcC* reduced bacterial survival. These effects could be complemented by introducing the $\Delta yjcC$ mutant with the YjcC-expression plasmid pJR1. The recombinant protein containing only the YjcC-EAL domain exhibited phosphodiesterase (PDE) activity; overexpression of *yjcC* has lower levels of cyclic di-GMP. The *yjcC* deletion mutant also exhibited increased reactive oxygen species (ROS) formation, oxidation damage, and oxidative stress scavenging activity. In addition, the *yjcC* deletion reduced capsular polysaccharide production in the bacteria, but increased the LD50 in mice, biofilm formation, and type 3 fimbriae major pilin MrkA production. Finally, a comparative transcriptome analysis showed 34 upregulated and 29 downregulated genes with the increased production of YjcC. The activated gene products include glutaredoxin I, thioredoxin, heat shock proteins, chaperone, and MrkHI, and proteins for energy metabolism (transporters, cell surface structure, and transcriptional regulation). In conclusion, the results of this study suggest that YjcC positively regulates the oxidative stress response and mouse

virulence but negatively affects the biofilm formation and type 3 fimbriae expression by altering the c-di-GMP levels after receiving oxidative stress signaling inputs.

2.2. Introduction

During infection, pathogens protect themselves from the oxidative burst of phagocytic cells and the challenging oxidative environments within cellular and extracellular compartments. Upon exposure to oxidative stress such as tellurite, paraquat or hydrogen peroxide, *E. coli* exhibits an increase in the intracellular ROS and the content of protein carbonyl groups [136-138]. Reactive oxygen species (ROS), including superoxide anion (O_2^-), hydrogen peroxide (H_2O_2), and hydroxyl radicals (HO^\cdot), may damage DNA, proteins, and cell membranes and often lead to cell death [117,118]. The bacterial defense mechanism includes sensing, avoiding, and removing the ROS [123]. In general, SodA, SodB, and SodC remove superoxide, whereas catalases (KatE and KatG) and peroxidases (AhpC and GST) remove hydrogen peroxide [139,140]. These various stress defenses are controlled by regulators that respond to superoxide and redox-cycling drugs (e.g., SoxRS), hydrogen peroxide (e.g., OxyR), iron (e.g., Fur), or oxygen tension (e.g., FNR and ArcAB) [140-143]. Diguanylate cyclases (DGCs) and phosphodiesterases (PDEs) regulate the levels of bacterial second messenger cyclic di-GMP (c-di-GMP) by

catalyzing molecular synthesis and hydrolysis, respectively [71,81]. The regulatory roles of c-di-GMP appear in numerous bacteria in various cellular functions, including cell surface remodeling [144], cellulose synthesis [111], virulence [145], motility [107], and biofilm formation [146-148]. *E. coli* YfgF, which exhibits PDE activity, regulates not only surface cell remodeling but also the oxidative stress response by modulating c-di-GMP levels [11]. The disruption of *Salmonella enteric* Var. *typhimurium* *cdgR*, which encodes a PDE protein, also decreases bacterial resistance to hydrogen peroxide and accelerates death by macrophages [149].

Klebsiella pneumoniae pyogenic liver abscess isolates often carry heavy capsular polysaccharides (CPS) to avoid phagocytosis or death by serum factors [33,150]. This thick and viscous structure also helps regulate the bacterial colonization and biofilm formation at the infection site [151]. Several regulators, such as RcsB, RmpA, RmpA2, KvhR, KvgA, and KvhA, help control the CPS biosynthesis by regulating the *cps* transcriptions in *K. pneumoniae* [39,152]. An increase in CPS synthesis protects *K. pneumoniae* from oxidative stress [32,153,154]. However, whether the modulation of c-di-GMP affects CPS synthesis remains unclear.

The expression of *yjcC*, an IVE gene isolated from the liver abscess isolate *K. pneumoniae* CG43, is inducible in the presence of 10 μ M paraquat [115]. Sequence analysis of YjcC shows a signal peptide followed by 2 transmembrane domains and a

CSS motif at the N-terminal region, whereas the C-terminal contains a conserved EAL domain of the PDE enzyme [155]. In addition, the encoding gene *yjcC* is cluster-located with *soxRS* genes, suggesting that it plays a role in the oxidative stress response. This study investigates whether YjcC plays a role in oxidative stress defenses and if YjcC uses PDE activity to execute its regulation.

2.3. Results

2.3.1 The YjcC expression is paraquat inducible, and SoxRS and RpoS dependent

To confirm the previously reported paraquat-induced expression phenotype [115], the IVE DNA containing the 5' non-coding region and part of the coding sequence of *yjcC* was isolated from *K. pneumoniae* CG43S3 and cloned in front of the promoterless *lacZ* gene of pLacZ15 [152]. The resulting plasmid was called pP_{*yjcC1*}. The sequence analysis of P_{*yjcC1*} shows a conserved Fnr box TGTGA-N₆-TCACA [156] centered approximately 400-bp upstream of the *yjcC* start codon. This process also generated recombinant plasmids pP_{*yjcC2*} and pP_{*yjcC0*} carrying truncated forms of P_{*yjcC1*}. These plasmids respectively removed the putative Fnr box and the small stem-loop sequence of the 33-bp coding region shown in Fig.2.1 (A). As Fig. 2.1 (B) shows, the bacteria containing pP_{*yjcC1*} exhibited the highest level of β -galactosidase activity, whereas CG43S3[pP_{*yjcC2*}] had the lowest activity. In addition, the activity of P_{*yjcC1*}, but

not P_{yjcC2} nor P_{yjcC0} , increased after adding 10 μM of paraquat to the culture medium. This paraquat-induced characteristic also appeared when the concentration increased to 30 μM , further enhancing the activity of P_{yjcC1} .

As Fig. 2.1 (C) shows, the addition 30 μM paraquat to the bacterial culture significantly increased the *yjcC* mRNA level. Compared to the expression of the well-characterized stress response regulators SoxS, SoxR, RpoS, and Fnr, the *yjcC* gene expression was more responsive to paraquat than to hydrogen peroxide exposure. This study also investigates whether *yjcC* is subjected to regulation by SoxRS or RpoS. As Fig.2.1 (D) shows, the deletion of *soxR*, *soxS*, or *rpoS* reduces the *yjcC* expression, implying that SoxRS and RpoS play a positive role in *yjcC* expression.

2.3.2 YjcC plays a positive role in the oxidative stress response

Paraquat is a superoxide anion generator. Thus, the paraquat-inducible expression suggests that YjcC plays a role in the oxidative stress response. To investigate this possibility, an *yjcC* deletion mutant was generated through an allelic exchange strategy. As Fig. 2.2 (A) shows, the *yjcC* deletion mutant was more sensitive to paraquat and hydrogen peroxide when compared to the wild type bacteria *K. pneumoniae* CG43S3. The deletion effect could be complemented by transforming the *yjcC* expression plasmid pJR1 into the mutant. However, introducing the mutant pJR2,

which expresses the mutant form of YjcC with the conserved E residue of the EAL domain replaced by A or pJR3 (which carries the coding region of the YjcC EAL domain), had no complementation effect. Neither of the two EAL-domain protein encoding plasmids *pmrkJ* and *pfimK*, which carry PDE activity, could complement the *yjcC* deletion effect. These results suggest that the stress response is YjcC dependent and both the N-terminal signaling receiving region and the EAL domain of YjcC are required and specific for an oxidative stress response.

To determine if the YjcC-EAL domain exhibits PDE activity, the recombinant expression plasmid containing the DNA coding for the EAL domain of YjcC or the AAL coding region of pJR2 was constructed and overexpressed in *E. coli*, and the recombinant proteins were purified. Figure 2.2 (B) shows that the purified EAL domain protein exhibits PDE activity towards pNpp. This activity is lower than the level of the recombinant MrkJ [157], but considerably higher than the activity of the recombinant protein AAL_{*yjcC*}. As Fig.2.2 (C) shows, the c-di-GMP level of CG43S3Δ*yjcC*[pJR1] was significantly lower than those of CG43S3[pRK415], CG43S3Δ*yjcC*[pJR2], or CG43S3Δ*yjcC*[pJR3]. This suggests that YjcC in vivo functions as a PDE enzyme capable of reducing the intracellular c-di-GMP levels. The deletion of *yjcC* gene from CG43S3 increased the c-di-GMP amounts and the difference between the levels was much more apparent after the bacteria exposure to

30 μ M paraquat Fig. 2.2(D). This also suggests that YjcC is able to degrade c-di-GMP and the catalytic activity could be enhanced by oxidative stress.

2.3.3 Deletion of *yjcC* places bacteria in an oxidative stress state

As Figs. 2.3 (A) and (B) show, the deletion of *yjcC* after treatment of H₂O₂ or paraquat significantly raised the levels of the fluorescent probe H2DCFDA (used to monitor the formation of ROS) and carbonyl proteins. The introduction of pJR1 into CG43S3 Δ *yjcC* mutant appeared to reduce the levels of ROS and the carbonyl proteins, showing that YjcC is involved in the removal of ROS or damaged molecules. Thus, this study also investigates the anti-oxidant activity of YjcC. As Fig. 3C shows, the deletion of *yjcC* reduced the oxidant scavenging activity, as assessed by the absorbance change at 517 nm for the decolorization degree of the purple color, supporting the possibility that YjcC modulates anti-oxidant activity in a certain manner. Numerous studies have shown that Fur and RpoS affect and regulate numerous SODs and catalases [139,158-161]. Figure 2.3 (D) shows that zymogel analysis and total activity measurement exhibit significant changes in the SOD or catalase activity after the deletion of *fur* or *rpoS*. However, the deletion of *yjcC* has no apparent influence on SOD or catalase activity, suggesting that the YjcC-dependent anti-oxidant enzyme remains to be identified.

2.3.4 YjcC plays a regulatory role in the virulence, CPS production, biofilm formation, and type 3 fimbriae expression

YjcC, previously identified as an IVE gene product, is likely involved in infection [115]. To investigate whether YjcC is a virulence factor for the bacteria to establish infection, a mouse peritonitis model was employed. As Table 1 shows, the LD50 to Balb/c mice increased approximately 10-fold after *yjcC* deletion; introducing $\Delta yjcC$ with pJR1, but not pJR2 or pJR3, could restore the LD50. This indicates that YjcC expression at a certain stage is required for mouse infection. It is interesting to note that the $\Delta yjcC$ colony is smaller and less mucoid, as determined by a string test [39], than its parental strain on LB agar plate. Therefore, sedimentation analysis and glucuronic acid content measurement are carried out to determine the CPS production. As Fig. 2.4 (A) shows the deletion of *yjcC* reduces CPS production. The CPS deficient phenotype can be fully complemented with the transformation of pJR1 into the $\Delta yjcC$ mutant. However, transforming the mutant with pJR2 or pJR3 partially restores glucuronic acid production.

The second messenger c-di-GMP plays an important role in bacterial biofilm formation [14-16]. Figure 2.4 (B) shows that the biofilm formation activity of $\Delta yjcC$ appears to increase compared to the parental strain, whereas that transformed with pJR1 decreases biofilm formation. This can be attributed to the level changes of

c-di-GMP (Fig. 2.2 C), which indicates that the YjcC expression of pJR1 significantly reduces the c-di-GMP level, thus reducing biofilm forming activity. Moreover, type 3 fimbriae is a major determinant of biofilm formation in *K. pneumoniae* [64]. Therefore, this study also investigates the deletion effect on type 3 fimbriae expression. As Fig. 2.4 (C) shows, the western blot hybridization with anti-Mrka antibody shows that the *yjcC* deletion also increased the major pilin MrkA production of type 3 fimbriae.

2.3.5 Effects of YjcC overexpression assessed using a transcriptome study

This study uses comparative transcriptome analysis between CG43S3[pRK415] and CG43S3[pJR1] to gain further insights into how YjcC executes its regulation. Analysis of the genome annotation of liver abscess isolate *K. pneumoniae* NTHU-K2044 [112] shows that the increased expression of *yjcC* significantly enhances the expression of 34 genes. As Table 2.2 shows, the YjcC-activated genes can be categorized into 12 functional groups. These include the oxidative stress response genes *grxA*, *ybbN*, *dinI*, *priB*, and *stpA*, which are involved in anti-oxidation [162,163] or DNA repair [163], the heat shock chaperone protein encoding genes *ibpB*, *ibpA*, *htpG*, and *dnaK*, which are generally induced in stress conditions [164], and the genes coding for chaperone ClpB and PspB to protect protein from

aggregation and help maintain proton motive force (PMF) to counteract stress conditions [165,166]. Increasing the expression of *yjcC* also enhanced the expression of PilZ domain protein MrkH and the LuxR-type transcription factor MrkI. Conversely, 29 genes whose expressions were significantly repressed by the increase of YjcC expression include *fumB*, which is regulated by *fnr* under limited oxygen and anaerobic conditions [124]. Other YjcC negatively affected genes are metabolite transporter genes and genes coding for permease and energy metabolism involved in the synthesis of amino acids (Table 2.3).

As assessed by qRT-PCR analysis, Fig. 2.5 shows that the mRNA level of *mrkH* and *mrkI*, respectively increased 2.87- and 3.24-fold in CG43S3[pJR1] compared to that of CG43S3[pRK415]. In contrast, the *mrkA* transcript levels dropped to approximately 1/3 of that of CG43S3[pRK415].

2.4. Discussion

In *E. coli*, all the described genes inducible by paraquat are a part of the SoxRS regulon [167-169]. The expression of *yjcC* is RpoS-dependent in *E. coli* [170]. Consistent with this finding, the *yjcC* expression in *K. pneumoniae* is affected by RpoS and by SoxRS at the transcriptional level. No SoxRS or RpoS binding box appears within the putative promoter sequence, suggesting the possibility of an indirect control. In *E. coli*, the FNR regulator controls the transition between aerobic

and anaerobic growth at the transcriptional level [171]. The conserved *fnr* binding box present in the upstream non-coding region of *yjcC* implies an FNR dependent control of YjcC expression. Thus, the *yjcC* regulation by FNR likely occurs in poorly oxygenated environments.

The *K. pneumoniae* NTUH K2044 genome contains 27 genes encoding GGDEF-, EAL-, and GGDEF-EAL-domain proteins of potential DGC and PDE enzyme activity [172]. The *yjcC* encoding gene is also identified as member of the protein family. The family regulation specificity is determined by the sensory domain of the DGC or PDE proteins. Figure 2.2 (A) shows that the PDE expression plasmids *pfimK* and *pmrkJ*, which contain the respective coding region with putative promoter, failed to complement *yjcC* deletion. This may be due to *fimK* and *mrkJ* genes are not induced in comparison to *yjcC* in the presence of paraquat. There is also the possibility that the N-terminal peptide of approximately 300 aa of YjcC plays a role in the oxidative stress response besides signal sensing. Various sensory domains can bind to small molecular signals, and through this connection, modulate the levels of c-di-GMP [173,174]. Although the signal for the CSS-motif remains unknown, we speculate that YjcC-mediated signaling sensing may occur in the periplasmic space because of the signal peptide and the transmembrane domain at the N-terminal region. The purified recombinant EAL domain of YjcC exhibits PDE activity. However, the

amount of c-di-GMP in CG43S3 Δ *yjcC*[pJR3] is approximately the same as that in CG43S3 Δ *yjcC*[pRK415] and CG43S3 Δ *yjcC*[pJR2], suggesting that the EAL domain has extremely low levels of PDE activity. The N terminal region of YjcC likely requires receiving some signal from outside, and the interaction of the sensory domain with signaling molecules activates the PDE activity. This is supported by Fig. 2.2 (D) showing that the deletion of *yjcC* gene from CG43S3 raised the c-di-GMP levels and the influence was much more apparent after the bacteria exposure to 30 μ M of paraquat.

The deletion of *yjcC* decreases the CPS production and the virulence attenuation, indicating that YjcC is required to avoid the damage of oxidative stress. In bacteria, superoxide dismutase and catalase are common antioxidant enzymes that scavenge ROS from oxidative stress. The redox proteins (including GrxA and YbbN) required for maintaining redox status in bacteria are also protect bacteria from oxidative stress [175,176]. The deletion of *yjcC* has no apparent effect on the SOD and catalase activity, but appears to increase the transcription of *grxA* and *ybbN*. This suggests that YjcC is involved in regulating the redox levels in bacteria after oxidative stress. The chaperone protein ClpB stabilizes protein and suppresses the protein aggregation induced by heat or other stresses [165,177]. The phage shock proteins, PspB and PspC, act as positive regulators to transduce stress signal(s) to PspA through protein–protein

interaction, maintaining the proton-motive force under extracytoplasmic stress conditions [166]. Transcriptome analysis shows that an increase in YjcC induces the expression of several heat shock proteins and chaperones, suggesting that YjcC is involved in regulating anti-stress responses. The fumarase gene *fumB*, which is expressed under anaerobic cell growth conditions, is regulated by Fnr and ArcA [178,179]. The result of *yjcC* expression reduced the *fumB* transcripts implies that YjcC is a component of the Fnr and ArcA regulatory pathway.

In *K. pneumoniae*, the second messenger c-di-GMP activates type 3 fimbriae expression through MrkHI activation [146]. However, the increased synthesis of *mrkH* and *mrkI* transcripts by the overexpression of *yjcC* remains unclear. We have found that *mrkHI* expression is barely detected under LB culture (unpublished observation). Under oxidative stress pressure, the N-terminal region of YjcC may turn on the expression of MrkHI. Thus, the N-terminal region likely plays a determinant role in YjcC-dependent regulation. *E. coli* YdeH has c-di-GMP cyclase activity [180]. The transcriptome analysis as shown in Table S3 revealed that the transcript levels of *mrkA*, *mrkH*, and *mrkI* in CG43[pRK415-*ydeH*], with c-di-GMP level of 23.1 fmole/mg⁻¹ (data not shown), significantly increased compared to those of CG43S3[pJR1]. This also indicates that *mrkHI* expression is c-di-GMP level-dependent and the N-terminal part of YjcC plays a positive regulatory role in the expression of *mrkHI*.

Overall, these results indicate that the YjcC-mediated regulatory system is considerably more complex than expected. During infection, the transition from aerobic to microaerobic conditions or the transition from a microaerobic to oxidative stress environment, YjcC may be activated through sensory regulatory systems on the N-terminal region. Thereafter, YjcC modulates the levels of c-di-GMP to affect the expression of the downstream regulatory pathways. In conclusion, YjcC regulates the oxidative stress response, mouse virulence, CPS synthesis, biofilm formation, and type 3 fimbriae expression. This most likely occurs through the adjustment of c-di-GMP levels after receiving outside signals.

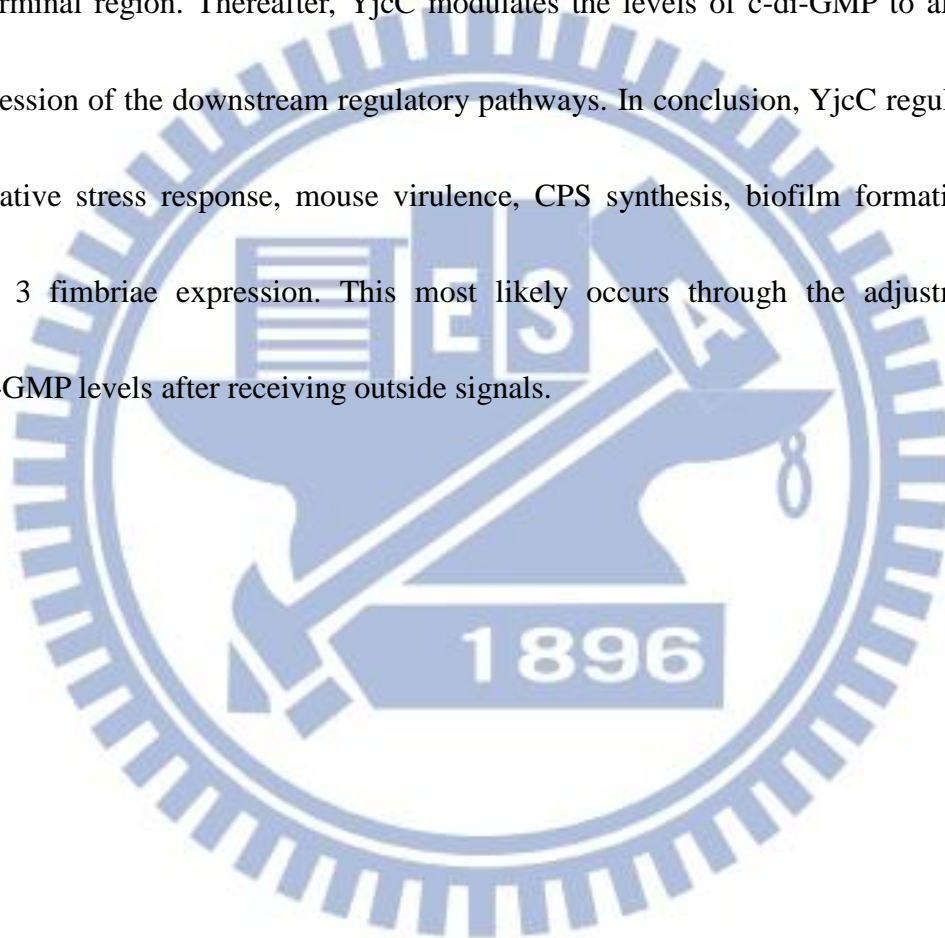


Table 2.1. YjcC effect on the mouse virulence.

Strain	LD50
CG43S3	1x10 ⁴
CG43S3ΔyjcC	7.8 x10 ⁵
CG43S3ΔyjcC [pJR1]	3.3 x10 ⁴
CG43S3ΔyjcC [pJR2]	1.1 x10 ⁶

The tested bacterial strains CG43S3, CG43S3ΔyjcC, CG43S3ΔyjcC[pJR1] and CG43S3ΔyjcC[pJR2] were cultured in LB medium at 37°C for overnight.

Five mice of a group were injected intraperitoneally with bacteria resuspended in 0.2 ml of saline in 10-fold steps graded doses. The LD₅₀, based on the number of survivors after one week, were calculated by the method of Reed and Muench [215] and expressed as CFU.

Table 2.2 Significantly upregulated genes by *yjcC* overexpression

Proposed function	Gene name	Fold ^a expression	ORF ^b ID
Oxidative response/repair/sos responsive			
Glutaredoxin I	<i>grxA</i>	2.6	KP1_1843
Thioredoxin	<i>ybbN</i>	2.4	KP1_1349
DNA damage inducible protein I	<i>dinI</i>	2.1	KP1_2061
Heat shock response/chaperones/protein modification			
Heat shock protein	<i>ibpB</i>	5.9	KP1_5467
Heat shock protein	<i>ibpA</i>	5.6	KP1_2622
Heat shock protein 90	<i>htpG</i>	2.9	KP1_1331
Heat shock protein 70	<i>dnaK</i>	3.5	KP1_0835
Protein disaggregation chaperon	<i>clpB</i>	3.2	KP1_4170
Phage shock protein B	<i>pspB</i>	2.1	KP1_2344
Ci-di GMP metabolite			
EAL containing protein	<i>yjcC</i>	6.3	KP1_0324
PilZ domain protein	<i>mrkH</i>	3.2	KP1_4551
Energy/intermediary metabolism			
Carbamoyl phosphate synthase	<i>carA</i>	3.2	KP1_0853
Ascorbate specific PTS family enzyme		3.1	KP1_2793
D-arabinitol dehydrogenase		2.9	KP1_3760
Allulose-6-phosphate 3-epimerase		2.3	KP1_2791
Xylulokinase		2	KP1_3759
Transporter			
ABC transporter ATP-binding protein		2.5	KP1_5267
Putative transport protein/kinase	<i>ydjN</i>	2	KP1_2272
Amino acid biosynthesis			
Sulfate adenylate transferase subunit 2	<i>cysD</i>	2.4	KP1_4384
Nucleotide biosynthesis and metabolism			
Methionine sulfoxide reductase A	<i>msrA</i>	2.5	KP1_0489
DNA replication/recombination/repair			
Primosomal replication protein N	<i>priB</i>	2.1	KP1_0469
DNA binding protein, nucleoid associated	<i>stpA</i>	2.6	KP1_4260
Cell surface structures			
Prepillin peptidase dependent protein		2.6	KP1_0311
Two component system connector	<i>ycgZ</i>	2.6	KP1_1728
Pullulanase-specific type II secretion system outer membrane lipoprotein	<i>pspD</i>	2.3	KP1_0998
Regulators			
LysR family transcriptional regulator		2.8	KP1_4352
Transcriptional activator	<i>nhaR</i>	2.1	KP1_0838
LuxR family regulatory protein	<i>mrkI</i>	2.6	KP1_4552
Hemolysin modulating protein	<i>hha</i>	2.6	KP1_1317
Transcriptional antiterminator of glycerol uptake operon		2.1	KP1_1112
DNA binding transcriptional activator	<i>pspC</i>	2.1	KP1_2344
Hypothetical proteins			
ParB family protein HP		3.3	KP1_2152
formylglycine generating sulfatase		2.6	KP1_3378

Table 2.3. Significantly downregulated genes by *yjcC* overexpression

Proposed function	Gene name	Fold ^a expression	ORF ^b ID
Anaerobic response protein			
Anaerobic class I fumarate hydratase	<i>fumB</i>	-5.7	KP1_2562
Transporter			
Alanine/serine/glycine transport protein		-6.8	KP1_2505
ABC transport system ATP binding protein		-4.5	KP1_3173
PTS transporter subunits II ABC		-5.0	KP1_3804
Methylgalactoside transporter inner membrane component	<i>mglC</i>	-4.8	KP1_0277
Methylgalactoside transporter system Substrate-binding component	<i>mglB</i>	-4.2	KP1_3815
Putative ABC transport system component		-4.6	KP1_3175
Molybdate ABC transporter system		-4.4	KP1_3995
Maltose/maltodextrin transporter ATP binding protein	<i>malK</i>	-4.2	KP1_0276
Sugar ABC transport system permease component		-4.1	KP1_1424
Putative ABC transporter	<i>mocB</i>	-3.7	KP1_1423
Putative rhizopine uptake ABC transporter	<i>proY</i>	-3.7	KP1_1422
Permease			
Putative PTS permease		-6.5	KP1_0760
Putative amino acid permease		-4.3	KP1_1204
Amino acid biosynthesis			
Arginine succinyltransferase		-4.5	KP1_2499
Acetylornithine transaminase		-5.0	KP1_2498
Putative glutamine synthetase		-3.3	KP1_2006
Energy/intermediary metabolism			
Succinate antiporter		-6.4	KP1_2563
Succinylarginine dihydrolase		-5.3	KP1_2502
Glucosamine-fructose-6-phosphate aminotransferase		-6.0	KP1_0764
NADH: flavin oxidoreductase		-5.8	KP1_2565
Phospho-beta glucosidase		-5.2	KP1_3803
Acetyl-CoA synthetase	<i>asc</i>	-4.3	KP1_0342
Succinylglutamate desuccinylase	<i>astE</i>	-4.0	KP1_2256
Phosphomannosemutase	<i>manB</i>	-3.4	KP1_3702
Putative monooxygenase subunit		-3.1	KP1_1996
Putative acid phosphatase		-3.1	KP1_3725
Regulators			
DNA binding transcriptional repressor	<i>lldR</i>	-4.5	KP1_5297
Cell surface structures			
Maltoporin	<i>lamB</i>	-4.8	KP1_0277

Table2 and 3. Significantly upregulated and downregulated genes by YjcC overexpression. The selected genes show more than 2 log₂ fold change (in absolute value) in the abundance of transcript between *K. pneumoniae* CG43S3[pRK415] and

CG43S3[pJR1]. ^a Log₂ fold change represents the log₂ ratio of mRNA transcript levels of CG43S3[pJR1] to CG43S3[pRK415]. ^b Open reading frame (ORF) ID is as annotated from *K. pneumoniae* NTUH K2044.

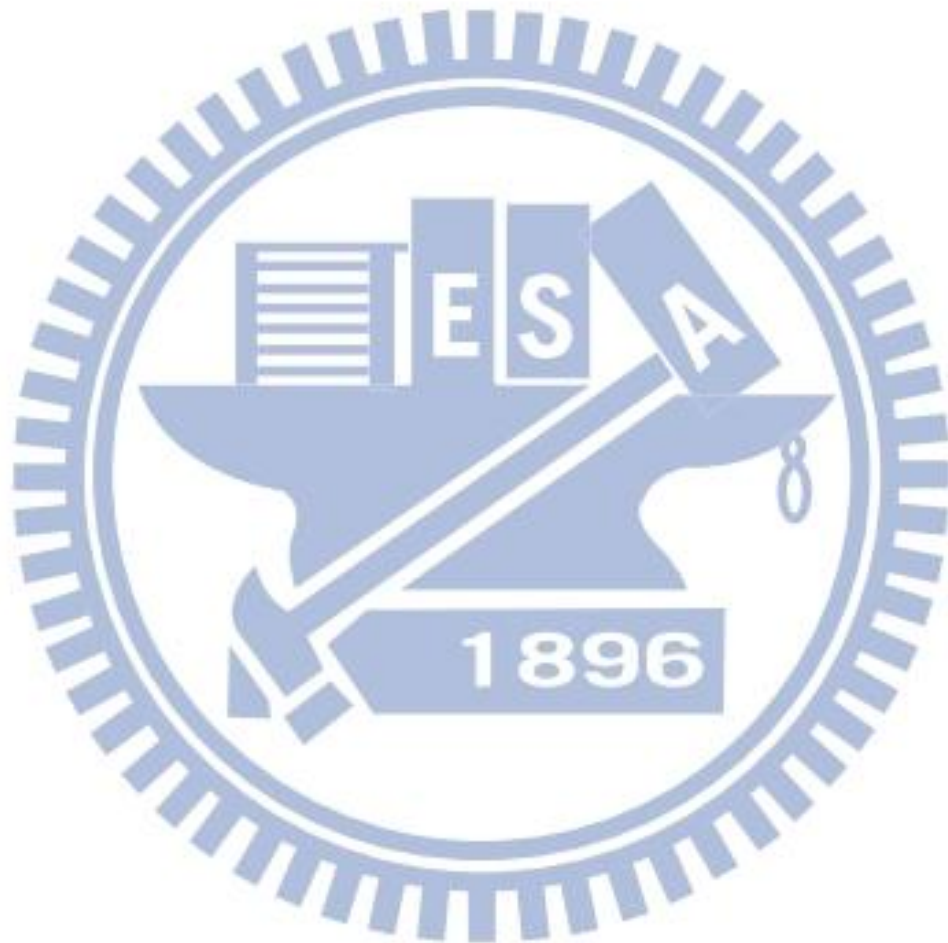
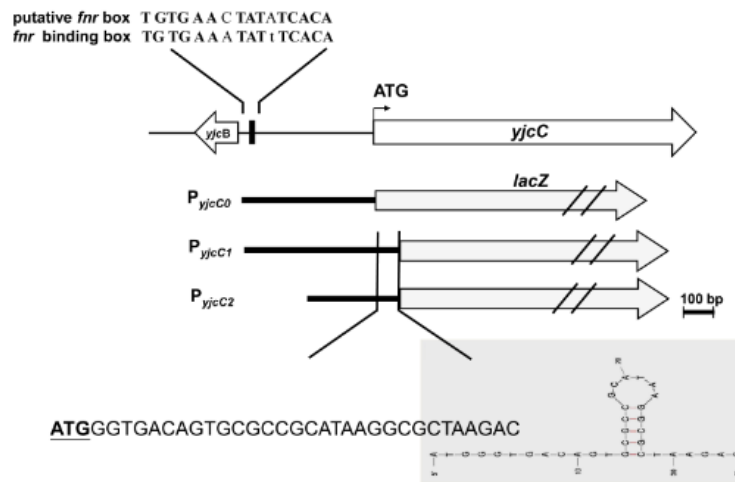


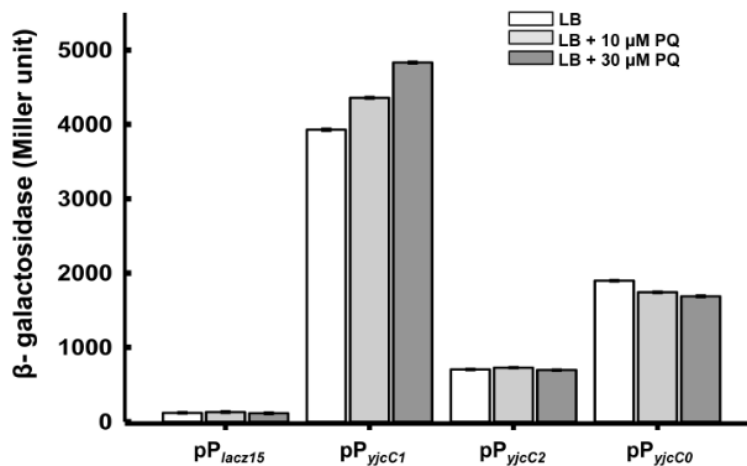
Fig. 2.1. The *yjcC* is paraquat inducible, and *SoxRS* and *RpoS* dependent.

(A)



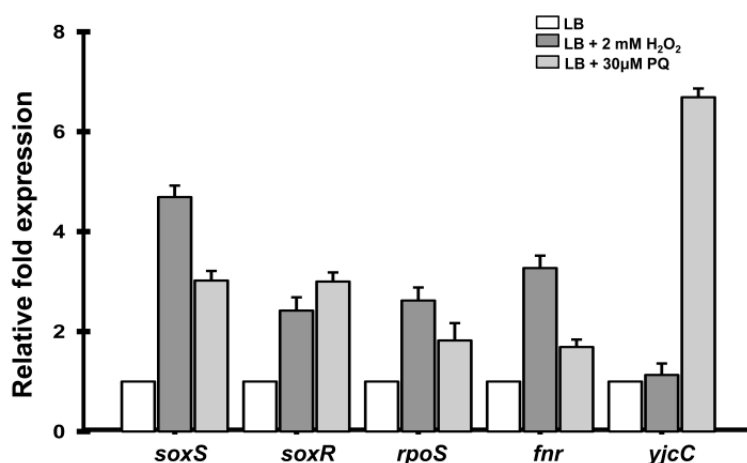
(A) The putative promoters respectively containing 525 bp (P_{yjcC1}), 385 bp (P_{yjcC2}) and 415 bp (P_{yjcC0}) of *yjcC* were isolated and cloned into the LacZ reporter plasmid *placZ15*.

(B)



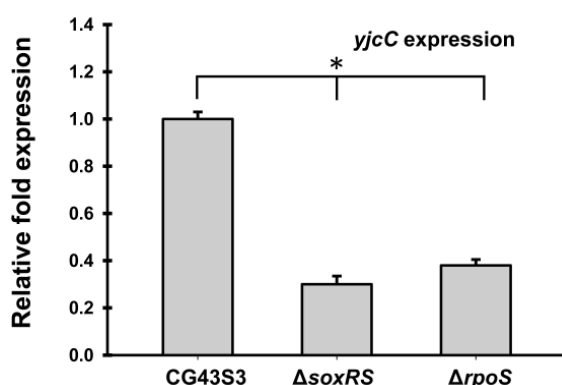
(B) The recombinant plasmids *placZ15*, pP_{yjcC1} , pP_{yjcC2} and pP_{yjcC0} were then transformed to *K. pneumoniae* CG43Z01 and the β -galactosidase activities of the transformants grown to log-phase in LB broth were determined. The results are shown as an average of triplicate samples. Error bars indicate standard deviations.

(C)



(C) Total RNA of *K. pneumoniae* CG43S3 was isolated after the bacteria were grown in 2 mM H₂O₂ or 30 μM of paraquat. Specific primer pairs used to detect the expression of *soxR*, *soxS*, *rpoS*, and *yjcC* are listed in Table 5.2. Relative fold expression was compared with the non-induced condition and determined by the 2^{-ΔΔCt} method [207]. Error bars indicate standard deviation of the mean. Data are representative of three independent experiments.

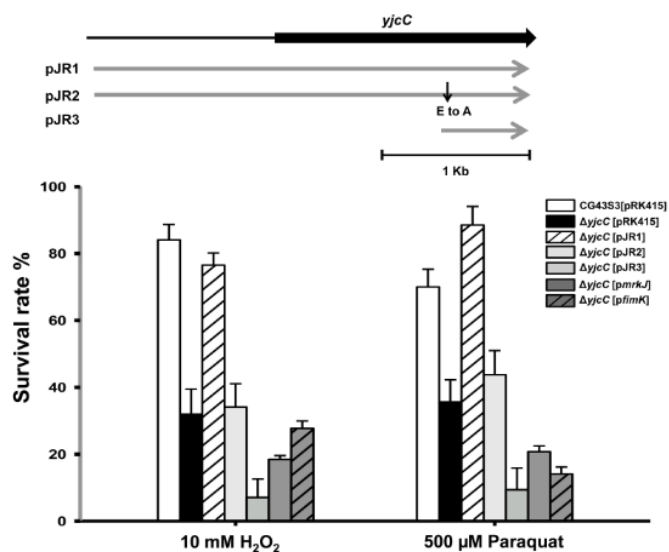
(D)



(D) The expression of *yjcC* was determined in Δ*soxRS* and Δ*rpoS* mutant by qRT-PCR. Data are representative of three independent experiments, *, P < 0.001.

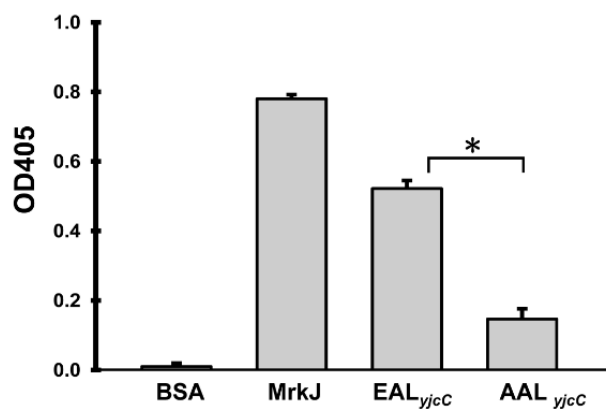
Fig. 2.2. Analysis of the deletion effects of *yjcC* upon exposure to oxidative stress.

(A)



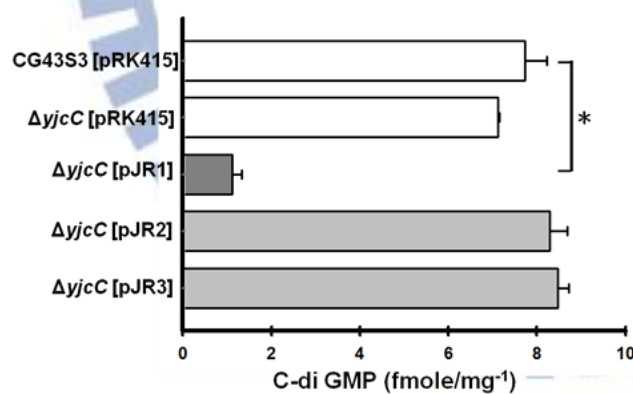
(A) Diagrammatic depiction of the YjcC complementation plasmids is shown in the upper panel. The plasmid pJR2 is identical to pJR1 except that the E residue was replaced with A by site directed mutagenesis. The plasmid pJR3 carries only the EAL domain region of YjcC. Overnight cultures were collected and refreshed grown in LB until OD₆₀₀ reached 0.6-0.7. 500 μM paraquat or 10 mM H₂O₂ was then added and the cultures continued for 35 min and finally the cultures plated onto LB plates for colony formation.

(B)

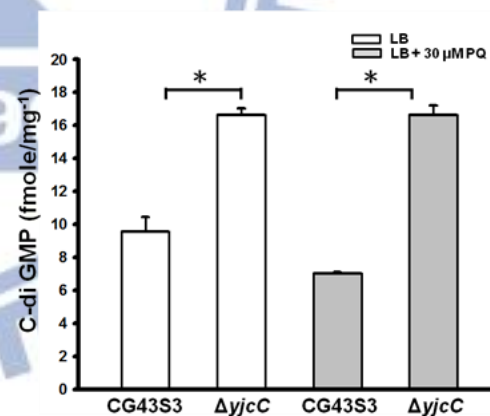


(B) The phosphodiesterase activity of purify recombinant MrkJ protein, YjcC-EAL domain and YjcC-AAL domain proteins. BSA was used as a negative control. The activity is demonstrated using bis (pNpp) as substrate by the release of p-nitrophenol.

(C)



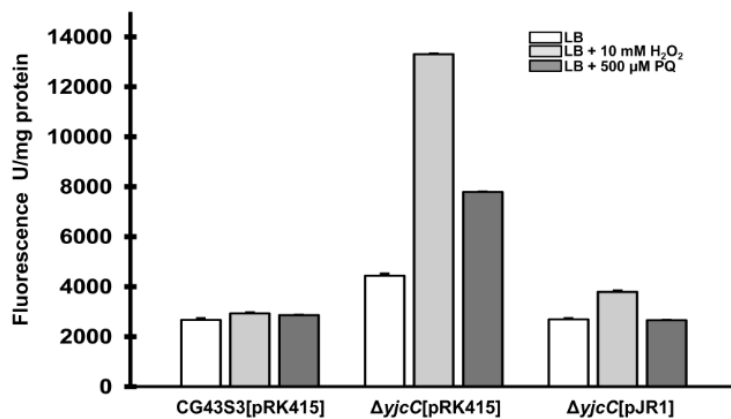
(D)



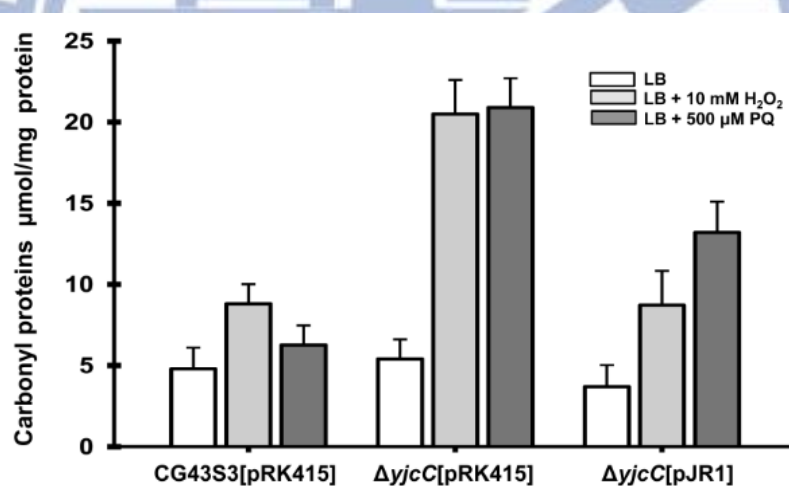
(C), (D) Quantification of the c-di-GMP levels in *K. pneumoniae* CG43S3 using the ELISA kit according to the manual (Wuhan EIAab Science Co., Ltd). Three independent experiments were performed for the measurement Error bars shown are standard deviations, and asterisks indicate the differences with a statistical significance, $P < 0.001$.

Fig. 2.3. Deletion of *yjcC* places bacteria in an oxidative stress state.

(A)

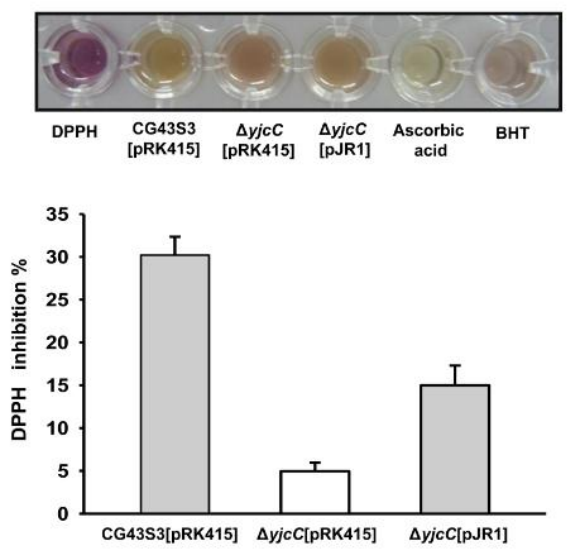


(B)



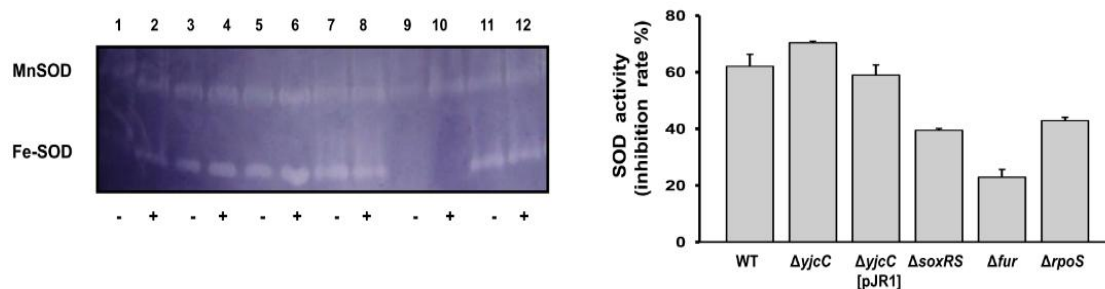
(A) Cytoplasmic ROS content determination. (B) The oxidation determination of the cytoplasmic proteins and membrane lipids. The log-phased bacteria *K. pneumoniae* CG43S3[pRK415], $\Delta yjcC$ [pRK415] and $\Delta yjcC$ [pJR1] were exposed to 500 μ M paraquat or 10 mM H₂O₂ for 40 min and the intracellular peroxide levels and the carbonyl groups were determined. Bars represent standard deviations (n= 4).

(C)

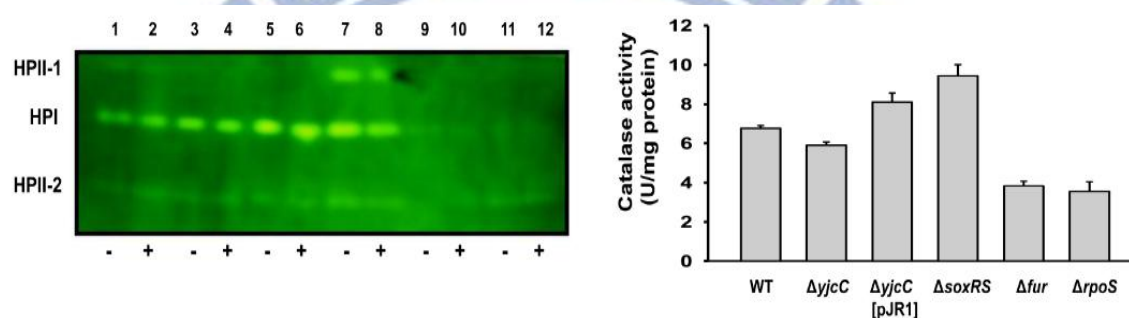


(C) The DPPH radical scavenging activity measurement. The upper panel shows that, correlating with the antioxidant activity, the color of DPPH gradually changes from purple to yellow. Ascorbic acid and Butylated hydroxytoluene (BHT) were used as positive control. The lower panel shows quantitative measurement of the DPPH scavenging activity of the log-phased bacteria *K. pneumoniae* CG43S3[pRK415], $\Delta yjcC$ [pRK415] and $\Delta yjcC$ [pJR1]. Bars represent standard deviations (n= 4).

(D)



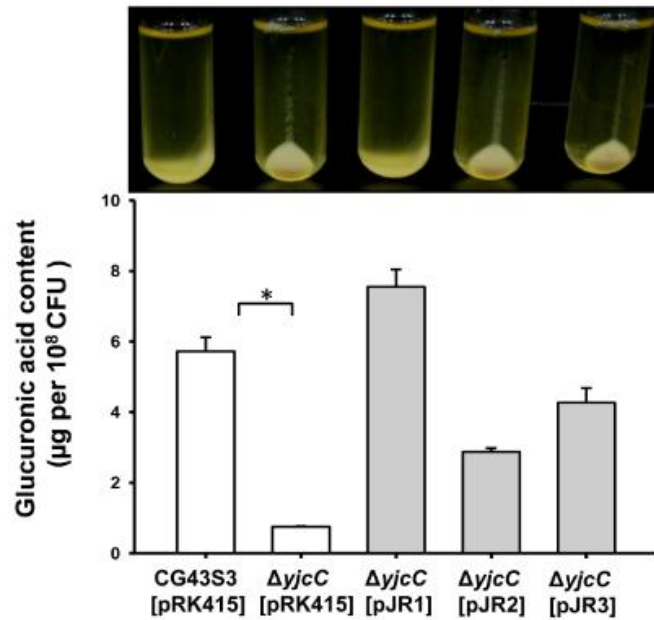
(E)



(D) SOD and (E) catalase activity determination as described in Materials and Methods. Left panels, in gel staining for the activity of Mn-SOD and Fe-SOD (D) and catalase HPI and HPIIs (E); Lanes 1, 2: CG43S3; 3, 4: $\Delta yjcC$; 5, 6: $\Delta yjcC$ [pRK415-pJR1]; 7, 8: $\Delta soxRS$; 9, 10: Δfur ; 11, 12: $\Delta rpoS$. Lanes 1, 3, 5, 7, 9, and 11 are protein extracts of the bacteria with no stress treatment; 2, 4, 6, 8, and 10 are protein extracts of the bacteria with paraquat. Right panels, quantitative measurement of the total SOD (D) and catalase activity (E).

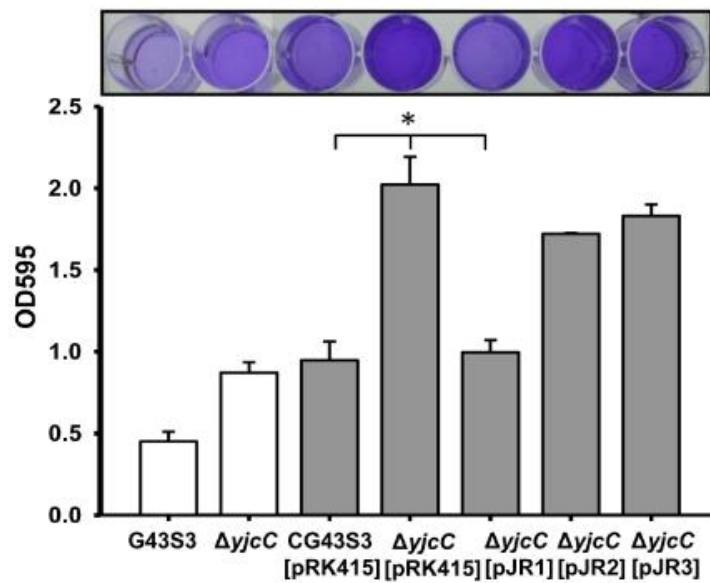
Fig. 2.4. YjcC affects the CPS biosynthesis, biofilm formation and MrkA production.

(A)



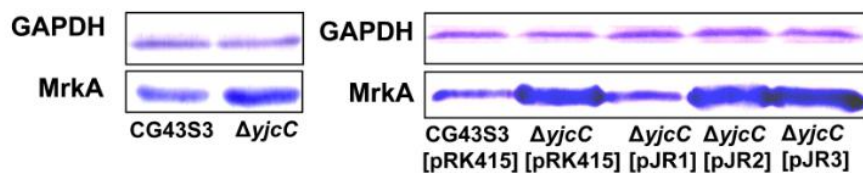
(A) Sedimentation analysis (upper panel) and glucuronic acid content measurement (lower panel). Bacteria were grown overnight in LB broth at 37°C and subjected to centrifugation at 4000 rpm for 5 min. The glucuronic acid contents are expressed as the average of the triplicate samples. Error bars indicate standard deviations. *, $P < 0.001$ compared to the parental strain CG43S3 ($n \geq 3$). Biofilm formation as assessed using crystal violet staining (upper panel) and spectrometry (lower panel).

(B)



(B) Bacteria were grown at 37°C in polystyrene plates for 24 h, the sessile bacteria stained with crystal violet, and then the stained cells eluted with 95% ethanol. *, $p < 0.001$. Data are representative of three independent experiments (triplicate in each experiment).

(C)



(B) Western blotting analysis for the expression of MrkA. Bacteria were grown overnight at 37°C with agitation in LB broth, and then total proteins extracted for western blot analysis. GAPDH was probed as a protein loading control.

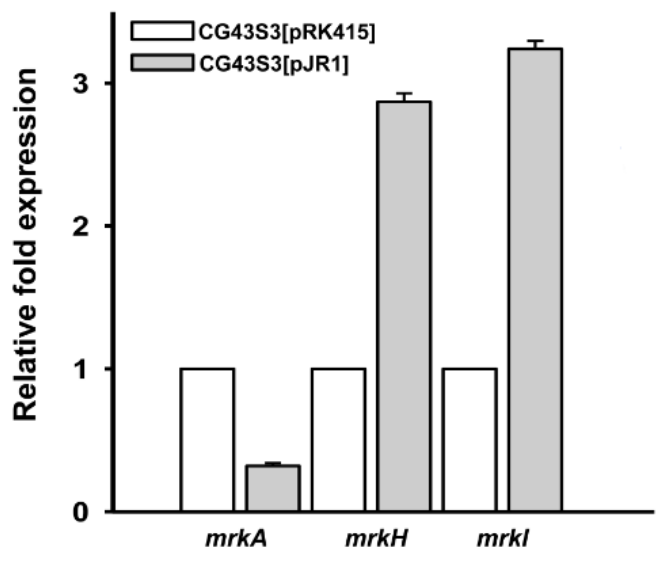
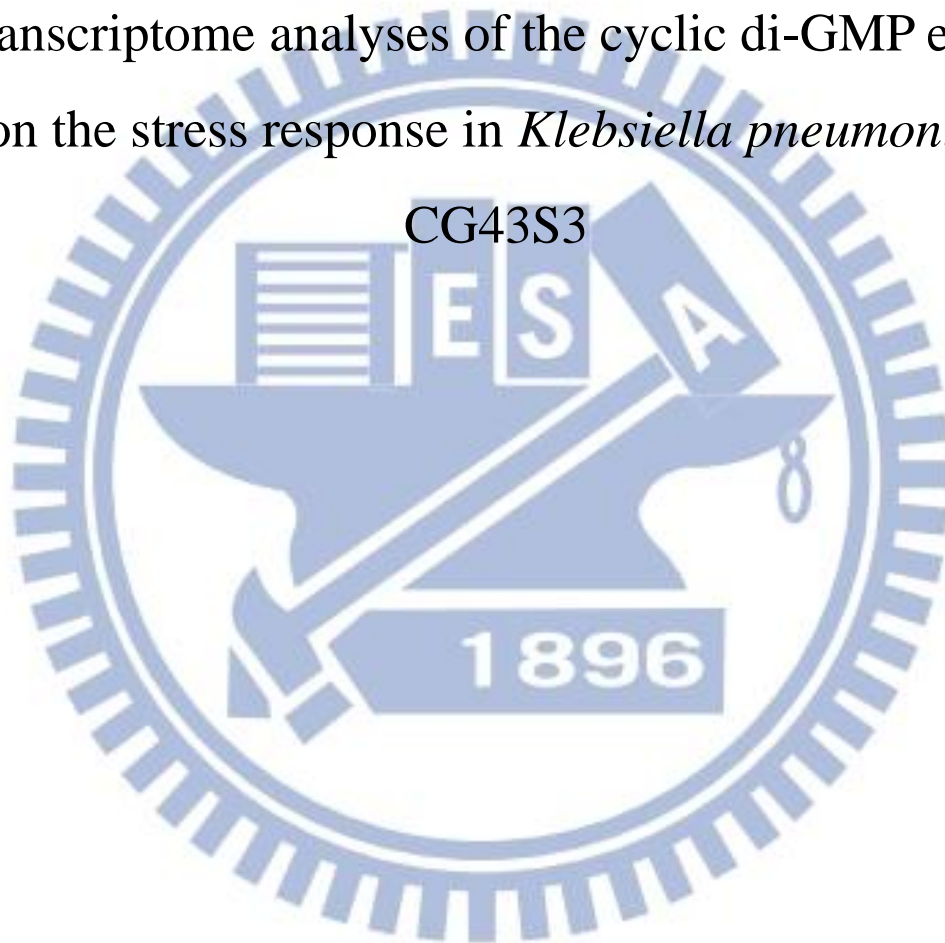


Fig. 2.5. qRT-PCR analysis of the expression of *mrkA*, *mrkH*, and *mrkI*. Total RNA of *K. pneumoniae* CG43S3[pRK415] and CG43S3[pJR1] were isolated after the bacteria were grown overnight in LB supplemented with 12.5 μ g/ml tetracycline. Specific primer pairs used to detect the expression of *mrkA*, *mrkH*, and *mrkI* are listed in Table S2. Relative fold expression was compared with the non-induced condition and determined by the $2^{-\Delta\Delta Ct}$ method. Error bars indicate standard deviation of the mean. Data are representative of three independent experiments.

Chapter 3

Transcriptome analyses of the cyclic di-GMP effect
on the stress response in *Klebsiella pneumoniae*

CG43S3



3.1 Abstract

A comparative transcriptome analysis via RNA sequencing is employed to determine if the second messenger cyclic di-GMP plays a role in the pathogenesis of *Klebsiella pneumoniae*-associated liver abscess. The analysis reveals 94 upregulated (>1.5-fold change) and 154 downregulated genes (< 2-fold change) with the increased production of diguanylate cyclase YdeH in *K. pneumoniae* CG43S3, a liver abscess isolate. The significantly activated genes included KP_0384 (*perA*), KP1_0385 (*perC*), *ibpA*, *ibpB* for heat shock response, *pspB* and *pspD* for phage shock response, and *mrkABCDF* and *mrkHIJ* respectively for type 3 fimbriae expression and the fimbrial regulation. Quantitative PCR analysis has been performed to validate the up-regulated genes which include *ibpA*, *clpB*, *dnaK*, *grxA*, *dinI*, *mrkA*, *mrkH* and *mrkI*. Compared to CG43S3[pRK415], the bacteria CG43S3[pRK415-*ydeH*] had increased the c-di-GMP levels and also the heat shock stress response, while decreased the acid stress and oxidative stress survivals.

3.2 Introduction

During the last decade, *K. pneumoniae* causing community-acquired primary pyogenic liver abscess (PLA) has become an emerging disease which receiving increasing attention. Many studies on the PLA pathogenesis have been reported [181-185], however, no conclusive points could be presented. The bacterial second

messenger c-di-GMP is a global signaling molecule that has been shown to influence a lot of physiological activity [186-188]. In recent year, its regulation on the stress response has been reported such as *E.coli* K12 YfgF, *S. Typhimurium* STM1344 in oxidative stress response[110,144], anti-toxin *mqsA* resistance of *E. coli* in acid stress[189], and *V. cholera* HapR in the stress response regulation [190]. However, c-di GMP regulation on the heat shock stress response has not been reported yet.

In the liver abscess isolate *K. pneumoniae* CG43, c-di-GMP has been shown as an effector for the expression of the PilZ domain protein MrkH and also the type 3 fimbriae expression [191]. Here we examine the effect of increasing c-di-GMP levels by transforming into *K. pneumoniae* CG43 with *E. coli ydeH*, which encodes a GGDEF domain protein and has been shown a high DGC activity [180,192]. A comparative transcriptome analysis of CG43S3[pRK415] and CG43S3[pRK415-*ydeH*] using RNA-seq approach is then carried out in order to identify the genes responding to c-di- GMP regulation.

3.3 Results

3.3.1 The *ydeH* expression increased the c-di-GMP levels and biofilm formation

As shown in Fig.3.1A, the intracellular c-di-GMP content is increased 2.4-fold by the introducing the *ydeH* expression plasmid pRK415-*ydeH* into CG43S3. The biofilm forming activity analysis also supports the c-di-GMP mediated effect which is

to increase the biofilm formation activity (Fig. 3.1B). The results confirmed that the GGDEF domain protein YdeH carries a c-di-GMP DGC activity.

3.3.2 Up-regulated genes and down-regulated genes by the increase of c-di-GMP levels

The comparative transcriptome analysis, on the basis of the genome annotation of *K. pneumoniae* NTHU-K2044 which is also a liver abscess isolate [112] revealed 19 genes significantly upregulated (> 2.3 fold expression) and 31 genes downregulated (< 4 fold expression). As shown in Table 3.1, the transcript levels of KP1_0384, KP1_0385, heat shock protein encoding genes *ibpA*, *ibpB*, *clpB* and *psp* as well as *mrkH* and *mrkABCDF* are increased. By contrast, the downregulated genes include many metabolite transporters and permease (Table 3.2).

3.3.3 qRT-PCR analysis validates the c-di-GMP dependent expression manner

In order to confirm the RNAseq data, we have selected 8 genes including *mrkA*, *mrkH*, *mrkI*, *grxA*, *ibpA*, *ibpB*, *clpB*, and *dnaK* for qRT-PCR analysis. Fig.3.2 shows *mrkA* and *dnaK* transcript levels are respectively increased 3.0 and 3.5 fold by the increasing levels of c-di-GMP, other transcripts are increased at least 1 fold compared to wild type.

3.3.4 Increased c-di-GMP level upregulates the heat shock stress response but downregulated the response to acid stress or oxidative stress

The transcriptome analysis implies a c-di-GMP dependent regulation of the stress response. The survival analysis against the stresses including heat (50°C), acid (pH 3), and oxidants (H₂O₂) revealed the increased c-di GMP level increased the heat shock survival rates but reduced the survival rates after bacteria exposure to 10 mM H₂O₂ or acid (Fig.3.3).

3.4 Discussion

In addition to *mrkABCDF*, *mrkHI*, and the stress response genes, the up-regulated genes also include KP1_0384 (*perA*) and KP1_0385 (*perC*) both coding for transcription factors. For enteropathogenic *E coli*, *perA* gene is a transcriptional activator carried by the virulence related *perABC* operon [193-196].

Gene annotation analysis of the CG43 genome revealed only *perA* and *perC*, implying *per* operon may play different role in regulation of the virulence in *K. pneumoniae*. The *dnaK* transcript which is significantly increased by the increase of c-di-GMP level encodes a molecular chaperone important for protein protection against stress [197,198]. The protein quality maintenance is essential for bacteria under exposure to stresses and therefore DnaK is extremely important for bacterial survival in harsh environment such as the infection site in the host body. Interestingly, phage shock related genes are also induced expression by c-di-GMP induced (Table 3.1). This implies the c-di-GMP level changes may be related to the bacterial resistance

to phage infection or to maintain the lysogenic state [199-201].

Table 3.1 and 3.2 Up-regulated genes and down-regulated genes from the comparison of CG43S3[pRK415-*ydeH*] and CG43S3[pRK415]

Proposed function	Gene name	Fold ^a expression
heat shock chaperone IbpB	IbpB	6.17
PerC transcription regulator ,Transcriptional activator of <i>eaeA/bfpA</i> expression in enteropathogenic E.coli	KP1_0385	6.12
mrkH, pilZ domain	KP1_4551 (mrkH)	5.84
heat shock chaperone IbpA	ibpA	4.81
mrkB	mrkB	4.79
multiple drug resistance protein MarC	KP1_2622	4.61
mrkA	<i>mrkA</i>	4.48
mrkI	KP1_4552(mrkI)	4.17
mrkJ, EAL domain protein	KP1_4554 (mrkJ)	4.03
mrkC	mrkC	4.02
mrkF	mrkF	3.98
transcriptional antiterminator of glycerol uptake operon	KP1_1112	3.92
putative phospho-2-dehydro-3-deoxyheptonate aldolase	KP1_1114	3.38
sulfate/thiosulfate transporter subunit	<i>cysA</i>	3.32
putative L-xylulose kinase	<i>lyx</i>	3.25
putative oxidoreductase protein	KP1_1109	3.20
molecular chaperone DnaK	<i>dnaK</i>	3.14
mrkD	mrkD	3.13
3-ketoacyl-ACP reductase	<i>fabG</i> (NC_012731 1083687..1084494)	3.08
putative lactose/cellobiose-specific PTS family enzyme IIB component	KP1_5424	3.07
ABC transporter ATP-binding protein	KP1_5267	3.05
protein disaggregation chaperone	<i>clpB</i>	3.02
recombination and repair protein	<i>recN</i>	2.98
DNA-damage-inducible protein I	<i>dinI</i>	2.97
LuxR transcription factor	KP1_0384	2.94
putative acyltransferase	KP1_5452	2.80
putative enzyme	KP1_3482	2.74
sulfate adenylyltransferase subunit 2	<i>cysD</i>	2.69
thiosulfate transporter subunit	<i>cysP</i>	2.62
putative methyltransferase	KP1_1106	2.60
siroheme synthase	<i>cysG</i> (NC_012731 4204327..4205743)	2.59
bifunctional putative transport protein/putative kinase	<i>ydjN</i>	2.50
phage shock protein B	<i>pspB</i>	2.49
putative thioredoxin protein	<i>ybbN</i>	2.47
Glutaredoxin I	<i>grxA</i>	2.45
DNA binding protein, nucleoid associated	<i>htpG</i>	2.43
carbamoyl phosphate synthase small subunit	<i>carA</i>	2.41
PTS system, galactitol-specific IIC component	KP1_1108	2.39
peripheral inner membrane phage-shock protein	<i>pspD</i>	2.36

Table 3.2 downregulated

Proposed function	Gene name	Fold ^a expression
putative glyoxalase/bleomycin resistance protein/dioxygenase	KP1_2502	-5.48
L-lactate dehydrogenase	lldD	-5.47
putative PTS permease	KP1_0762	-5.34
putative Glucosamine-fructose-6-phosphate aminotransferase	KP1_0765	-5.17
putative ABC transport system inner membrane permease	KP1_3174	-5.08
putative PTS permease	KP1_0761	-5.04
putative NADH:flavin oxidoreductase	KP1_2565	-4.96
succinylglutamate desuccinylase	KP1_2504	-4.95
putative tartrate:succinate antiporter	KP1_2563	-4.92
succinylglutamic semialdehyde dehydrogenase	astD	-4.88
putative cytoplasmic protein	yiiL	-4.81
putative PTS permease	KP1_0763	-4.77
D-alanine/D-serine/glycine transport protein	KP1_2505	-4.71
putative glucosamine-fructose-6-phosphate aminotransferase	KP1_0764	-4.67
HP	KP1_0341	-4.62
putative PTS permease	KP1_0760	-4.62
putative ABC transporter	KP1_1423	-4.61
putative rhizopine uptake ABC transport system periplasmic solute-binding protein precursor	mocB (NC_012731 1369144..1370062)	-4.51
beta-methylgalactoside transporter inner membrane component	mgIC	-4.46
putative phospho-beta-glucosidase	KP1_3803	-4.45
putative ABC transport system periplasmic binding component	KP1_3175	-4.39
oxidoreductase	KP1_1248	-4.32
sugar ABC transport system permease component	KP1_1424	-4.27
lysine/cadaverine antiporter	cadB	-4.27
anaerobic class I fumarate hydratase/fumarase B	fumB	-4.25
putative myo-inositol catabolism protein	iolB	-4.23
maltoporin	lamB	-4.19
arginine succinyltransferase	KP1_2499	-4.14
methyl-galactoside transport system substrate-binding component	mgIB	-4.13
citrate/acetate antiporter	citW	-4.12
putative ABC transport system ATP-binding component	KP1_3173	-4.10
bifunctional succinylornithine transaminase/acetylornithine transaminase	KP1_2498	-4.06
acetolactate synthase	iolD	-3.91
galactose-proton symport of transport system	KP1_2730	-3.76
acetate permease	actP	-3.74
putative aldehyde dehydrogenase	KP1_0552	-3.70
putative POT family di-/tripeptide transport protein	yjdL	-3.66
putative aldehyde dehydrogenase	KP1_1995	-3.66

putative acetyltransferase	KP1_5342	-3.59
HP	KP1_3995	-3.53
histidine ammonia-lyase	hutH	-3.44
putative amino acid permease	proY (NC_012731 1688850..1690233)	-3.43
glutamate/aspartate transport system permease	gltJ (NC_012731 1578169..1578910)	-3.39
putative inner membrane protein	KP1_1483	-3.37
HP	KP1_2985	-3.34
glutamate/aspartate transport system ATP-binding component	gltL (NC_012731 1576770..1577496)	-3.33
HP	KP1_1396	-3.33
putative cytoplasmic protein	KP1_0509	-3.30
Predicted sugar epimerase	KP1_0551	-3.26
putative epimerase/isomerase	KP1_0562	-3.25
putative di(mono)oxygenase alpha subunit	KP1_1996	-3.23
type VI secretion system OmpA/MotB family protein	KP1_3385	-3.21
maltose ABC transporter periplasmic protein	malE	-3.17
glutamate and aspartate transporter subunit	gltI	-3.17
HP	KP1_2314	-3.10
phosphomannomutase	manB	-3.09
pullulanase-specific type II secretion system component J	puJ	-3.09
HP	KP1_0047	-3.09
aldehyde dehydrogenase	astD (NC_012731 2168051..2169530)	-3.06
putative glutamine synthetase	KP1_2006	-3.04
putative PTS system transport protein	KP1_1484	-3.01
PTS system beta-glucoside-specific transporter subunits IIABC	KP1_3804	-3.01

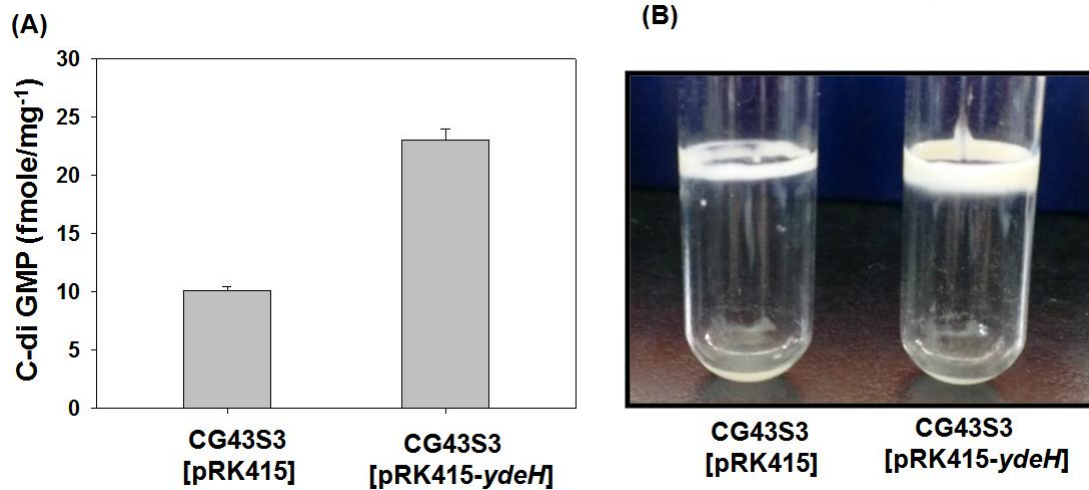


Fig.3.1. Cyclic di-GMP content. (A) C-di-GMP levels were determined using the ELISA kit (Wuhan EIAab Science Co., Ltd). Three independent experiments were performed and error bars shown. (B) Biofilm formation. 20 μ l of overnight bacteria were grown in LB at 37°C for 24 h. Biofilm development was observed visually as a function of pellicle formation and photographed. Data are representative of three independent experiments.

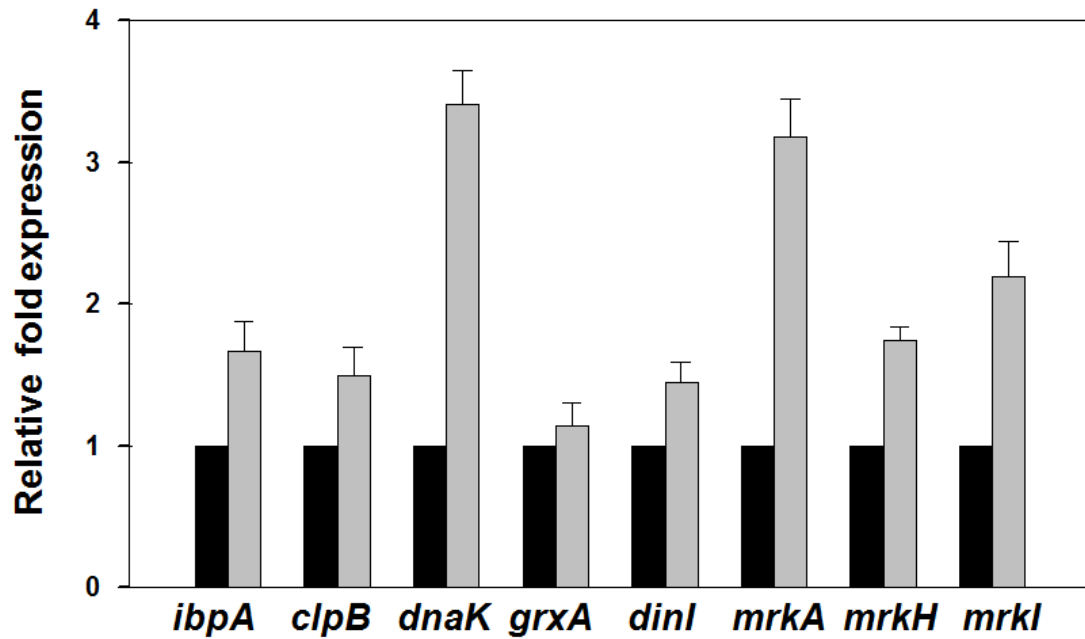


Fig. 3.2 qRT-PCR analysis of the selected up-regulated genes. Total RNA were isolated from the overnight culture of CG43S3[pRK415] and CG43S3[pRK415-*ydeH*]. Specific primer pairs selected for the up-regulated genes with over 3-fold increase of expression. Relative fold expression was determined by the $2^{-\Delta\Delta Ct}$ method. Data are representative of three independent experiments.

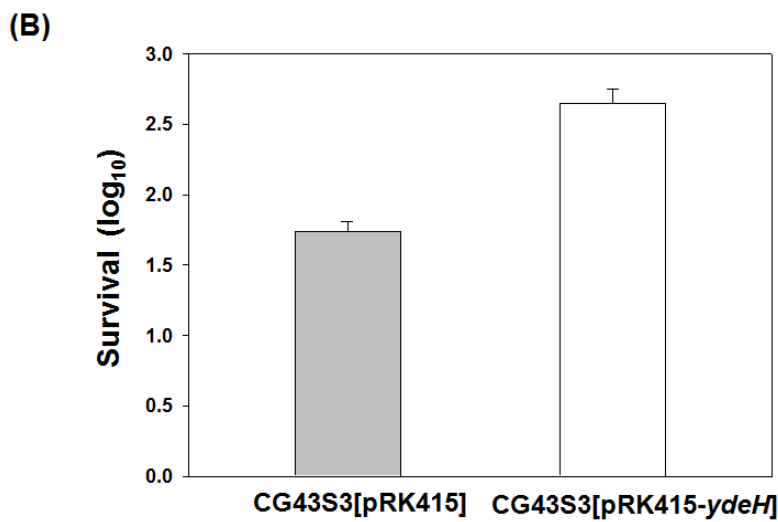
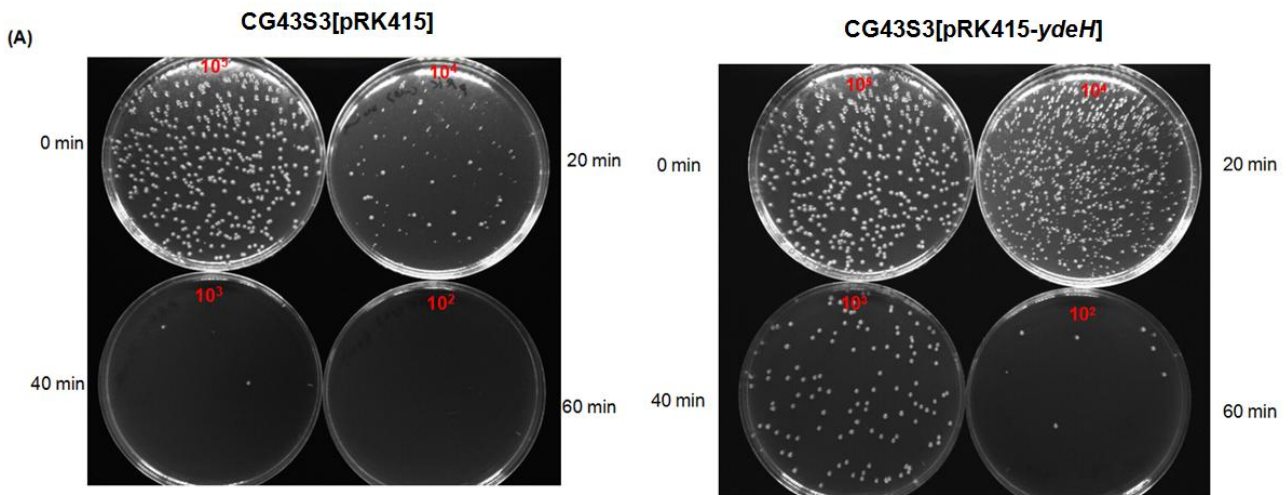


Fig. 3. 3 Heat shock stress survival analysis. The heat shock stress response was measured by colony formation (A) and survival rate (B). Overnight cultures of CG43S3[pRK415] and CG43S3[pRK415-ydeH] were collected and refreshed grown in LB until OD₆₀₀ reach 0.6~0.7. Aliquots of bacteria were then heated to 50 °C for 20, 40, and 60 min individually. Finally, the cultures were plated onto LB plates by 10-fold dilution for colony formation and the survival rate calculated. Error bars indicate standard deviation of the mean. Data are representative of three independent experiments.

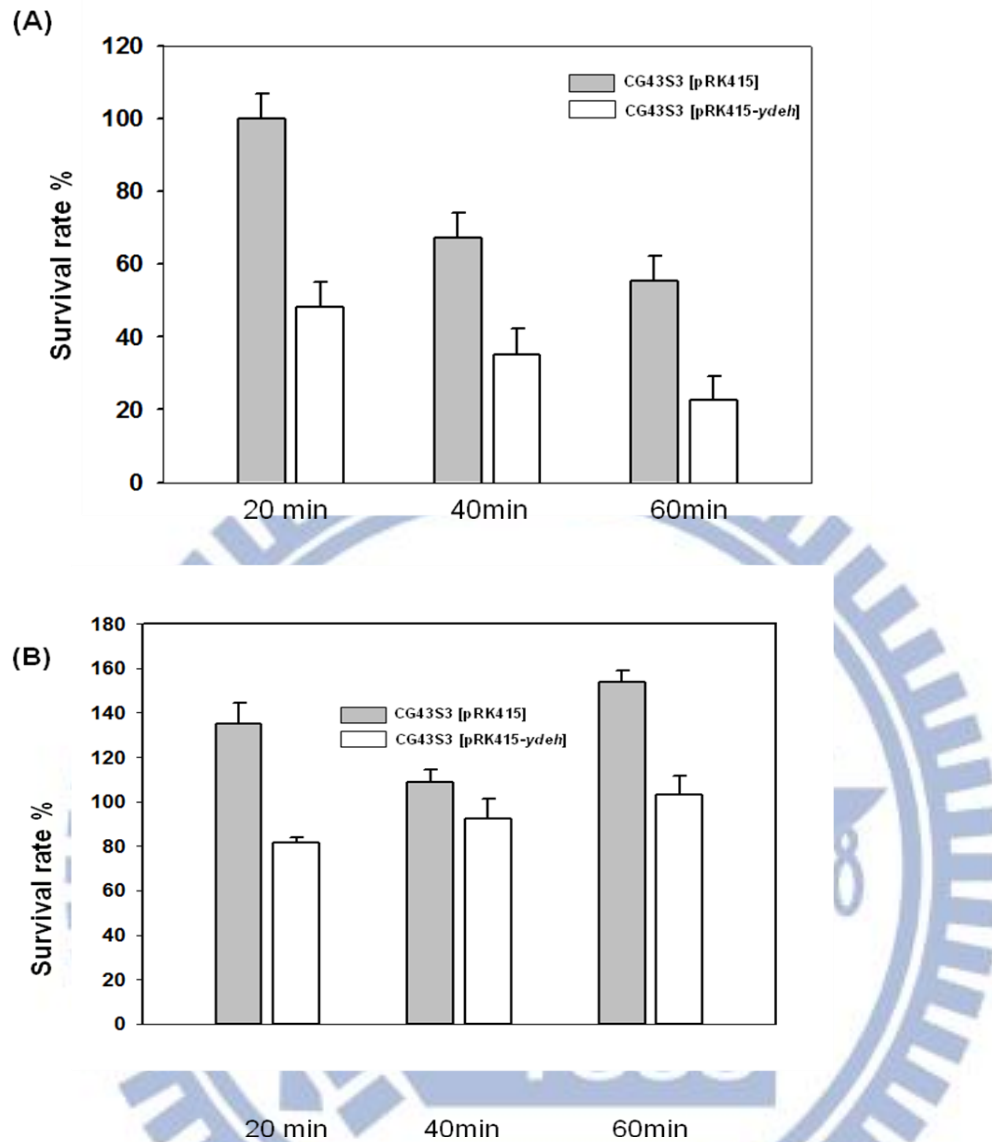
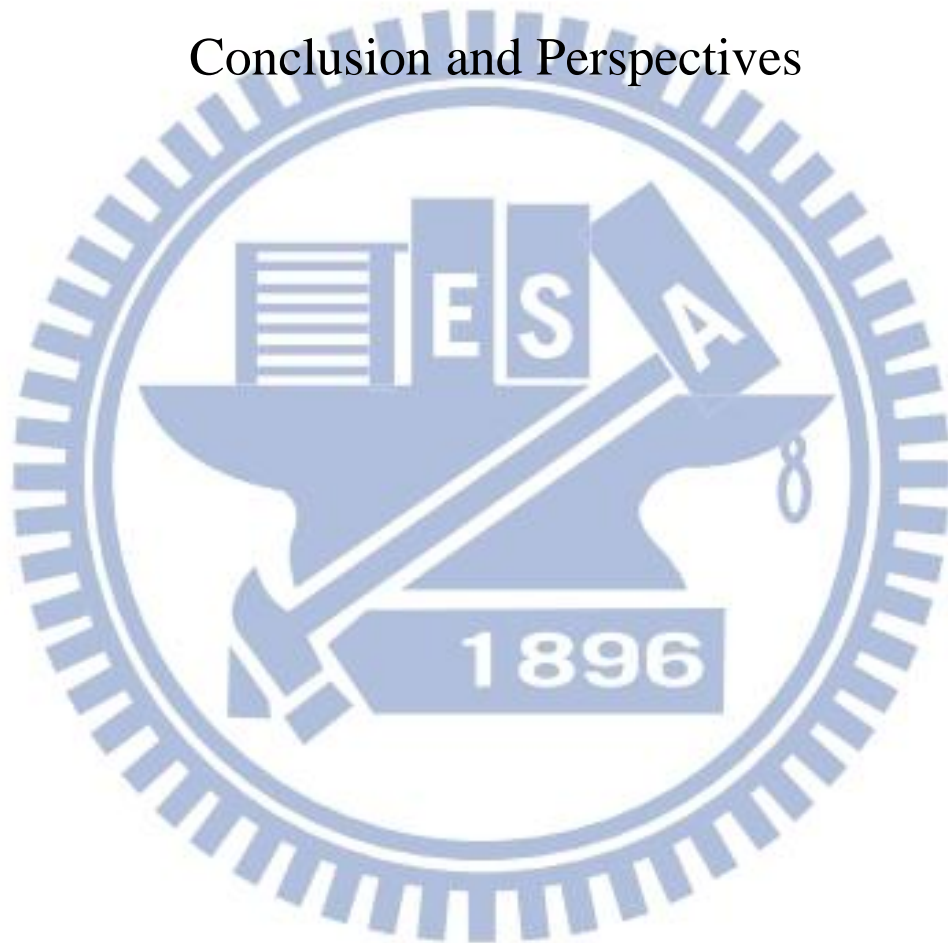


Fig. 3.4. Responses to acid stress (A) and oxidative stress (B). (A) Log-phased bacteria were grown in pH 4.4 LB 1 h for acid adaptation and then the cultures transferred to M9 (pH 3) for 20, 40, and 60 min. (B) Aliquots of log-phased bacteria (OD600 reaches 0.6~0.7) were treated with 10 mM H₂O₂ and the cultures continued at 37°C for 20, 40, and 60 min. Finally, the cultures were plated onto LB plates by 10-fold dilution for colony formation and the survival rate calculated.

Chapter 4

Conclusion and Perspectives



The c-di-GMP regulating network is complex and many unknown mechanisms remain to be explored, despite of the recent abundant information to characterize the function. We know only fragments of the c-di-GMP signaling networks, such as enzymes or receptors. However, the molecular regulation, signals reception and transduction, c-di-GMP-dependent circuits, or even targets of c-di-GMP action are often missing. Therefore, there is still a lot to be discovered in c-di-GMP signaling network.

In this thesis, we have demonstrated that YjcC exerts PDE activity, affects the virulence and resist oxidative stress in *K. pneumoniae* CG43S3. However, the upstream regulation of *yjcC* and how YjcC relay the c-di-GMP dependent resistance oxidative stress remains unclear. Moreover, if the CSS motif at the N-terminal region of YjcC plays a signal sensing role is also an interesting issue to be answered. We have also demonstrated that the increase of c-di-GMP levels by overexpression of the DGC encoding gene *ydeH* in the cells affects the stress responses to heat shock, oxidative stress and acid stress. As shown in Fig 3.3 and 3.4, increased *ydeH* expression enhanced the heat shock survivals but reduced the viability facing the stresses of oxidation and acidity. By contrast, increasing *yjcC* expression increased the survival rate after oxidative stress (Fig 2.2) indicating that different levels of c-di-GMP may modulate the stress responses differently.

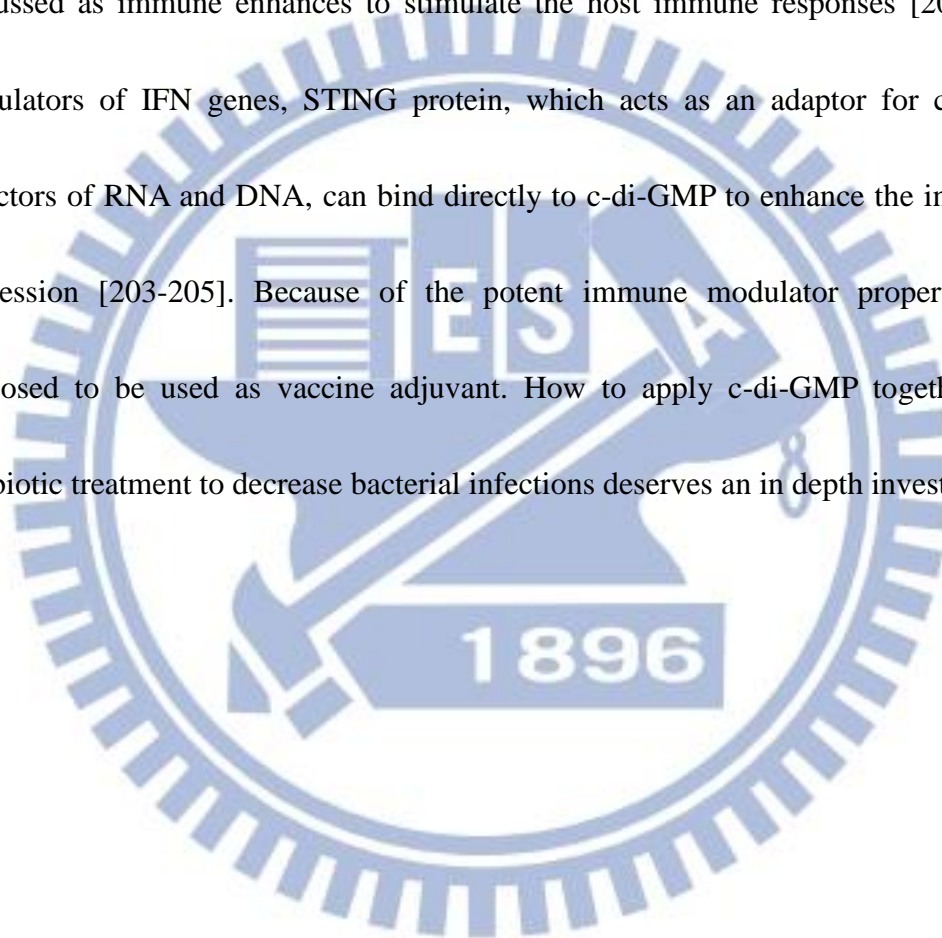
The c-di-GMP molecule has been shown to act on the transcriptional, posttranscriptional, and posttranslational levels for its regulation. In spite of numerous reports, the c-di-GMP targets and the c-di-GMP-mediated regulation mechanism remain a lot to be explored. In this thesis, we provide information to help elucidate the c-di-GMP mediated stress response in *K. pneumoniae* and toward understand how the c-di-GMP regulation functions to counter the stress condition.

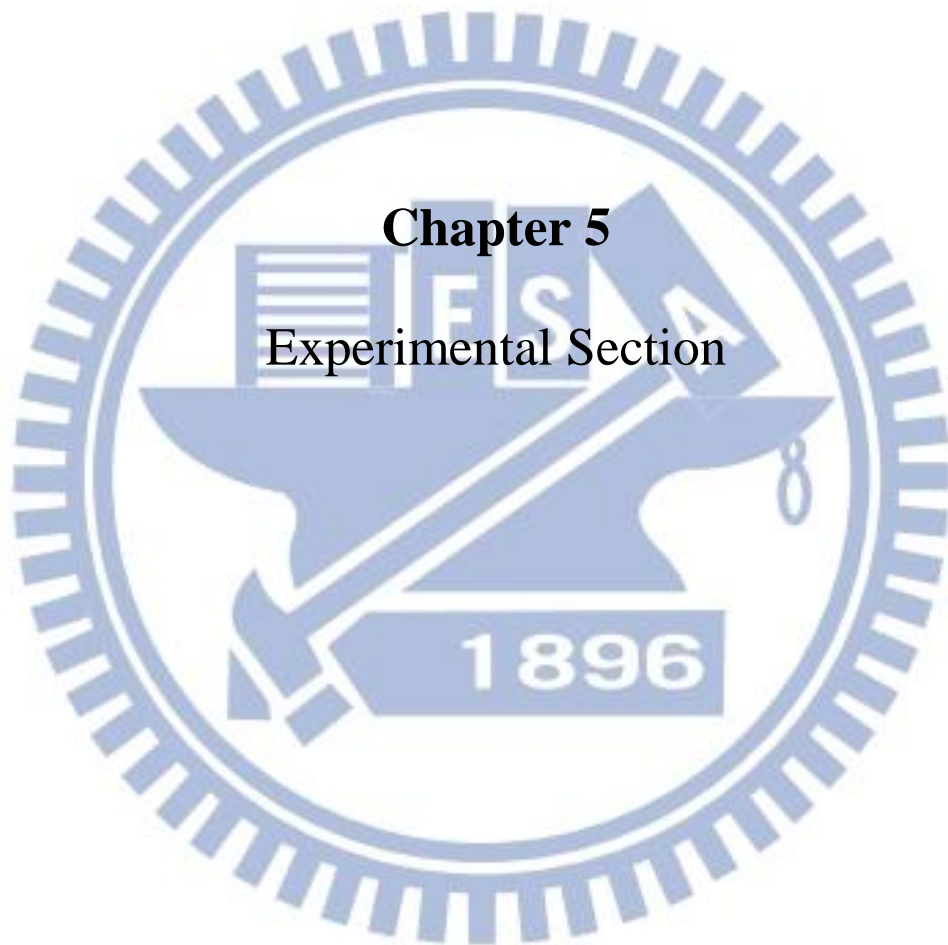
In the genome of *K. pneumoniae* CG43S3, there are overall 25 genes encoding the proteins, including GGDEF-, 11 EAL- and 4 GGDEF-EAL- domain proteins, to regulate the c-di-GMP levels. Four of the proteins including FimK, MrkJ, MrkH, and YjcC have been characterized and all are found to be involved in regulating the expression of type 3 fimbriae and biofilm formation at certain levels in the bacteria. However, the others remain uncharacterized. If they also play a role in affecting the expression of type 3 fimbriae, type 1 fimbriae, CPS biosynthesis, biofilm and virulence in *K. pneumoniae* is worth to further studying.

The transcriptome study via RNA sequencing is currently an intensively used approach for a genome-wide regulatory network. It is believed that a detailed analysis of the data from CG43[pRK415], CG43[pRK415-*ydeH*], and CG43[pRK415-*yjcC*] would provide much more information to help get insights of the c-di-GMP dependent regulatory mechanism in *K. pneumoniae*. The transcriptome data in Table 2.2 and

Table 3.1 revealed that the level change of c-di-GMP in *K. pneumoniae* CG43S3 induced expression of many heat shock chaperon gene suggesting that change of c-di-GMP level triggers the heat shock chaperon expression.

The cyclic dinucleotides such as c-di-GMP and c-di-AMP have recently been discussed as immune enhancers to stimulate the host immune responses [202]. The stimulators of IFN genes, STING protein, which acts as an adaptor for cytosolic detectors of RNA and DNA, can bind directly to c-di-GMP to enhance the interferon expression [203-205]. Because of the potent immune modulator property, it is proposed to be used as vaccine adjuvant. How to apply c-di-GMP together with antibiotic treatment to decrease bacterial infections deserves an in depth investigation.





5.1.1 Plasmids, bacterial strains, primers and growth conditions

Bacterial strains and plasmids used in this study are listed in Table 5.1 and Table 5.2, and the primers used are listed in Table 6.3. *K. pneumoniae* CG43, a clinical isolate of serotype K2, is high virulent to mice. *E. coli* and *K. pneumoniae* strains were generally propagated at 37°C in Luria-Bertani (LB) broth. M9 minimal medium and tryptic soy broth (TSB) were also used. Bacterial growth was assessed by measuring the absorbance of optical density at 600 nm (OD₆₀₀). Otherwise indicated, the antibiotics used include ampicillin (100 µg/mL), chloramphenicol (35 µg/mL), kanamycin (25 µg/mL), tetracycline (12.5 µg/mL) and streptomycin (500 µg/mL).

5.2 General Experimental Procedures

5.2.1 Construction of specific gene-deletion mutants and complementation

plasmids

Specific gene deletion was introduced into *K. pneumoniae* CG43 using an allelic-exchange strategy as previously described [152]. Two DNA fragments of approximately 1000-bp flanking both sides of the deleted region were cloned into pKAS46 [39]. The plasmid pKAS46 is a suicide vector containing *rpsL*, which allows positive selection with streptomycin for vector loss. The resulting plasmids were mobilized from *E. coli* S17-1λ *pir* to *K. pneumoniae* CG43S3 or CG43S3Δ*lacZ*, by conjugation, respectively. The transconjugants, with the plasmid integrated into the

chromosome through homologous recombination, were selected with ampicillin and kanamycin on M9 agar plates. Several of the colonies were grown overnight in LB broth at 37°C and then spread onto an LB agar plate containing 500 µg of streptomycin/mL. Streptomycin-resistant and kanamycin-sensitive colonies were selected, and the deletion was verified by PCR. Table 5.1 presents the resulting mutant strains. To obtain the complementation plasmids, DNA fragments containing the *yjcC*, and *soxRS* loci were PCR amplified using the primer pairs pjr1-F/pjr1-R, pjr2-F/pjr2-R, and pjr3-F/pjr3-R (Table 5.2). The PCR products were cloned in pRK415 [206] to generate pJR1(pRK415-*yjcC*), pJR2(pRK415-*yjcC*-AAL), pJR3(pRK415-EAL domain only of *yjcC*), *pmrkJ*, and *pfimK* respectively (Table S1).

5.2.2 Site-directed mutagenesis

Site-directed mutagenesis was performed on the plasmid pJR1 to substitute the critical residue E with A in the EAL domain of YjcC using a QuickChange site-directed mutagenesis kit and following the manufacturer protocols (Stratagene). The resulting PCR product contained one point mutation, corresponding to the E303-to-A303 change in the active EAL site. The resulting PCR product was digested with *Bam*HI and *Hind*III and ligated into *Bam*HI/*Hind*III-digested plasmid pRK415-pJR2.

5.2.3 Paraquat and H₂O₂ survival assessment

One hundred microliter of bacteria grown overnight were inoculated in LB and incubated at 37 °C to OD600 of 0.6-0.7. An aliquot of the bacteria was collected by centrifugation and then resuspended in 500 μM of paraquat and 10 mM H₂O₂ respectively, and then subjected to 37 °C incubation for 35 min. The colony-forming unit (CFU) of the bacteria was counted after the stress treatment, and the survival rate was determined by the CFU ratio. This study presents the representative data of at least 3 independent experiments. Every sample was assayed in triplicate, and this study presents the average activity and standard deviation.

5.2.4 Measurement of promoter activity

The promoter reporter plasmids were individually mobilized from *E.coli* S17-1λ *pir* to *K. pneumoniae* strains by conjugation. The β-galactosidase activity was measured as described previously [152]. The bacteria were grown to the log phase in the LB medium (OD600 of 0.6 - 0.7) and 100 μL of the culture was mixed with 900 μL of Z buffer (60 mM Na₂HPO₄, 40 mM NaH₂PO₄, 10 mM KCl, 1 mM MgSO₄, and 50 mM β-mercaptoethanol), 17 μL of 0.1% sodium dodecyl sulfate (SDS), and 35 μL of chloroform, followed by vigorous shaking. After incubation at 30 °C for 10 min, 200 μL of a 4-mg/mL concentration of o-nitrophenyl-β-D galactopyranoside (ONPG; Sigma-Aldrich, Milwaukee, WI) was added to the mixture to initiate the reaction. When yellow coloration appeared, the reaction was stopped by adding 500 μL of 1 M

Na₂CO₃ to the mixture. The absorbance at OD₄₂₀ was recorded, and the activity was expressed as Miller units. Each sample was assayed in triplicate, and at least 3 independent experiments were conducted. The data shown were calculated from one representative experiment, and are presented as the means and standard deviations from triplicate samples.

5.2.5 Real-time PCR analysis

Total RNA was isolated from bacteria using High Pure RNA isolation Kit (Roche, Germany), and the residual DNA was eliminated with RNase-free DNase I (Roche, Germany). The cDNAs used for PCR were synthesized from 1.5 µg RNA using random hexamer primer from RevertAidTM H Minus First strand cDNA synthesis Kit (Fermentas, Canada). An ABI Prism 7000 Detection system was used to perform PCR following the manufacturer instructions, and the products were detected using SYBR Green RCR Master Mix (Roche, Germany). The RNA samples were normalized to the level of 23S rRNA. PCR analysis was performed in triplicate in a reaction volume of 25 µL containing 12.5 µL of SYBR Green PCR Master Mix, 300 nM of primer pairs, 9.5 µL of distilled H₂O, and 1 µL of cDNA. Samples were heated for 10 min at 95 °C and amplified for 40 cycles for 15 s at 95 °C and 60 s at 60 °C. Quantification was performed using the $2^{-\Delta\Delta C_t}$ method [207].

5.2.6 Cloning, expression, and purification of the recombinant proteins

The coding regions of the EAL or AAL domains of *yjcC* were PCR amplified with the primer sets yEAL-F/yEAL-R and yAAL-F/yAAL-R (Table S2) and cloned in the NdeI/XhoI site in pET30b (Novagen, Madison, WI). This process generated pET30b-EAL or pET30b-AAL with a carboxyl-terminus His tag (RcsB-His6). The resulting plasmids pEAL (pET30b-EAL of *yjcC*) and pAAL (pET30b-AAL of *yjcC*) were individually transformed into *E. coli* BL21(DE3)/pLysS (Invitrogen), and the overproduction of the recombinant protein was induced by adding 0.5 mM IPTG for 4 h at 37 °C. The recombinant proteins were then purified from the soluble fraction of the total cell lysate by affinity chromatography using His-Bind resin (Novagen). The purified proteins were then dialyzed against 1 TBS (Tris-buffered saline; pH 7.4) containing 10% glycerol at 4 °C overnight, followed by condensation with PEG 20000. The purity was determined by SDS-PAGE.

5.2.7 Phosphodiesterase activity assay

The recombinant plasmids pET30b-EAL_{*yjcC*}, pET30b-AAL_{*yjcC*}, and pET30b-*mrkJ* were transformed into *E. coli* BL21(DE3), and the protein induced expression using 0.5 mM IPTG at 22 °C for 12 h. The PDE activity was determined using the synthetic chromogenic substrate *bis*(*p*-nitrophenyl) phosphate (*bis*-pNPP) (Sigma-Aldrich) as previously described [90,208]. The specific PDE activity was determined using purified proteins and by measuring the release of *p*-nitrophenol (*p*NP) at 405 nm. The

calculations in this study use an extinction coefficient of $1.78 \times 10^4 / \text{M} \cdot \text{cm}$ for *p*-nitrophenol. Control BSA without extracts was included to account for any non-enzymatic bis-pNPP hydrolysis and MrkJ, which carries PDE activity as a positive control [157].

5.2.8 In vivo ci-di GMP content

To measure the c-di-GMP contents, cellular extracts were prepared as described [209]. The cultured bacteria were collected and treated with formaldehyde (0.19% final concentration) and then pelleted by centrifugation. The pellet was suspended in water and heated to 95 °C for 10 min before the nucleotides were extracted by 65% ethanol. The lyophilized samples were then resuspended in water and this suspension was used for c-di-GMP detection with a cyclic diguanylate ELISA kit (Wuhan EIAab Science co., Ltd). The ci-di GMP activity of crude extracts (1 mg of total protein/mL) containing WT-pRK415 vector only, pJR1, and pJR2 in ΔyjC was also assayed as described above.

5.2.9 Determination of intracellular ROS concentration

Bacterial cultures were grown exponentially ($\text{OD}_{600} = 0.6 - 0.7$) and exposed to 10 mM of hydrogen peroxide or 500 μM of paraquat for 40 min. Cells were centrifuged at 13000 *g*, washed with 10 mM potassium phosphate (pH 7.0) buffer (Buffer A), and suspended in 500 μL of the same buffer, which contained 10 μM

2',7'-dihydrodichlorofluorescein diacetate (H2DCFDA). After shaking for defined periods in darkness at room temperature, cells were centrifuged as mentioned and washed twice with 500 μ L of Buffer A. Cells were suspended in 500 μ L of Buffer A and disrupted by sonication. After centrifugation at 13000 g, aliquots of 100 μ L supernatants were used to determine fluorescence intensity (excitation 490 nm and emission 519 nm) as described [136,137].

5.2.10 Oxidation of cytoplasmic proteins

Bacteria was grown to an OD600 0.6 - 0.7 in the presence of 10 mM hydrogen peroxide. After incubating for 30 min at 37 °C, crude extracts were prepared and suspended in 500 μ L of Buffer A and then disrupted by sonication. After centrifugation at 13000 g, 4 aliquots of 10 mM dinitrophenylhydrazine (DNPH) were added to the supernatant and the mixture was incubated at room temperature for 1 h with occasional stirring. Proteins were precipitated by adding one volume of 20% trichloroacetic acid (TCA) and centrifuged at 13000 g for 5 min. The precipitate was washed 3 times with a mixture of ethanol: ethyl acetate (1:1). Finally, the sediment was dissolved in 450 μ L of 6M guanidine hydrochloride/dithiothreitol and carbonyl concentration was determined spectrophotometrically at 370 nm ($\epsilon = 22000 \text{ M}^{-1} \text{ cm}^{-1}$).

5.2.11 Evaluation of antioxidant activity with DPPH assay

DPPH radical scavenging activity was estimated using the method of Liyana-Pathirana and Adedapo [210,211]. When DPPH accepts an electron donated by an antioxidant compound, the free radical is decolorized from a stable purple color to yellow which can be quantitatively measured from the changes in absorbance. A solution of 0.135 mM DPPH in methanol was prepared, and 1.0 mL of this solution was mixed with 1.0 mL of extract in methanol containing 0.02-0.1 mg of the extract. The reaction mixture was thoroughly vortexed and left in the dark at room temperature for 30 min. The absorbance of the mixture was measured with a spectrophotometer at 517 nm, with ascorbic acid and BHT as references. The scavenge ability to remove DPPH radicals was calculated using the following equation: DPPH radical scavenging activity (%) = $[(\text{Abs control} - \text{Abs sample}) / (\text{Abs control})] \times 100$, where Abs control is the absorbance of DPPH radical + methanol, and Abs sample is the absorbance of DPPH radical + sample extract/standard.

5.2.12 Determination of SOD and catalase enzyme activity

Cell-free extracts were harvested (15000 rpm, 4 °C, 20 min) from the exponential phased bacteria ($\text{OD}_{600} = 0.7 - 0.8$) and suspended in ice-cold potassium phosphate buffer (50 mM, pH 7). After cells were disrupted by ultra-sonication, cell debris was removed by 12000 rpm centrifugation for 10 min at 4 °C, and the supernatant was

collected. The extraction of total proteins was conducted on ice and the concentrations were estimated using the Bradford method [212]. Aliquots of the extracted proteins were individually loaded onto 10% native polyacrylamide gels and the proteins were separated at a constant voltage of 150 V for 2 h. The gels were then removed and stained for SOD and CAT activity using the methods of Beauchamp and Fridovich [213] and Woodbury et al. [214], respectively. The SODs were localized by soaking gels in 2.45 mM nitro blue tetrazolium for 20 min, followed by immersion in a solution of 50 mM phosphate buffer (pH 7.0), 0.028 mM riboflavin, and 0.028 M TEMED (*N,N,N',N'*-tetramethylethylenediamine). The gels were then removed from the solution and exposed to light for approximately 20 min. The SOD activity produced achromatic zones in the purple gel. The expression of CAT activity was identified by soaking gels in 10 mM hydrogen peroxide for 30 min with gentle shaking and then transferring the gels to a solution of 1% ferric chloride and 1% potassium ferricyanide for 10 min. The localized-CAT produced colorless bands on a dark green background.

The SOD activity was determined using a spectrophotometer at 25 °C using the xanthine oxidase–cytochrome C method [213]. The assay mixture in 0.7 mL contained 50 mM potassium phosphate (pH 7.8), 0.1 mM EDTA, 50 mM xanthine, 1.7 mU xanthine oxidase, and 10 mM cytochrome C. The reduction of cytochrome C

was measured at A550. One unit (U) of SOD activity was defined as the amount of enzyme required to inhibit the reduction rate of cytochrome C by 50%. Catalase activity was also determined spectrophotometrically at 25 °C by monitoring the decrease in A240 in 50 mM Tris/HCl buffer (pH 8.0) [136]. One unit (U) of activity was defined as the amount of enzyme that catalyses the oxidation of 1 mmol H₂O₂ min⁻¹ under assay conditions.

5.2.13 Mouse lethality assay

The bacterial virulence in mice was determined as described [39]. Female BALB/c mice (aged 4 to 5 wk) were obtained from the National Laboratory Animal Center and acclimatized in an animal house for 7 d. The tested bacterial strains were cultured overnight in LB medium at 37 °C. Four mice in each group were injected intraperitoneally with 0.2 mL of bacterial suspension in saline in 10-fold graded doses. The LD₅₀ values were calculated using the Reed and Muench method [215] based on the number of survivors after 14 day.

5.2.14 Extraction and quantification of capsular polysaccharides

The bacterial CPS was extracted using the method described [39,216]. A 500 µL sample of overnight-grown bacteria was mixed with 100 µL of 1% Zwittergent 3-14 (Sigma-Aldrich, Milwaukee, WI) in 100 mM citric acid (pH 2.0) and then incubated at 50 °C for 20 min. After centrifugation, a 250 µL sample of the supernatant was

transferred to a new tube, and the CPS was precipitated with 1 mL of absolute ethanol. The pellet was dried and dissolved in 200 μL of distilled water, and 1200 μL of 12.5 mM borax in H_2SO_4 was then added. The mixture was vigorously mixed, boiled for 5 min, and cooled before adding 20 μL of 0.15% 3-hydroxydiphenol (Sigma-Aldrich, Milwaukee, WI). The absorbance at 520 nm was measured, and the uronic acid content was determined from a standard curve of glucuronic acid and expressed as micrograms per 10^8 or 10^9 CFU.

5.2.15 Biofilm formation assay

The ability of bacteria to form biofilm was analyzed as described, with a minor modification. Bacteria were diluted 1/100 in LB broth supplemented with the appropriate antibiotics, and this dilution was inoculated into each well of a 96-well micro titre dish (Orange Scientific) and statically incubated at 37 °C for 48 h. Planktonic cells were removed, and the wells were washed once with distilled water to remove unattached cells. Crystal violet (0.1% w/v; Sigma) was used to stain the attached cells for 30 min. Unattached dye was rinsed by washing 3 times with distilled water, and the stained biomass was solubilized in 1% (w/v) SDS. The absorbance was determined at 595 nm, and relative bacterial biofilm-forming activities were observed.

5.2.16 Western blot analysis

K. pneumoniae CG43S3 and its derived mutants were grown in LB broth with agitation at 37 °C. The bacterial total protein, approximately 5 µg per lane, was then subjected to western blot analysis using MrkA antiserum. Aliquots of total cellular lysates were resolved by SDS-PAGE, and the proteins were electrophoretically transferred onto a polyvinylidene difluoride (PVDF) membrane (Millipore, Billerica, MA, USA). After incubation with 5% skim milk at room temperature for 1 h, the membrane was washed 3 times with 1X PBS. The membrane was subsequently incubated with diluted anti-GAPDH (GeneTex Inc.) and anti-MrkA serum at room temperature for 1 h. After 3 washes with 1X PBS, a 5000-fold diluted alkaline phosphatase-conjugated anti-rabbit immunoglobulin G was added and incubated for 1 h. The blot was washed again and the bound antibodies were detected using the chromogenic reagents BCIP (5-bromo-4-chloro-3-indolyl phosphate) and NBT (Nitro blue tetrazolium).

5.2.17 Transcriptome analysis

Total RNA from CG43S3[pRK415] and CG43S3[pJR1] were isolated using Trizol reagent (Invitrogen), subsequently purified using RNeasy MinElute Cleanup Kit (Qiagen), and eluted in RNase-free water. The RNA samples were sequenced on Illumina's sequencing instrument. In the data analysis pipeline, we used the

FASTX-Toolkit to remove or trim deep sequencing reads containing low quality bases or adaptor sequences. To estimate expression levels of genes, all the remaining reads were mapped to the *Klebsiella pneumoniae* NTUH-K2044 genome using TopHat and determined using Cufflinks package. The genes were identified as significantly transcript abundance changed in CG43S3[pRK415] as compared to that in CG43S3[pJR1] if the log₂ fold change was greater than 2 (up and down). Finally, functional annotation tools, such as DAVID, can be used to illustrate the biological regulation role from Gene Ontology or KEGG pathway database.

5.1.18 Acid tolerance response

Bacterial resistance to acid challenge was determined essentially as previously described (94). To investigate the effect of pre-adaptation in different growth conditions, the parental strain CG43S3[pRK415] and CG43S3[pRK415-*ydeH*] was grown separately in LB and M9 medium, and the log-phased cultures were further divided into two groups. One group (approximately 1×10^8 CFU/mL) was first centrifuged and resuspended in LB or M9 medium (pH 4.5) for a 30 min adaption period before the acid challenge, while the other group (approximately 2×10^8 CFU/mL) was directly acid challenged by re-suspending bacterial cultures in M9 medium (pH 3.0). Upon acid challenge, 100 μ L of each culture was immediately removed for serial tenfold dilution in PBS, and 100 μ L of each culture to the 10^{-5}

dilution was plated onto LB agar plates at what was considered to be the initial time point (t_0). The bacterial survival was expressed as the CFU of each strain after acid challenge divided by the CFU of each strain at t_0 . Then the bacterial cultures were subjected to pre-adaptation at pH 4.5, acid challenged, and the survival rates at 20, 40 and 60 min were determined as described above. Three independent assays were performed, and data shown were the average and standard deviation of samples from one of the trials.

5.1.19 Heat shock stress response

One hundred microliter of bacteria grown overnight were inoculated in LB and incubated at 37 °C to OD600 of 0.6-0.7. An aliquot of the bacteria were collected before and after 20, 30, and 40 min of 50 °C heat exposure. The colony-forming unit (CFU) of the bacteria was counted after the stress treatment, and the survival rate was determined by the CFU ratio. This study presents the representative data of at least 3 independent experiments. Every sample was assayed in triplicate, and this study presents the average activity and standard deviation.

5.2.20 Statistical methods

The results of the survival rate, CPS amounts, biofilm-forming activity, enzyme activity assay and β -galactosidase activity assays were derived from a single experiment that was representative at least of three independent experiments. Each

sample was assayed in triplicate and the data were presented as the mean \pm standard deviation (SD). Differences between groups were evaluated by a two-tailed Student's *t*-test. *P*-values less than 0.01 were considered statistically significant difference.

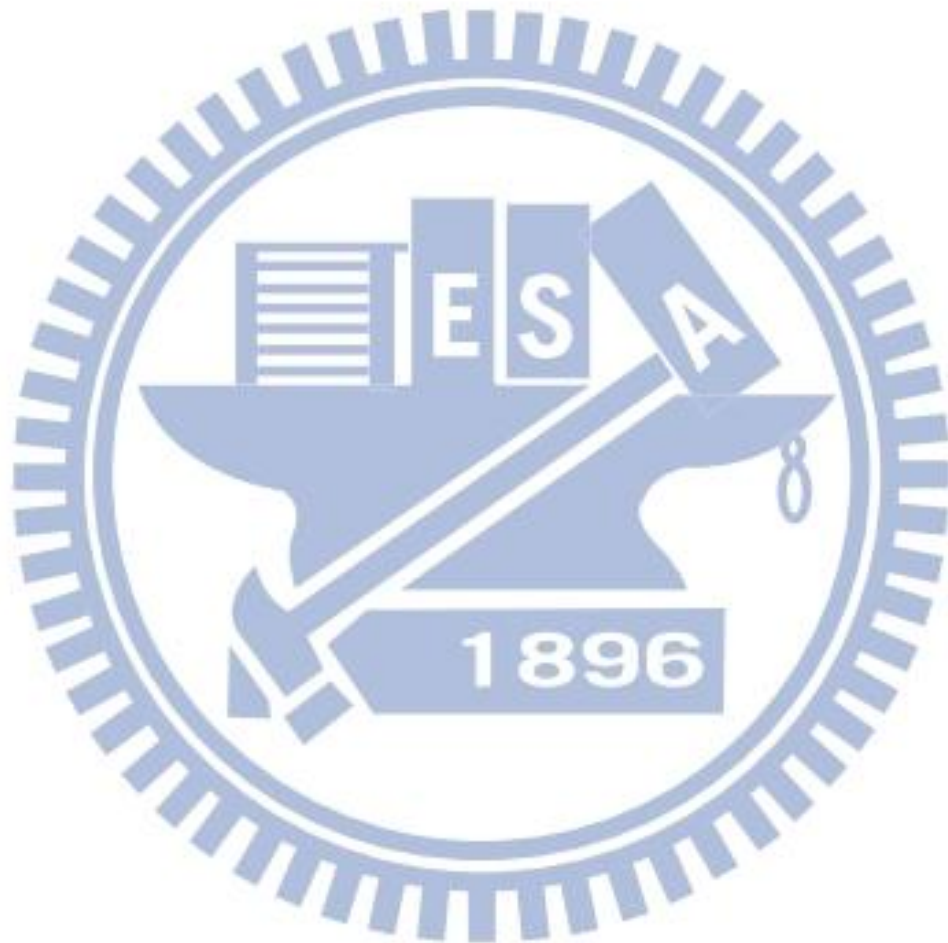


Table 5.1 Strains and plasmids used in this study

Strains or plasmids	Descriptions	Reference or source
<i>K. pneumoniae</i>		
CG43S3	CG43 Sm ^r	Laboratory stock
$\Delta yjcC$	CG43S3 $\Delta yjcC$	This study
$\Delta soxRS$	CG43S3 $\Delta soxRS$	This study
$\Delta rpoS$	CG43S3 $\Delta rpoS$	This study
$\Delta lacZ$	CG43S3 $\Delta lacZ$	Laboratory stock
$\Delta lacZ soxRS$	CG43S3 $\Delta lacZ \Delta soxRS$	This study
$\Delta lacZ rpoS$	CG43S3 $\Delta lacZ \Delta rpoS$	This study
<i>E. coli</i>		
JM109	F' (<i>traD36, proAB⁺ lacI^q, (lacZ)M15</i>) <i>endA1 recA1 hsdR17</i> (r _k ⁻ , m _k ⁺) <i>mcrA supE44⁻ gyrA96 relA1 (lacproAB) thi-1</i>	Laboratory stock
BL21 (DE3)	F' <i>ompT hsdS_B[r_B⁻ m_B⁻]</i> <i>gal dcm trxB15::kan</i> (DE3)	Novagen
S17-1 λpir	<i>hsdR recA pro</i> RP4-2 (Tc::Mu; Km::Tn7) (λpir)	
Plasmids		
yT&A	Ap ^r , TA cloning vector	Yeastern
pKAS46	Ap ^r Km ^r , positive selection suicide vector, <i>rpsL</i>	
<i>pyjcC</i>	2.1-kb fragment containing a 1300-bp deletion in <i>yjcC</i> locus cloned into pKAS46	This study
<i>psoxRS</i>	2 kb fragment containing a 700-bp deletion in <i>soxRS</i> locus cloned into pKAS46	This study
pRK415	Tc ^r , shuttle vector, <i>mob⁺</i>	Laboratory stock
pJR1	Tc ^r , full length <i>yjcC</i> with putative promoter cloned into pRK415	This study
pJR2	Tc ^r , ~ 2 kb fragment encoding YjcC with the domain of EAL _{E303A} cloned into pRK415	This study
pJR3	Tc ^r , 813-bp fragment of EAL domain only of <i>yjcC</i> cloned into pRK415	This study
<i>pfimK</i>	Tc ^r , 1242-bp fragment of <i>fimK</i> cloned into pRK415	Laboratory stock
<i>pmrkJ</i>	Tc ^r , 714-bp fragment of <i>mrkJ</i> cloned into pRK415	Laboratory stock
<i>pydeH</i>	Tc ^r , 894-bp fragment of <i>ydeH</i> , from <i>E.coli</i> W3110, cloned into pRK415	Laboratory stock
pET30b	Km ^r , protein expression vector	Novagen
pEAL	813-bp fragment encoding EAL coding region of <i>yjcC</i> cloned from CG43S3 into pET30b	This study
pAAL	813-bp fragment encoding EAL _{E303A} coding region of <i>yjcC</i> cloned from CG43S3 into pET30b	This study
placZ15	Cm ^r , promoter selection vector, <i>lacZ⁺</i>	Laboratory stock
<i>pyjcC0</i>	Cm ^r , 415-bp fragment of the upstream region of <i>yjcC</i>	This study
<i>PyjcC1</i>	Cm ^r , 525-bp fragment of the upstream region of <i>yjcC</i>	This study
<i>PyjcC2</i>	Cm ^r , 385-bp fragment of the upstream region of <i>yjcC</i>	This study

Table 5.2 Oligonucleotide primers used in this study

Function	Primer name	Sequence (5'→3')
Gene deletions		
<i>yjcC</i>	<i>yjcC</i> -A(XbaI)F	TA TCTAGA GGCTGCAGAAAACGAAAAAGC
	<i>yjcC</i> -A(BamHI)R	TA GGATCC ACCATTTCCGTTTTTTTGC
	<i>yjcC</i> -B(BamHI)F	AT GGATCC CTCTACAAGCGCGGCGTAC
	<i>yjcC</i> -B(EcoRI)R	AT GAATTC CTCGCTGCAGACAAAAC
<i>soxRS</i>	<i>soxRS</i> -A(XbaI)F	AT TCTAGA ATACTTTTTTAATCAGAATG
	<i>soxRS</i> -A(BamHI)R	AT GGATTC CGCCATCAGATCTCCGCGTG
	<i>soxRS</i> -B(BamHI)F	AT GGATTC GAAGACGAGTGATAAAAC
	<i>soxRS</i> -B(EcoRI)R	AT GAATTC CGCTAACAAATTTTTAGTGAG
Recombinant constructs		
yEAL	EAL(EcoRI)F	TA GAATCC ATGCTGCAGCGGGCTCTG
	EAL(HindIII)R	TA AAGCTT TCACTCCC GCGCCGGCAT
yAAL	EAL(EcoRI)F	TA GAATCC ATGCTGCAGCGGGCTCTG
	EAL(HindIII)R	TA AAGCTT TCACTCCC GCGCCGGCAT
Complementation constructs		
pJR1	pjr1(BamHI)F	AAGGATTCTAACCTATCCTCAAAGAAAGTGC
	pjr1(EcoRI)R	AAGAATTCTCAGATCTCCGCGTGAC
pJR2	pjr2(BamHI)F	AAGGATTCTAACCTATCCTCAAAGAAAGTGC
	pjr2(EcoRI)R	AAGAATTCTCAGATCTCCGCGTGAC
pJR3	pjr3(BamHI)F	AAGGATTCCGCGGACAGTATC
	pjr3(EcoRI)R	AAGAATTCTCAGATCTCCGCGTGAC
site-directed mutagenesis		
	<i>yjcC</i> -ala F	CCGCTGCGTTGGGGCGGCAGCGCTGCTG
	<i>yjcC</i> -ala R	CAGCAGCGCTGCCGCCCAACGCAGCGG
Promoter constructs		
P_{yjc0}	415p(BamHI)-F	AAGGATTGTGGACGACCTGGCGCGACTG
	415p(BglII)-R	ATAGATCTTTACGCTTACATCCATGCGA
P_{yjc1}	525p(BamHI)-F	AAGGATTGTGGACGACCTGGCGCGACTG
	525p(BglII)-R	AGATCTGTCTTAGCGCCTTATGCG
P_{yjc2}	385p(BamHI)-F	GGATCCTGTGGATATTGGTGAGC
	385p(BglII)-R	AGATCTGTCTTAGCGCCTTATGCG
Quantitative RT-PCR		
23S	F	AGCGACTAAGCGTACACGGTGG
	R	GATGTTTCAGTTCCCCCGGTTT
<i>soxR</i>	F	AATCACCCCGCATCAAATGCTG
	R	CAGCGGGATGCCAATACGTTG
<i>soxS</i>	F	AGCGGATGTTCCGTACCGTGATG
	R	AGAAGGTTTGCTGCGAGACGTAGC
<i>rpoS</i>	F	AGACGCGGAATTTGATGAGAACG
	R	AGCTGAGTGGCGTCAAGTACGC
<i>yjcC</i>	F	ATGGGTGACAGTGCGCCGCATAAG
	R	TCGGCTTTAGCCCCGAGCT
<i>mrkA</i>	F	TAACGGCCAGGGCAGCATG
	R	AGCCAGCAGGTTACCGCCGG
<i>mrkH</i>	F	ACCCAAGTACGCGCGTG
	R	GCGACGCTGCACTACCTGCA
<i>mrkI</i>	F	TCTATCGTCCAGCGCGCCA
	R	TGGATGCGGTGGCTATGAACC

Reference

1. Chang FY, Chou MY, Fan RL, Shaio MF (1988) A clinical study of Klebsiella liver abscess. *Taiwan Yi Xue Hui Za Zhi* 87: 282-287.
2. Chang FY, Chou MY (1995) Comparison of pyogenic liver abscesses caused by Klebsiella pneumoniae and non-K. pneumoniae pathogens. *J Formos Med Assoc* 94: 232-237.
3. Liu YC, Cheng DL, Lin CL (1986) Klebsiella pneumoniae liver abscess associated with septic endophthalmitis. *Arch Intern Med* 146: 1913-1916.
4. Fang CT, Chuang YP, Shun CT, Chang SC, Wang JT (2004) A novel virulence gene in Klebsiella pneumoniae strains causing primary liver abscess and septic metastatic complications. *J Exp Med* 199: 697-705.
5. Hawkey PM (2008) Prevalence and clonality of extended-spectrum beta-lactamases in Asia. *Clin Microbiol Infect* 14 Suppl 1: 159-165.
6. Saccente M (1999) Klebsiella pneumoniae liver abscess, endophthalmitis, and meningitis in a man with newly recognized diabetes mellitus. *Clin Infect Dis* 29: 1570-1571.
7. Yu WL, Chan KS, Ko WC, Lee CC, Chuang YC (2007) Lower prevalence of diabetes mellitus in patients with Klebsiella pneumoniae primary liver abscess caused by isolates of K1/K2 than with non-K1/K2 capsular serotypes. *Clin Infect Dis* 45: 1529-1530; author reply 1532-1523.
8. Nadasy KA, Domiati-Saad R, Tribble MA (2007) Invasive Klebsiella pneumoniae syndrome in North America. *Clin Infect Dis* 45: e25-28.
9. Karama EM, Willermann F, Janssens X, Claus M, Van den Wijngaert S, et al. (2008) Endogenous endophthalmitis complicating Klebsiella pneumoniae liver abscess in Europe: case report. *Int Ophthalmol* 28: 111-113.
10. Meric de Bellefon L, Legrand JC, Codden T, Carlier E, Vanhaeverbeek M (2007) [Klebsiella pneumoniae septicemia and meningitis in a diabetic patient with an hepatic abscess]. *Rev Med Brux* 28: 460-463.
11. Sobirk SK, Struve C, Jacobsson SG (2010) Primary Klebsiella pneumoniae Liver Abscess with Metastatic Spread to Lung and Eye, a North-European Case Report of an Emerging Syndrome. *Open Microbiol J* 4: 5-7.
12. Merlet A, Cazanave C, Dutronc H, de Barbeyrac B, Brisse S, et al. (2012) Primary

- liver abscess due to CC23-K1 virulent clone of *Klebsiella pneumoniae* in France. *Clin Microbiol Infect* 18: E338-339.
13. Curiao T, Morosini MI, Ruiz-Garbajosa P, Robustillo A, Baquero F, et al. (2010) Emergence of bla KPC-3-Tn4401a associated with a pKPN3/4-like plasmid within ST384 and ST388 *Klebsiella pneumoniae* clones in Spain. *J Antimicrob Chemother* 65: 1608-1614.
 14. Decre D, Verdet C, Emirian A, Le Gourrierec T, Petit JC, et al. (2011) Emerging severe and fatal infections due to *Klebsiella pneumoniae* in two university hospitals in France. *J Clin Microbiol* 49: 3012-3014.
 15. Rahimian J, Wilson T, Oram V, Holzman RS (2004) Pyogenic liver abscess: recent trends in etiology and mortality. *Clin Infect Dis* 39: 1654-1659.
 16. Yeh KM, Kurup A, Siu LK, Koh YL, Fung CP, et al. (2007) Capsular serotype K1 or K2, rather than magA and rmpA, is a major virulence determinant for *Klebsiella pneumoniae* liver abscess in Singapore and Taiwan. *J Clin Microbiol* 45: 466-471.
 17. Yu WL, Ko WC, Cheng KC, Lee HC, Ke DS, et al. (2006) Association between rmpA and magA genes and clinical syndromes caused by *Klebsiella pneumoniae* in Taiwan. *Clin Infect Dis* 42: 1351-1358.
 18. Yu WL, Ko WC, Cheng KC, Lee CC, Lai CC, et al. (2008) Comparison of prevalence of virulence factors for *Klebsiella pneumoniae* liver abscesses between isolates with capsular K1/K2 and non-K1/K2 serotypes. *Diagn Microbiol Infect Dis* 62: 1-6.
 19. Lin JC, Siu LK, Fung CP, Yeh KM, Chang FY (2007) Nosocomial liver abscess caused by extended-spectrum beta-lactamase-producing *Klebsiella pneumoniae*. *J Clin Microbiol* 45: 266-269.
 20. Su SC, Siu LK, Ma L, Yeh KM, Fung CP, et al. (2008) Community-acquired liver abscess caused by serotype K1 *Klebsiella pneumoniae* with CTX-M-15-type extended-spectrum beta-lactamase. *Antimicrob Agents Chemother* 52: 804-805.
 21. Kumarasamy KK, Toleman MA, Walsh TR, Bagaria J, Butt F, et al. (2010) Emergence of a new antibiotic resistance mechanism in India, Pakistan, and the UK: a molecular, biological, and epidemiological study. *Lancet Infect Dis* 10: 597-602.

22. Sentochnik DE, Eliopoulos GM, Ferraro MJ, Moellering RC, Jr. (1989) Comparative in vitro activity of SM7338, a new carbapenem antimicrobial agent. *Antimicrob Agents Chemother* 33: 1232-1236.
23. Trautmann M, Bruckner O, Marre R, Hahn H (1986) Comparative efficacy of different beta-lactam antibiotics and gentamicin in *Klebsiella pneumoniae* septicaemia in neutropenic mice. *J Antimicrob Chemother* 18: 387-391.
24. Hernandez JR, Martinez-Martinez L, Canton R, Coque TM, Pascual A, et al. (2005) Nationwide study of *Escherichia coli* and *Klebsiella pneumoniae* producing extended-spectrum beta-lactamases in Spain. *Antimicrob Agents Chemother* 49: 2122-2125.
25. Gil-Romero Y, Sanz-Rodriguez N, Almagro-Molto M, Gomez-Garces JL (2012) [New description of a NDM-1 carbapenemase producing *Klebsiella pneumoniae* carrier in Spain.]. *Enferm Infecc Microbiol Clin*.
26. Oteo J, Domingo-Garcia D, Fernandez-Romero S, Saez D, Guiu A, et al. (2012) Abdominal abscess due to NDM-1-producing *Klebsiella pneumoniae* in Spain. *J Med Microbiol* 61: 864-867.
27. Cheng HP, Siu LK, Chang FY (2003) Extended-spectrum cephalosporin compared to cefazolin for treatment of *Klebsiella pneumoniae*-caused liver abscess. *Antimicrob Agents Chemother* 47: 2088-2092.
28. Nassif X, Fournier JM, Arondel J, Sansonetti PJ (1989) Mucoid phenotype of *Klebsiella pneumoniae* is a plasmid-encoded virulence factor. *Infect Immun* 57: 546-552.
29. Wiskur BJ, Hunt JJ, Callegan MC (2008) Hypermucoviscosity as a virulence factor in experimental *Klebsiella pneumoniae* endophthalmitis. *Invest Ophthalmol Vis Sci* 49: 4931-4938.
30. Evrard B, Balestrino D, Dosgilbert A, Bouya-Gachancard JL, Charbonnel N, et al. (2010) Roles of capsule and lipopolysaccharide O antigen in interactions of human monocyte-derived dendritic cells and *Klebsiella pneumoniae*. *Infect Immun* 78: 210-219.
31. Flannagan RS, Cosio G, Grinstein S (2009) Antimicrobial mechanisms of phagocytes and bacterial evasion strategies. *Nat Rev Microbiol* 7: 355-366.
32. Lin JC, Chang FY, Fung CP, Xu JZ, Cheng HP, et al. (2004) High prevalence of phagocytic-resistant capsular serotypes of *Klebsiella pneumoniae* in liver

- abscess. *Microbes Infect* 6: 1191-1198.
33. Campos MA, Vargas MA, Regueiro V, Llompert CM, Alberti S, et al. (2004) Capsule polysaccharide mediates bacterial resistance to antimicrobial peptides. *Infect Immun* 72: 7107-7114.
 34. Llobet E, Tomas JM, Bengoechea JA (2008) Capsule polysaccharide is a bacterial decoy for antimicrobial peptides. *Microbiology-Sgm* 154: 3877-3886.
 35. Mizuta K, Ohta M, Mori M, Hasegawa T, Nakashima I, et al. (1983) Virulence for mice of *Klebsiella* strains belonging to the O1 group: relationship to their capsular (K) types. *Infect Immun* 40: 56-61.
 36. Pan YJ, Fang HC, Yang HC, Lin TL, Hsieh PF, et al. (2008) Capsular polysaccharide synthesis regions in *Klebsiella pneumoniae* serotype K57 and a new capsular serotype. *J Clin Microbiol* 46: 2231-2240.
 37. Turton JF, Baklan H, Siu LK, Kaufmann ME, Pitt TL (2008) Evaluation of a multiplex PCR for detection of serotypes K1, K2 and K5 in *Klebsiella* sp. and comparison of isolates within these serotypes. *FEMS Microbiol Lett* 284: 247-252.
 38. Hsu CR, Lin TL, Chen YC, Chou HC, Wang JT (2011) The role of *Klebsiella pneumoniae* *rmpA* in capsular polysaccharide synthesis and virulence revisited. *Microbiology* 157: 3446-3457.
 39. Lai YC, Peng HL, Chang HY (2003) *RmpA2*, an activator of capsule biosynthesis in *Klebsiella pneumoniae* CG43, regulates K2 *cps* gene expression at the transcriptional level. *J Bacteriol* 185: 788-800.
 40. Podschun R, Ullmann U (1998) *Klebsiella* spp. as nosocomial pathogens: epidemiology, taxonomy, typing methods, and pathogenicity factors. *Clin Microbiol Rev* 11: 589-603.
 41. Hsieh PF, Lin TL, Lee CZ, Tsai SF, Wang JT (2008) Serum-induced iron-acquisition systems and TonB contribute to virulence in *Klebsiella pneumoniae* causing primary pyogenic liver abscess. *J Infect Dis* 197: 1717-1727.
 42. Lin CT, Wu CC, Chen YS, Lai YC, Chi C, et al. (2011) Fur regulation of the capsular polysaccharide biosynthesis and iron-acquisition systems in *Klebsiella pneumoniae* CG43. *Microbiology* 157: 419-429.

43. Hirakawa H, Nishino K, Yamada J, Hirata T, Yamaguchi A (2003) Beta-lactam resistance modulated by the overexpression of response regulators of two-component signal transduction systems in *Escherichia coli*. *J Antimicrob Chemother* 52: 576-582.
44. Hancock RE (1997) Peptide antibiotics. *Lancet* 349: 418-422.
45. Zavascki AP, Goldani LZ, Li J, Nation RL (2007) Polymyxin B for the treatment of multidrug-resistant pathogens: a critical review. *J Antimicrob Chemother* 60: 1206-1215.
46. Stahlhut SG, Tchesnokova V, Struve C, Weissman SJ, Chattopadhyay S, et al. (2009) Comparative structure-function analysis of mannose-specific FimH adhesins from *Klebsiella pneumoniae* and *Escherichia coli*. *J Bacteriol* 191: 6592-6601.
47. Struve C, Bojer M, Krogfelt KA (2008) Characterization of *Klebsiella pneumoniae* type 1 fimbriae by detection of phase variation during colonization and infection and impact on virulence. *Infect Immun* 76: 4055-4065.
48. Struve C, Bojer M, Krogfelt KA (2009) Identification of a conserved chromosomal region encoding *Klebsiella pneumoniae* type 1 and type 3 fimbriae and assessment of the role of fimbriae in pathogenicity. *Infect Immun* 77: 5016-5024.
49. Hanson MS, Hempel J, Brinton CC, Jr. (1988) Purification of the *Escherichia coli* type 1 pilin and minor pilus proteins and partial characterization of the adhesin protein. *J Bacteriol* 170: 3350-3358.
50. Klemm P, Schembri MA (2000) Bacterial adhesins: function and structure. *Int J Med Microbiol* 290: 27-35.
51. Wright KJ, Seed PC, Hultgren SJ (2007) Development of intracellular bacterial communities of uropathogenic *Escherichia coli* depends on type 1 pili. *Cell Microbiol* 9: 2230-2241.
52. Zavialov A, Zav'yalova G, Korpela T, Zav'yalov V (2007) FGL chaperone-assembled fimbrial polyadhesins: anti-immune armament of Gram-negative bacterial pathogens. *FEMS Microbiol Rev* 31: 478-514.
53. Connell I, Agace W, Klemm P, Schembri M, Marild S, et al. (1996) Type 1 fimbrial expression enhances *Escherichia coli* virulence for the urinary tract.

Proc Natl Acad Sci U S A 93: 9827-9832.

54. Kil KS, Darouiche RO, Hull RA, Mansouri MD, Musher DM (1997) Identification of a *Klebsiella pneumoniae* strain associated with nosocomial urinary tract infection. *J Clin Microbiol* 35: 2370-2374.
55. Mulvey MA, Lopez-Boado YS, Wilson CL, Roth R, Parks WC, et al. (1998) Induction and evasion of host defenses by type 1-piliated uropathogenic *Escherichia coli*. *Science* 282: 1494-1497.
56. Rosen DA, Pinkner JS, Jones JM, Walker JN, Clegg S, et al. (2008) Utilization of an intracellular bacterial community pathway in *Klebsiella pneumoniae* urinary tract infection and the effects of FimK on type 1 pilus expression. *Infect Immun* 76: 3337-3345.
57. Sokurenko EV, Chesnokova V, Dykhuizen DE, Ofek I, Wu XR, et al. (1998) Pathogenic adaptation of *Escherichia coli* by natural variation of the FimH adhesin. *Proc Natl Acad Sci U S A* 95: 8922-8926.
58. Wang ZC, Huang CJ, Huang YJ, Wu CC, Peng HL (2013) FimK regulation on the expression of type 1 fimbriae in *Klebsiella pneumoniae* CG43S3. *Microbiology*.
59. Duguid JP (1959) Fimbriae and adhesive properties in *Klebsiella* strains. *J Gen Microbiol* 21: 271-286.
60. Boddicker JD, Anderson RA, Jagnow J, Clegg S (2006) Signature-tagged mutagenesis of *Klebsiella pneumoniae* to identify genes that influence biofilm formation on extracellular matrix material. *Infect Immun* 74: 4590-4597.
61. Burmolle M, Bahl MI, Jensen LB, Sorensen SJ, Hansen LH (2008) Type 3 fimbriae, encoded by the conjugative plasmid pOLA52, enhance biofilm formation and transfer frequencies in *Enterobacteriaceae* strains. *Microbiology* 154: 187-195.
62. Di Martino P, Cafferini N, Joly B, Darfeuille-Michaud A (2003) *Klebsiella pneumoniae* type 3 pili facilitate adherence and biofilm formation on abiotic surfaces. *Res Microbiol* 154: 9-16.
63. Jagnow J, Clegg S (2003) *Klebsiella pneumoniae* MrkD-mediated biofilm formation on extracellular matrix- and collagen-coated surfaces. *Microbiology* 149: 2397-2405.

64. Langstraat J, Bohse M, Clegg S (2001) Type 3 fimbrial shaft (MrkA) of *Klebsiella pneumoniae*, but not the fimbrial adhesin (MrkD), facilitates biofilm formation. *Infect Immun* 69: 5805-5812.
65. Ong CL, Beatson SA, Totsika M, Forestier C, McEwan AG, et al. (2010) Molecular analysis of type 3 fimbrial genes from *Escherichia coli*, *Klebsiella* and *Citrobacter* species. *BMC Microbiol* 10: 183.
66. Ong CL, Ulett GC, Mabbett AN, Beatson SA, Webb RI, et al. (2008) Identification of type 3 fimbriae in uropathogenic *Escherichia coli* reveals a role in biofilm formation. *J Bacteriol* 190: 1054-1063.
67. Ross P, Weinhouse H, Aloni Y, Michaeli D, Weinberger-Ohana P, et al. (1987) Regulation of cellulose synthesis in *Acetobacter xylinum* by cyclic diguanylic acid. *Nature* 325: 279-281.
68. D'Argenio DA, Miller SI (2004) Cyclic di-GMP as a bacterial second messenger. *Microbiology* 150: 2497-2502.
69. Romling U, Amikam D (2006) Cyclic di-GMP as a second messenger. *Curr Opin Microbiol* 9: 218-228.
70. Romling U, Galperin MY, Gomelsky M (2013) Cyclic di-GMP: the first 25 years of a universal bacterial second messenger. *Microbiol Mol Biol Rev* 77: 1-52.
71. Romling U, Gomelsky M, Galperin MY (2005) C-di-GMP: the dawning of a novel bacterial signalling system. *Mol Microbiol* 57: 629-639.
72. Chan C, Paul R, Samoray D, Amiot NC, Giese B, et al. (2004) Structural basis of activity and allosteric control of diguanylate cyclase. *Proc Natl Acad Sci U S A* 101: 17084-17089.
73. Schmidt AJ, Ryjenkov DA, Gomelsky M (2005) The ubiquitous protein domain EAL is a cyclic diguanylate-specific phosphodiesterase: Enzymatically active and inactive EAL domains. *Journal of Bacteriology* 187: 4774-4781.
74. Ausmees N, Mayer R, Weinhouse H, Volman G, Amikam D, et al. (2001) Genetic data indicate that proteins containing the GGDEF domain possess diguanylate cyclase activity. *FEMS Microbiol Lett* 204: 163-167.
75. Petersen E, Chaudhuri P, Gourley C, Harms J, Splitter G (2011) *Brucella melitensis* cyclic di-GMP phosphodiesterase BpdA controls expression of flagellar genes. *J Bacteriol* 193: 5683-5691.

76. Shanahan CA, Strobel SA (2012) The bacterial second messenger c-di-GMP: probing interactions with protein and RNA binding partners using cyclic dinucleotide analogs. *Org Biomol Chem* 10: 9113-9129.
77. Galperin MY, Nikolskaya AN, Koonin EV (2001) Novel domains of the prokaryotic two-component signal transduction systems. *FEMS Microbiol Lett* 203: 11-21.
78. Taylor BL, Zhulin IB (1999) PAS domains: internal sensors of oxygen, redox potential, and light. *Microbiol Mol Biol Rev* 63: 479-506.
79. Aldridge P, Paul R, Goymer P, Rainey P, Jenal U (2003) Role of the GGDEF regulator PleD in polar development of *Caulobacter crescentus*. *Mol Microbiol* 47: 1695-1708.
80. Simm R, Morr M, Kader A, Nimtz M, Romling U (2004) GGDEF and EAL domains inversely regulate cyclic di-GMP levels and transition from sessility to motility. *Mol Microbiol* 53: 1123-1134.
81. Ryan RP, Fouhy Y, Lucey JF, Dow JM (2006) Cyclic di-GMP signaling in bacteria: recent advances and new puzzles. *J Bacteriol* 188: 8327-8334.
82. Meissner A, Wild V, Simm R, Rohde M, Erck C, et al. (2007) *Pseudomonas aeruginosa* cupA-encoded fimbriae expression is regulated by a GGDEF and EAL domain-dependent modulation of the intracellular level of cyclic diguanylate. *Environ Microbiol* 9: 2475-2485.
83. Ryan RP, Dow JM (2010) Cell-cell signal dependent dynamic interactions between HD-GYP and GGDEF domain proteins mediate virulence in *Xanthomonas campestris*. *Virulence* 1: 404-408.
84. Amikam D, Galperin MY (2006) PilZ domain is part of the bacterial c-di-GMP binding protein. *Bioinformatics* 22: 3-6.
85. Ryjenkov DA, Simm R, Romling U, Gomelsky M (2006) The PilZ domain is a receptor for the second messenger c-di-GMP: the PilZ domain protein YcgR controls motility in enterobacteria. *J Biol Chem* 281: 30310-30314.
86. Ryan RP, Tolker-Nielsen T, Dow JM (2012) When the PilZ don't work: effectors for cyclic di-GMP action in bacteria. *Trends Microbiol* 20: 235-242.
87. Guzzo CR, Salinas RK, Andrade MO, Farah CS (2009) PILZ protein structure and interactions with PILB and the FIMX EAL domain: implications for control of

- type IV pilus biogenesis. *J Mol Biol* 393: 848-866.
88. Lee VT, Matewish JM, Kessler JL, Hyodo M, Hayakawa Y, et al. (2007) A cyclic-di-GMP receptor required for bacterial exopolysaccharide production. *Mol Microbiol* 65: 1474-1484.
 89. Steiner S, Lori C, Boehm A, Jenal U (2013) Allosteric activation of exopolysaccharide synthesis through cyclic di-GMP-stimulated protein-protein interaction. *EMBO J* 32: 354-368.
 90. Kuchma SL, Brothers KM, Merritt JH, Liberati NT, Ausubel FM, et al. (2007) BifA, a cyclic-Di-GMP phosphodiesterase, inversely regulates biofilm formation and swarming motility by *Pseudomonas aeruginosa* PA14. *J Bacteriol* 189: 8165-8178.
 91. Johnson JG, Clegg S (2010) Role of MrkJ, a phosphodiesterase, in type 3 fimbrial expression and biofilm formation in *Klebsiella pneumoniae*. *J Bacteriol* 192: 3944-3950.
 92. Zogaj X, Wyatt GC, Klose KE (2012) Cyclic di-GMP stimulates biofilm formation and inhibits virulence of *Francisella novicida*. *Infect Immun* 80: 4239-4247.
 93. Sisti F, Ha DG, O'Toole GA, Hozbor D, Fernandez J (2013) Cyclic-di-GMP signalling regulates motility and biofilm formation in *Bordetella bronchiseptica*. *Microbiology* 159: 869-879.
 94. Jain R, Behrens AJ, Kaefer V, Kazmierczak BI (2012) Type IV pilus assembly in *Pseudomonas aeruginosa* over a broad range of cyclic di-GMP concentrations. *J Bacteriol* 194: 4285-4294.
 95. Van Parys A, Boyen F, Volf J, Verbrugge E, Leyman B, et al. (2010) *Salmonella* Typhimurium resides largely as an extracellular pathogen in porcine tonsils, independently of biofilm-associated genes *csgA*, *csgD* and *adrA*. *Vet Microbiol* 144: 93-99.
 96. Frye J, Karlinsey JE, Felise HR, Marzolf B, Dowidar N, et al. (2006) Identification of new flagellar genes of *Salmonella enterica* serovar Typhimurium. *J Bacteriol* 188: 2233-2243.
 97. Girgis HS, Liu Y, Ryu WS, Tavazoie S (2007) A comprehensive genetic characterization of bacterial motility. *PLoS Genet* 3: 1644-1660.

98. Zorraquino V, Garcia B, Latasa C, Echeverz M, Toledo-Arana A, et al. (2013) Coordinated cyclic-di-GMP repression of Salmonella motility through YcgR and cellulose. *J Bacteriol* 195: 417-428.
99. Paul K, Nieto V, Carlquist WC, Blair DF, Harshey RM (2010) The c-di-GMP binding protein YcgR controls flagellar motor direction and speed to affect chemotaxis by a "backstop brake" mechanism. *Mol Cell* 38: 128-139.
100. Claret L, Miquel S, Vieille N, Ryjenkov DA, Gomelsky M, et al. (2007) The flagellar sigma factor FliA regulates adhesion and invasion of Crohn disease-associated Escherichia coli via a cyclic dimeric GMP-dependent pathway. *J Biol Chem* 282: 33275-33283.
101. Borlee BR, Goldman AD, Murakami K, Samudrala R, Wozniak DJ, et al. (2010) Pseudomonas aeruginosa uses a cyclic-di-GMP-regulated adhesin to reinforce the biofilm extracellular matrix. *Mol Microbiol* 75: 827-842.
102. Ryan RP, Fouhy Y, Lucey JF, Jiang BL, He YQ, et al. (2007) Cyclic di-GMP signalling in the virulence and environmental adaptation of Xanthomonas campestris. *Mol Microbiol* 63: 429-442.
103. Bruggemann H, Hagman A, Jules M, Sismeiro O, Dillies MA, et al. (2006) Virulence strategies for infecting phagocytes deduced from the in vivo transcriptional program of Legionella pneumophila. *Cell Microbiol* 8: 1228-1240.
104. Lai TH, Kumagai Y, Hyodo M, Hayakawa Y, Rikihisa Y (2009) The Anaplasma phagocytophilum PleC histidine kinase and PleD diguanylate cyclase two-component system and role of cyclic Di-GMP in host cell infection. *J Bacteriol* 191: 693-700.
105. Romling U (2009) Cyclic Di-GMP (c-Di-GMP) goes into host cells--c-Di-GMP signaling in the obligate intracellular pathogen Anaplasma phagocytophilum. *J Bacteriol* 191: 683-686.
106. Dey AK, Bhagat A, Chowdhury R (2013) Host cell contact induces expression of virulence factors and VieA, a cyclic di-GMP phosphodiesterase, in Vibrio cholerae. *J Bacteriol* 195: 2004-2010.
107. Kazmierczak BI, Lebron MB, Murray TS (2006) Analysis of FimX, a phosphodiesterase that governs twitching motility in Pseudomonas aeruginosa. *Mol Microbiol* 60: 1026-1043.

108. Malone JG, Jaeger T, Spangler C, Ritz D, Spang A, et al. (2010) YfiBNR mediates cyclic di-GMP dependent small colony variant formation and persistence in *Pseudomonas aeruginosa*. *PLoS Pathog* 6: e1000804.
109. Slater H, Alvarez-Morales A, Barber CE, Daniels MJ, Dow JM (2000) A two-component system involving an HD-GYP domain protein links cell-cell signalling to pathogenicity gene expression in *Xanthomonas campestris*. *Mol Microbiol* 38: 986-1003.
110. Simm R, Remminghorst U, Ahmad I, Zakikhany K, Romling U (2009) A role for the EAL-like protein STM1344 in regulation of CsgD expression and motility in *Salmonella enterica* serovar Typhimurium. *J Bacteriol* 191: 3928-3937.
111. Tal R, Wong HC, Calhoun R, Gelfand D, Fear AL, et al. (1998) Three *cdg* operons control cellular turnover of cyclic di-GMP in *Acetobacter xylinum*: genetic organization and occurrence of conserved domains in isoenzymes. *J Bacteriol* 180: 4416-4425.
112. Wu KM, Li LH, Yan JJ, Tsao N, Liao TL, et al. (2009) Genome sequencing and comparative analysis of *Klebsiella pneumoniae* NTUH-K2044, a strain causing liver abscess and meningitis. *J Bacteriol* 191: 4492-4501.
113. Punta M, Coggill PC, Eberhardt RY, Mistry J, Tate J, et al. (2012) The Pfam protein families database. *Nucleic Acids Res* 40: D290-301.
114. Barends TR, Hartmann E, Griese JJ, Beitlich T, Kirienko NV, et al. (2009) Structure and mechanism of a bacterial light-regulated cyclic nucleotide phosphodiesterase. *Nature* 459: 1015-1018.
115. Lai YC, Peng HL, Chang HY (2001) Identification of genes induced in vivo during *Klebsiella pneumoniae* CG43 infection. *Infect Immun* 69: 7140-7145.
116. Chang W, Small DA, Toghrol F, Bentley WE (2005) Microarray analysis of *Pseudomonas aeruginosa* reveals induction of pyocin genes in response to hydrogen peroxide. *BMC Genomics* 6: 115.
117. Imlay JA (2003) Pathways of oxidative damage. *Annu Rev Microbiol* 57: 395-418.
118. Imlay JA (2008) Cellular defenses against superoxide and hydrogen peroxide. *Annu Rev Biochem* 77: 755-776.
119. Pomposiello PJ, Demple B (2001) Redox-operated genetic switches: the SoxR

- and OxyR transcription factors. *Trends Biotechnol* 19: 109-114.
120. Benov LT, Fridovich I (1994) *Escherichia coli* expresses a copper- and zinc-containing superoxide dismutase. *J Biol Chem* 269: 25310-25314.
 121. McCord JM, Fridovich I (1969) Superoxide dismutase. An enzymic function for erythrocyte hemocuprein (hemocuprein). *J Biol Chem* 244: 6049-6055.
 122. Palma M, Zurita J, Ferreras JA, Worgall S, Larone DH, et al. (2005) *Pseudomonas aeruginosa* SoxR does not conform to the archetypal paradigm for SoxR-dependent regulation of the bacterial oxidative stress adaptive response. *Infect Immun* 73: 2958-2966.
 123. Lushchak VI (2001) Oxidative stress and mechanisms of protection against it in bacteria. *Biochemistry (Mosc)* 66: 476-489.
 124. Park SJ, Gunsalus RP (1995) Oxygen, iron, carbon, and superoxide control of the fumarase *fumA* and *fumC* genes of *Escherichia coli*: role of the *arcA*, *fnr*, and *soxR* gene products. *J Bacteriol* 177: 6255-6262.
 125. Park KJ, Kang MJ, Kim SH, Lee HJ, Lim JK, et al. (2004) Isolation and characterization of *rpoS* from a pathogenic bacterium, *Vibrio vulnificus*: role of sigmaS in survival of exponential-phase cells under oxidative stress. *J Bacteriol* 186: 3304-3312.
 126. Peterson CN, Carabetta VJ, Chowdhury T, Silhavy TJ (2006) LrhA regulates *rpoS* translation in response to the Rcs phosphorelay system in *Escherichia coli*. *J Bacteriol* 188: 3175-3181.
 127. Repoila F, Majdalani N, Gottesman S (2003) Small non-coding RNAs, co-ordinators of adaptation processes in *Escherichia coli*: the RpoS paradigm. *Mol Microbiol* 48: 855-861.
 128. Lin CT, Peng HL (2006) Regulation of the homologous two-component systems KvgAS and KvhAS in *Klebsiella pneumoniae* CG43. *J Biochem* 140: 639-648.
 129. Velculescu VE, Zhang L, Vogelstein B, Kinzler KW (1995) Serial analysis of gene expression. *Science* 270: 484-487.
 130. Schena M, Shalon D, Davis RW, Brown PO (1995) Quantitative monitoring of gene expression patterns with a complementary DNA microarray. *Science* 270: 467-470.

131. Adams MD, Kerlavage AR, Fleischmann RD, Fuldner RA, Bult CJ, et al. (1995) Initial assessment of human gene diversity and expression patterns based upon 83 million nucleotides of cDNA sequence. *Nature* 377: 3-174.
132. Mardis ER (2008) Next-generation DNA sequencing methods. *Annu Rev Genomics Hum Genet* 9: 387-402.
133. Wold B, Myers RM (2008) Sequence census methods for functional genomics. *Nat Methods* 5: 19-21.
134. Sultan M, Schulz MH, Richard H, Magen A, Klingenhoff A, et al. (2008) A global view of gene activity and alternative splicing by deep sequencing of the human transcriptome. *Science* 321: 956-960.
135. Mortazavi A, Williams BA, McCue K, Schaeffer L, Wold B (2008) Mapping and quantifying mammalian transcriptomes by RNA-Seq. *Nat Methods* 5: 621-628.
136. Acuna LG, Calderon IL, Elias AO, Castro ME, Vasquez CC (2009) Expression of the *yggE* gene protects *Escherichia coli* from potassium tellurite-generated oxidative stress. *Arch Microbiol* 191: 473-476.
137. Perez JM, Arenas FA, Pradenas GA, Sandoval JM, Vasquez CC (2008) *Escherichia coli* YqhD exhibits aldehyde reductase activity and protects from the harmful effect of lipid peroxidation-derived aldehydes. *J Biol Chem* 283: 7346-7353.
138. Perez JM, Calderon IL, Arenas FA, Fuentes DE, Pradenas GA, et al. (2007) Bacterial toxicity of potassium tellurite: unveiling an ancient enigma. *PLoS One* 2: e211.
139. Niederhoffer EC, Naranjo CM, Bradley KL, Fee JA (1990) Control of *Escherichia coli* superoxide dismutase (*sodA* and *sodB*) genes by the ferric uptake regulation (*fur*) locus. *J Bacteriol* 172: 1930-1938.
140. Farr SB, Kogoma T (1991) Oxidative stress responses in *Escherichia coli* and *Salmonella typhimurium*. *Microbiol Rev* 55: 561-585.
141. Semchyshyn H, Bagnyukova T, Storey K, Lushchak V (2005) Hydrogen peroxide increases the activities of *soxRS* regulon enzymes and the levels of oxidized proteins and lipids in *Escherichia coli*. *Cell Biol Int* 29: 898-902.
142. Zheng M, Doan B, Schneider TD, Storz G (1999) OxyR and SoxRS regulation of

- fur. *J Bacteriol* 181: 4639-4643.
143. Chattopadhyay S, Wu Y, Datta P (1997) Involvement of Fnr and ArcA in anaerobic expression of the *tdc* operon of *Escherichia coli*. *J Bacteriol* 179: 4868-4873.
 144. Lacey MM, Partridge JD, Green J (2010) *Escherichia coli* K-12 YfgF is an anaerobic cyclic di-GMP phosphodiesterase with roles in cell surface remodelling and the oxidative stress response. *Microbiology* 156: 2873-2886.
 145. Chin KH, Lee YC, Tu ZL, Chen CH, Tseng YH, et al. The cAMP receptor-like protein CLP is a novel c-di-GMP receptor linking cell-cell signaling to virulence gene expression in *Xanthomonas campestris*. *J Mol Biol* 396: 646-662.
 146. Wilksch JJ, Yang J, Clements A, Gabbe JL, Short KR, et al. MrkH, a novel c-di-GMP-dependent transcriptional activator, controls *Klebsiella pneumoniae* biofilm formation by regulating type 3 fimbriae expression. *PLoS Pathog* 7: e1002204.
 147. Li TN, Chin KH, Liu JH, Wang AH, Chou SH (2009) XC1028 from *Xanthomonas campestris* adopts a PilZ domain-like structure without a c-di-GMP switch. *Proteins* 75: 282-288.
 148. Krasteva PV, Fong JC, Shikuma NJ, Beyhan S, Navarro MV, et al. *Vibrio cholerae* VpsT regulates matrix production and motility by directly sensing cyclic di-GMP. *Science* 327: 866-868.
 149. Hisert KB, MacCoss M, Shiloh MU, Darwin KH, Singh S, et al. (2005) A glutamate-alanine-leucine (EAL) domain protein of *Salmonella* controls bacterial survival in mice, antioxidant defence and killing of macrophages: role of cyclic diGMP. *Mol Microbiol* 56: 1234-1245.
 150. Keynan Y, Karlowsky JA, Walus T, Rubinstein E (2007) Pyogenic liver abscess caused by hypermucoviscous *Klebsiella pneumoniae*. *Scand J Infect Dis* 39: 828-830.
 151. Wu MC, Lin TL, Hsieh PF, Yang HC, Wang JT Isolation of genes involved in biofilm formation of a *Klebsiella pneumoniae* strain causing pyogenic liver abscess. *PLoS One* 6: e23500.
 152. Lin CT, Huang TY, Liang WC, Peng HL (2006) Homologous response regulators KvgA, KvhA and KvhR regulate the synthesis of capsular polysaccharide in

- Klebsiella pneumoniae* CG43 in a coordinated manner. *J Biochem* 140: 429-438.
153. Lin CT, Wu CC, Chen YS, Lai YC, Chi C, et al. Fur regulation of the capsular polysaccharide biosynthesis and iron-acquisition systems in *Klebsiella pneumoniae* CG43. *Microbiology* 157: 419-429.
 154. Sahly H, Podschun R, Oelschlaeger TA, Greiwe M, Parolis H, et al. (2000) Capsule impedes adhesion to and invasion of epithelial cells by *Klebsiella pneumoniae*. *Infect Immun* 68: 6744-6749.
 155. Spurbeck RR, Tarrien RJ, Mobley HL Enzymatically Active and Inactive Phosphodiesterases and Diguanylate Cyclases Are Involved in Regulation of Motility or Sessility in *Escherichia coli* CFT073. *MBio* 3.
 156. Reents H, Munch R, Dammeyer T, Jahn D, Hartig E (2006) The Fnr regulon of *Bacillus subtilis*. *J Bacteriol* 188: 1103-1112.
 157. Johnson JG, Clegg S (2011) Role of MrkJ, a phosphodiesterase, in type 3 fimbrial expression and biofilm formation in *Klebsiella pneumoniae*. *J Bacteriol* 192: 3944-3950.
 158. Dubrac S, Touati D (2000) Fur positive regulation of iron superoxide dismutase in *Escherichia coli*: functional analysis of the *sodB* promoter. *J Bacteriol* 182: 3802-3808.
 159. Italiani VC, da Silva Neto JF, Braz VS, Marques MV Regulation of catalase-peroxidase *KatG* is OxyR dependent and Fur independent in *Caulobacter crescentus*. *J Bacteriol* 193: 1734-1744.
 160. Tanaka K, Handel K, Loewen PC, Takahashi H (1997) Identification and analysis of the *rpoS*-dependent promoter of *katE*, encoding catalase HPII in *Escherichia coli*. *Biochim Biophys Acta* 1352: 161-166.
 161. Visick JE, Clarke S (1997) RpoS- and OxyR-independent induction of HPI catalase at stationary phase in *Escherichia coli* and identification of *rpoS* mutations in common laboratory strains. *J Bacteriol* 179: 4158-4163.
 162. Prieto-Alamo MJ, Jurado J, Gallardo-Madueno R, Monje-Casas F, Holmgren A, et al. (2000) Transcriptional regulation of glutaredoxin and thioredoxin pathways and related enzymes in response to oxidative stress. *J Biol Chem* 275: 13398-13405.

163. Renzette N, Gumlaw N, Sandler SJ (2007) DinI and RecX modulate RecA-DNA structures in *Escherichia coli* K-12. *Mol Microbiol* 63: 103-115.
164. Kitagawa M, Matsumura Y, Tsuchido T (2000) Small heat shock proteins, IbpA and IbpB, are involved in resistances to heat and superoxide stresses in *Escherichia coli*. *FEMS Microbiol Lett* 184: 165-171.
165. Nagy M, Guenther I, Akoyev V, Barnett ME, Zavodszky MI, et al. Synergistic cooperation between two ClpB isoforms in aggregate reactivation. *J Mol Biol* 396: 697-707.
166. Jovanovic G, Engl C, Mayhew AJ, Burrows PC, Buck M Properties of the phage-shock-protein (Psp) regulatory complex that govern signal transduction and induction of the Psp response in *Escherichia coli*. *Microbiology* 156: 2920-2932.
167. Membrillo-Hernandez J, Kim SO, Cook GM, Poole RK (1997) Paraquat regulation of hmp (flavo-hemoglobin) gene expression in *Escherichia coli* K-12 is SoxRS independent but modulated by sigma S. *J Bacteriol* 179: 3164-3170.
168. Koh YS, Roe JH (1995) Isolation of a novel paraquat-inducible (pqi) gene regulated by the soxRS locus in *Escherichia coli*. *J Bacteriol* 177: 2673-2678.
169. Liochev SI, Hausladen A, Beyer WF, Jr., Fridovich I (1994) NADPH: ferredoxin oxidoreductase acts as a paraquat diaphorase and is a member of the soxRS regulon. *Proc Natl Acad Sci U S A* 91: 1328-1331.
170. Sommerfeldt N, Possling A, Becker G, Pesavento C, Tschowri N, et al. (2009) Gene expression patterns and differential input into curli fimbriae regulation of all GGDEF/EAL domain proteins in *Escherichia coli*. *Microbiology* 155: 1318-1331.
171. Tolla DA, Savageau MA Regulation of aerobic-to-anaerobic transitions by the FNR cycle in *Escherichia coli*. *J Mol Biol* 397: 893-905.
172. Cruz DP, Huertas MG, Lozano M, Zarate L, Zambrano MM (2012) Comparative analysis of diguanylate cyclase and phosphodiesterase genes in *Klebsiella pneumoniae*. *BMC Microbiol* 12: 139.
173. Zhulin IB, Nikolskaya AN, Galperin MY (2003) Common extracellular sensory domains in transmembrane receptors for diverse signal transduction pathways in bacteria and archaea. *J Bacteriol* 185: 285-294.

174. Huang B, Whitchurch CB, Mattick JS (2003) FimX, a multidomain protein connecting environmental signals to twitching motility in *Pseudomonas aeruginosa*. *J Bacteriol* 185: 7068-7076.
175. Meyer Y, Buchanan BB, Vignols F, Reichheld JP (2009) Thioredoxins and glutaredoxins: unifying elements in redox biology. *Annu Rev Genet* 43: 335-367.
176. Caldas T, Malki A, Kern R, Abdallah J, Richarme G (2006) The *Escherichia coli* thioredoxin homolog YbbN/Trxsc is a chaperone and a weak protein oxidoreductase. *Biochem Biophys Res Commun* 343: 780-786.
177. Thomas JG, Baneyx F (2000) ClpB and HtpG facilitate de novo protein folding in stressed *Escherichia coli* cells. *Mol Microbiol* 36: 1360-1370.
178. Tseng CP (1997) Regulation of fumarase (fumB) gene expression in *Escherichia coli* in response to oxygen, iron and heme availability: role of the arcA, fur, and hemA gene products. *FEMS Microbiol Lett* 157: 67-72.
179. Tseng CP, Yu CC, Lin HH, Chang CY, Kuo JT (2001) Oxygen- and growth rate-dependent regulation of *Escherichia coli* fumarase (FumA, FumB, and FumC) activity. *J Bacteriol* 183: 461-467.
180. Zahringer F, Massa C, Schirmer T (2011) Efficient enzymatic production of the bacterial second messenger c-di-GMP by the diguanylate cyclase YdeH from *E. coli*. *Appl Biochem Biotechnol* 163: 71-79.
181. Fung CP, Lin YT, Lin JC, Chen TL, Yeh KM, et al. (2012) *Klebsiella pneumoniae* in gastrointestinal tract and pyogenic liver abscess. *Emerg Infect Dis* 18: 1322-1325.
182. Huang WK, Chang JW, See LC, Tu HT, Chen JS, et al. (2012) Higher rate of colorectal cancer among patients with pyogenic liver abscess with *Klebsiella pneumoniae* than those without: an 11-year follow-up study. *Colorectal Dis* 14: e794-801.
183. Wu MC, Lin TL, Hsieh PF, Yang HC, Wang JT (2011) Isolation of genes involved in biofilm formation of a *Klebsiella pneumoniae* strain causing pyogenic liver abscess. *PLoS One* 6: e23500.
184. Kohayagawa Y, Nakao K, Ushita M, Niino N, Koshizaki M, et al. (2009) Pyogenic liver abscess caused by *Klebsiella pneumoniae* genetic serotype K1 in Japan. *J Infect Chemother* 15: 248-251.

185. Basu S (2009) *Klebsiella pneumoniae*: An Emerging Pathogen of Pyogenic Liver Abscess. *Oman Med J* 24: 131-133.
186. Gomelsky M, Klug G (2002) BLUF: a novel FAD-binding domain involved in sensory transduction in microorganisms. *Trends Biochem Sci* 27: 497-500.
187. Srivastava D, Waters CM (2012) A tangled web: regulatory connections between quorum sensing and cyclic Di-GMP. *J Bacteriol* 194: 4485-4493.
188. An S, Wu J, Zhang LH (2010) Modulation of *Pseudomonas aeruginosa* biofilm dispersal by a cyclic-Di-GMP phosphodiesterase with a putative hypoxia-sensing domain. *Appl Environ Microbiol* 76: 8160-8173.
189. Wang X, Kim Y, Hong SH, Ma Q, Brown BL, et al. (2011) Antitoxin MqsA helps mediate the bacterial general stress response. *Nat Chem Biol* 7: 359-366.
190. Wang H, Wu JH, Ayala JC, Benitez JA, Silva AJ (2011) Interplay among cyclic diguanylate, HapR, and the general stress response regulator (RpoS) in the regulation of *Vibrio cholerae* hemagglutinin/protease. *J Bacteriol* 193: 6529-6538.
191. Wilksch JJ, Yang J, Clements A, Gabbe JL, Short KR, et al. (2011) MrkH, a novel c-di-GMP-dependent transcriptional activator, controls *Klebsiella pneumoniae* biofilm formation by regulating type 3 fimbriae expression. *PLoS Pathog* 7: e1002204.
192. Spangler C, Kaefer V, Seifert R (2011) Interaction of the diguanylate cyclase YdeH of *Escherichia coli* with 2',(3')-substituted purine and pyrimidine nucleotides. *J Pharmacol Exp Ther* 336: 234-241.
193. Maddox SM, Coburn PS, Shankar N, Conway T (2012) Transcriptional regulator PerA influences biofilm-associated, platelet binding, and metabolic gene expression in *Enterococcus faecalis*. *PLoS One* 7: e34398.
194. Loprasert S, Negoro S, Okada H (1989) Cloning, nucleotide sequence, and expression in *Escherichia coli* of the *Bacillus stearothermophilus* peroxidase gene (*perA*). *J Bacteriol* 171: 4871-4875.
195. Ibarra JA, Villalba MI, Puente JL (2003) Identification of the DNA binding sites of PerA, the transcriptional activator of the *bfp* and *per* operons in enteropathogenic *Escherichia coli*. *J Bacteriol* 185: 2835-2847.
196. Bustamante VH, Villalba MI, Garcia-Angulo VA, Vazquez A, Martinez LC, et al.

- (2011) PerC and GrlA independently regulate Ler expression in enteropathogenic *Escherichia coli*. *Mol Microbiol* 82: 398-415.
197. Tomoyasu T, Tabata A, Imaki H, Tsuruno K, Miyazaki A, et al. (2012) Role of *Streptococcus intermedius* DnaK chaperone system in stress tolerance and pathogenicity. *Cell Stress Chaperones* 17: 41-55.
198. Winter J, Linke K, Jatzek A, Jakob U (2005) Severe oxidative stress causes inactivation of DnaK and activation of the redox-regulated chaperone Hsp33. *Mol Cell* 17: 381-392.
199. Weiner L, Brissette JL, Model P (1991) Stress-induced expression of the *Escherichia coli* phage shock protein operon is dependent on sigma 54 and modulated by positive and negative feedback mechanisms. *Genes Dev* 5: 1912-1923.
200. Flores-Kim J, Darwin AJ (2012) Phage shock protein C (PspC) of *Yersinia enterocolitica* is a polytopic membrane protein with implications for regulation of the Psp stress response. *J Bacteriol* 194: 6548-6559.
201. Yamaguchi S, Reid DA, Rothenberg E, Darwin AJ (2013) Changes in Psp protein binding partners, localization and behaviour upon activation of the *Yersinia enterocolitica* phage shock protein response. *Mol Microbiol* 87: 656-671.
202. Burdette DL, Monroe KM, Sotelo-Troha K, Iwig JS, Eckert B, et al. (2011) STING is a direct innate immune sensor of cyclic di-GMP. *Nature* 478: 515-518.
203. Keating SE, Baran M, Bowie AG (2011) Cytosolic DNA sensors regulating type I interferon induction. *Trends Immunol* 32: 574-581.
204. Shaw N, Ouyang S, Liu ZJ (2013) Binding of bacterial secondary messenger molecule c di-GMP is a STING operation. *Protein Cell* 4: 117-129.
205. Wu J, Sun L, Chen X, Du F, Shi H, et al. (2013) Cyclic GMP-AMP is an endogenous second messenger in innate immune signaling by cytosolic DNA. *Science* 339: 826-830.
206. Mather MW, McReynolds LM, Yu CA (1995) An enhanced broad-host-range vector for gram-negative bacteria: avoiding tetracycline phototoxicity during the growth of photosynthetic bacteria. *Gene* 156: 85-88.
207. Livak KJ, Schmittgen TD (2001) Analysis of relative gene expression data using

- real-time quantitative PCR and the 2(-Delta Delta C(T)) Method. *Methods* 25: 402-408.
208. Bobrov AG, Kirillina O, Perry RD (2005) The phosphodiesterase activity of the HmsP EAL domain is required for negative regulation of biofilm formation in *Yersinia pestis*. *FEMS Microbiol Lett* 247: 123-130.
209. Schmidt AJ, Ryjenkov DA, Gomelsky M (2005) The ubiquitous protein domain EAL is a cyclic diguanylate-specific phosphodiesterase: enzymatically active and inactive EAL domains. *J Bacteriol* 187: 4774-4781.
210. Liyana-Pathirana CM, Shahidi F (2005) Antioxidant activity of commercial soft and hard wheat (*Triticum aestivum* L.) as affected by gastric pH conditions. *J Agric Food Chem* 53: 2433-2440.
211. Adedapo AA, Jimoh FO, Koduru S, Afolayan AJ, Masika PJ (2008) Antibacterial and antioxidant properties of the methanol extracts of the leaves and stems of *Calpurnia aurea*. *BMC Complement Altern Med* 8: 53.
212. Bradford MM (1976) A rapid and sensitive method for the quantitation of microgram quantities of protein utilizing the principle of protein-dye binding. *Anal Biochem* 72: 248-254.
213. Beauchamp C, Fridovich I (1971) Superoxide dismutase: improved assays and an assay applicable to acrylamide gels. *Anal Biochem* 44: 276-287.
214. Woodbury W, Spencer AK, Stahman MA (1971) An improved procedure using ferricyanide for detecting catalase isozymes. *Anal Biochem* 44: 301-305.
215. MUENCH LJRAH (1937) A SIMPLE METHOD OF ESTIMATING FIFTY PER CENT ENDPOINTS 1 ' 2. *THE AMERICAN JOURNAL OF HYGIENE* 27: 493-497.
216. Cheng HY, Chen YS, Wu CY, Chang HY, Lai YC, et al. (2010) RmpA regulation of capsular polysaccharide biosynthesis in *Klebsiella pneumoniae* CG43. *J Bacteriol* 192: 3144-3158.

Publication

1. Chen LH, Kathaperumal K, **Huang CJ**, McDonough SP, Stehman S, Akey B, Huntley J, Bannantine JP, Chang CF, Chang YF (2008) Immune responses in mice to *Mycobacterium avium* subsp. *paratuberculosis* following vaccination with a novel 74F recombinant polyprotein. *Vaccine* 26(9):1253-62.
2. Wu CC, Lin CT, Cheng WY, **Huang CJ**, Wang ZC, Peng HL (2012) Fur-dependent MrkHI regulation of type 3 fimbriae in *Klebsiella pneumoniae* CG43. *Microbiology-SGM* 158: 1045-56.
3. Wang ZC^a, **Huang CJ**^a, Huang YJ, Wu CC, Peng HL (2013) FimK positively regulates the expression of type 1 fimbriae in *Klebsiella pneumoniae* CG43. ^a equal contribution, *Microbiology-SGM* 159: 1402-1415. 2013 May 23.
4. **Huang CJ**, Wang ZC, Huang HY, Huang HD, Peng HL (2013) YjcC, a c-di GMP phosphodiesterase protein, regulates the oxidative stress response and virulence of *Klebsiella pneumoniae* CG43. *PLoS ONE* July: e66740.doi:10.1371/journal.pone.0066740



Vita



My research interest is to understand how cyclic di GMP signaling is involved in microbial pathogenesis. As a graduate student in Dr. Ming-Huei Liao's lab from 2001 to 2003, I focused on using molecular biology, cell biology and Immunology approaches to study and develop diagnostic methods for detection of duck viral enteritis. I was a visiting fellow in Dr. Yung-Fu Chang's lab at Cornell University from 2004 to 2005; I worked on a project developing a recombinant vaccine against *M. avium* subsp. *paratuberculosis* challenge. As a Ph.D. student, my research focused on stress responses, cyclic-di GMP signaling pathway and type 3 fimbriae regulation in *Klebsiella pneumoniae*. To better understand pathogenesis in bacteria, we used comparative genomics and transcriptome analysis to select cyclic di GMP and stress response induced genes to further investigate new related virulence factors in *K. pneumoniae*.